# Transcriptome analysis and identification of effector genes in *Phytophthora palmivora* (Butler) Butler, the bud rot pathogen of coconut (*Cocos nucifera* L.)

**Final Synopsis submission**

**For the award of**

**Doctor of Philosophy**
in
**Biosciences**

**Mangalore University**

By

**GANGARAJ K. P.**

(Registration number: 147798218)

(Ref.No: MU/EXB/Ph.D./CR.46/Biosc./2015-16/E.13)

December 2022

**Research Supervisor**

**Dr. M.K. Rajesh**
Principal Scientist
Division of Crop Improvement
ICAR-CPCRI, Kasaragod, Kerala.

# CONTENTS


| Sl. No. | Chapter | Page number |
|---|---|---|
| 1. | Introduction | 1 |
| 2. | Review of literature | 2 |
| 3. | Objectives | 5 |
| 3.1 | Objective 1. To standardize a rapid and reliable *in vitro* inoculation assay to investigate *Phytophthora palmivora*-coconut interactions | 6 |
| 3.2 | Objective 2. To carry out transcriptome analysis of coconut–*Phytophthora palmivora* interactions using RNA-Seq | 19 |
| 3.3 | Objective 3. To develop a transcriptome database of coconut –*Phytophthora palmivora* interactions | 33 |
| 3.4 | Objective 4. To identify effector genes involved in pathogenicity from the transcriptome data | 38 |
| 3.5 | Objective 5. To identify ligands capable of targeting these pathogenicity factors by molecular docking studies | 48 |
| 4. | Summary and conclusion | 60 |
| 5. | References | 63 |
| 6. | Publications from the research work | 70 |

## 1. INTRODUCTION

Coconut (*Cocos nucifera* L.) is eulogized as '*Kalpa Vriksha*' or 'Tree of Life'. Apart from the importance of copra and coconut oil, which find uses in the manufacture of hair oils, soaps, cosmetics and other industrial products, the husk is a source of fibre which supports the coir industry. The tender nut supplies coconut water, a popular thirst quencher of health and hygienic value. In recent times, coconut has been gaining popularity as a 'functional health food' with virgin coconut oil and inflorescence sap endorsed for health promotion and human disease prevention.

Pests and diseases are the major production constraints in coconut. Coconut palms are susceptible to several diseases, the chief being root (wilt), bud rot, stem bleeding, leaf rot, and basal stem rot. Bud rot is a fatal disease of the coconut palm. Typical symptoms of the disease include severe rotting of the terminal bud and its surrounding tissues. Palms of all ages are affected, with young palms experiencing moist conditions being the most susceptible. Though generally a sporadic disease, it can assume epidemic proportions when weather conditions are conducive. The oomycete *Phytophthora palmivora* causes bud rot disease. Integrated disease management (IDM) strategies should be adopted throughout the year to effectively manage the bud rot disease, especially in the disease-endemic areas. Badly affected palms need to be removed and burned. If disease detection is done at an early stage, the infected tissue has to be removed and the cut portion protected with Bordeaux paste (Srinivasulu and Raghava, 2009). Prophylactic spray with 1% Bordeaux mixture is recommended on all the healthy palms surrounding the infected palms before the onset of monsoon to prevent the spread of the disease (Ramesh *et al.*, 2013; Chidananda and Pandurang, 2001).

In recent years, advances in biotechnology and bioinformatics have allowed the identification and detailed functional analysis of genes involved in the interactions between pathogenic oomycetes and their host plants. Phytopathogenic oomycetes are known to secrete a diverse repertoire of effector proteins. These effectors modulate the host's innate immunity and enable infection (Bozkurt *et al.*, 2012). Hence, identifying

and inhibiting effector or virulent factors, which might decrease pathogen virulence, can be an effective means of phytopathogen control.

Host-pathogen interaction studies were earlier based on the microarray, real-time PCR (RT-PCR) and serial analysis of gene expression (SAGE) assays. With the advent of RNA-sequencing (RNA-seq) approaches, gene expression studies have become more comprehensive. A recent technique suitable for comprehending the molecular mechanisms of interactions between hosts and pathogens is the dual RNA-seq (Westermann *et al*., 2012). This technique allows the simultaneous detection of both hosts- and pathogen-specific transcripts in mixed samples. The method has been successfully applied to several plant-pathogen models, which have illustrated the suitability of the technique and clear advantages compared with previously used techniques

Dual RNA-seq of *P. palmivora*-infested coconut samples will provide a better understanding of the molecular basis of host-pathogen interactions. This area has not been previously explored in a perennial crop like coconut, especially in the context of biochemical pathways, receptor-ligand interactions, gene networks of relevant genes and their inferred evolutionary history. These detailed investigations will provide a fillip to developing novel strategies for controlling the bud rot pathogen.

## 2. REVIEW OF LITERATURE

### 2.1. Coconut palm

The coconut (*Cocos nucifera* L.) is one of the most useful plants in the world. The edible part of the coconut fruit is the endosperm tissue comprising coconut meat and water. Besides its use in the food and beverage industry, coconut is widely used for making soaps, cosmetics, coir, paints, varnishes, etc. Coconut water contains adequate nutrients and is one of the world's most versatile natural products.

### 2.2. Bud rot disease

Coconut production is badly affected due to recurring endemic and epidemic outbreaks of pests and diseases. Bud rot is a fatal disease of the coconut palm caused by *Phytophthora palmivora*. The disease was first noticed in Grand Cayman Island in 1834 but is now known to occur in almost all coconut-growing countries. In India, Butler first

reported the bud rot from the then Madras State in 1906. The incidence of the disease has spread rapidly in the southern states of Kerala, Tamil Nadu, Andhra Pradesh, Telangana and Karnataka, especially in hilly tracts and regions with high humidity. Early detection of the infection and treatment of the infected palms are the major factors in successfully managing the disease (Sharadraj and Chandra Mohanan, 2013).

Palms of all ages are affected by this disease, but the disease is more severe in young palms of 5-20 years. The first visible symptom of the disease is seen on the center shoot of the tree ('spindle'), which withers and turns pale in colour. The affected spindle could easily be pulled out, and the rotting of internal tissue could be observed. These tissues assumed pale pink colour with a brown border. With the spread of infection, the leaves next to the spindle are shed one by one, leaving only fully matured leaves in the outer whorl of the crown. Emission of a very foul smell, caused by the rotting of tissues, is a diagnostic symptom. The spread of infection in the terminal bud ultimately leads to the death of the palm. The leaflets also show lesions which, in severe cases, appear as a leaf-bitten symptom (Nambiar, 1994).

### 2.3. *Phytophthora palmivora*

The causative organism of bud rot disease is Phytophthora palmivora, an oomycete. Though the primary infection is caused by *P. palmivora*, subsequent colonization by bacteria enhances rotting (Radha and Joseph, 1974). *P. palmivora* produces different kinds of spores that may directly or indirectly cause infection.

### 2.4. *Phytophthora:* Mode of interaction and effectors

Plant pathogens can be classified, by their infection strategy, as biotrophs, hemibiotrophs and necrotrophs. Biotrophic pathogens multiply within and feed on living tissues; necrotrophs kill host tissue and feed on dead cells. In contrast, hemibiotrophic pathogens, such as *Phytophthora* spp., generally show an early asymptomatic biotrophic stage of infection followed by a necrotrophic phase (Zuluaga *et al.*, 2016).

*Phytophthora* spp. has evolved sophisticated mechanisms to manipulate plant cells and cause infections. Biotrophic pathogens often develop haustoria when invading host cells, which are intracellular structures for the resorption of nutrients and are surrounded by the extra haustorial matrix. The latter is formed between the pathogen and host plasma membranes and establishes the main field of interaction where all

potential effectors are secreted. Effectors encompass a broad range of molecules with diverse biological functions. They can act either at the host-pathogen interface ('apoplastic effectors') or inside the host cell ('cytoplasmic effectors') (Bozkurt *et al.*, 2012). The phytophthoral apoplastic effectors include cell wall-degrading enzymes, enzyme inhibitors, toxins and elicitins; the cytoplasmic effectors harbour an additional host-targeting (HT) leader sequence, which is required for translocation across the host plasma membrane. The HT signal of many *Phytophthora* effectors is composed of a highly conserved N-terminal RXLR and a dEER motif further downstream; such effectors are known as RXLR effectors. The second major group of suspected cytoplasmic effectors is CRN or 'crinkler effectors', devoid of the RXLR motif but possessing a KxLFLAK motif instead. While 'crinklers' are present in all investigated oomycete species, effectors with RXLRs seem to be specific to *Phytophthora* (Schornack *et al.*, 2010; Bozkurt *et al.*, 2012).

**2.5. Transcriptome-level approaches to identify effectors**

During the infection process, the interactions between the pathogen and plant host result in large-scale changes in gene expression within both organisms. Owing to technical limitations, previous transcriptomic studies using probe- and tag-based approaches often required the separation of the interacting host and pathogen. However, the development of a new technology, dual-RNA sequencing (dual RNA-seq), enables the analysis of both partners simultaneously (Westermann *et al.*, 2012).

Zuluaga *et al.* (2016a) examined the transcriptional dynamics of *P. infestans* in a compatible interaction with its host tomato at three infection stages: biotrophy, hemibiotrophic and necrotrophy. The expression data suggest a tight temporal regulation of many pathways associated with suppressing plant defence mechanisms and pathogenicity, including the induction of putative cytoplasmic and apoplastic effectors. Twelve of these were experimentally evaluated to determine their ability to suppress necrosis caused by the *P. infestans* necrosis-inducing protein PiNPP1.1 in *Nicotiana benthamiana*. Four effectors suppressed necrosis, suggesting that they might prolong the biotrophic phase.

Zuluaga *et al.* (2016b) analysed the tomato leaf transcriptome during successive hemibiotrophic stages of a compatible interaction with the oomycete pathogen *Phytophthora infestans*. Nearly 10000 genes, corresponding to proteins in

approximately 400 biochemical pathways, showed differential transcript abundance during the three infection stages, revealing a major reorganization of plant metabolism, including major changes in source-sink relations and secondary metabolites. In addition, more than 100 putative resistance genes and pattern recognition receptor genes were induced. Both jasmonic acid (JA) and salicylic acid (SA) levels and associated signalling pathways showed dynamic changes during the infection time course. The biotrophic phase was characterized by the induction of many defence systems, which were insufficient, evaded or suppressed by the pathogen.

Kovalchuk *et al.* (2019) investigated the host-pathogen interactions between *Heterobasidion* sp., which causes root and butt rot in conifer trees, by dual RNA-seq. The role of the phenylpropanoid and flavonoid pathways in imparting defence in confers was noteworthy. *Heterobasidion*-specific transcripts, correlating to genes encoding enzymes related to carbohydrate- and lignin-degradation, secondary metabolism genes and effectors, were found to be significantly up-regulated during colonization of the conifer hosts. In grapevine, dual RNA-seq of whole transcriptomes of Mgaloblishvili, Pinot noir (a susceptible cultivar), and Bianca (a resistant hybrid) leaves, inoculated and non-inoculated with *Plasmopara viticola*, the downy mildew pathogen, revealed numerous genes encoding the pathogen effector-encoding genes. These genes showed marked expression differences in relation to the inoculated grapevine cultivar. Interestingly, five of the *P. viticola* apoplastic effectors could be specifically associated with resistance in grapevine (Toffolatti *et al.*, 2020).

## 3. OBJECTIVES

The objectives of the present study were:

1) To standardize a rapid and reliable *in vitro* inoculation assay to investigate *Phytophthora palmivora*-coconut interactions
2) To carry out transcriptome analysis of coconut–*Phytophthora palmivora* interactions using RNA-seq
3) To develop a transcriptome database of coconut–*Phytophthora palmivora* interactions
4) To identify effector genes involved in pathogenicity from the transcriptome data
5) To identify ligands capable of targeting these pathogenicity factors by molecular docking studies

## 3.1. TO STANDARDIZE A RAPID AND RELIABLE *IN VITRO* INOCULATION ASSAY TO INVESTIGATE *PHYTOPHTHORA PALMIVORA*-COCONUT INTERACTIONS

### 3.1.1. Introduction

Crop breeding programmes aiming to develop disease-resistant cultivars assume significance in a crop like a coconut, given the cryptic nature of *P. palmivora* and its detection at a stage where successful control measures can be implemented. Whole plant testing is of limited relevance for large-scale screening of bud rot disease in coconut for apparent reasons; also, studies can be restricted only to seedlings in containment/quarantine facilities or assessment in regions with a history of disease outbreaks. A deep understanding of molecular mechanisms underlying plant-pathogen interactions could enable the development of novel approaches for crop protection. One of the techniques frequently used for investigating plant defence responses to pathogens under laboratory conditions is the detached leaf assay, which has been utilized in several studies such as soybean (Surin *et al*., 1993), wheat (Arraiano *et al*., 2001), alfalfa (Irwin *et al*., 2003), rice (Jia *et al*., 2003) and durian (Vawdrey *et al*., 2005). This laboratory assay possesses several advantages: higher reproducibility, the requirement of less space, labour, plant materials and inoculum, more consistent delivery of inoculum, uniform incubation conditions can be maintained, inoculation site can be localized to specific areas of the leaf, more accurate quantification of disease is possible (Dhingra and Sinclair, 1995). Besides, contamination can be controlled, more replicates can be maintained, and there is no risk of spreading the phytopathogen to the environment. However, this assay also possesses disadvantages: detached leaves may not be a typical reflection of the variability of whole plants in terms of actual physical condition and age/phyllotaxy of leaves, and some of the host defence responses may be attenuated in detached leaves (Parke *et al*., 2005).

Histo-pathological and molecular events occurring during *P. palmivora* infection has not been reported in coconut. In the current study, an *in vitro* assay was developed through challenge inoculation of *P. palmivora* on the coconut leaf segments cultured *in vitro*. The infection and disease progression process was tracked using histological studies, electrolyte leakage assays, and PCR and RT-PCR with specific primers. This

assay would enable detailed molecular investigations on the cascade of events that occur during *P. palmivora* infection in coconut.

### 3.1.2. Methodology

#### *Isolation and morphological characterization of the pathogen*

Samples were collected from bud rot-affected coconut palms from Kasaragod and Dakshina Kannada districts of Kerala and Karnataka state, respectively, India, during the South-West monsoon season (June-July) in 2017. Bud region, along with young infected leaves, were collected in an autoclaved polythene bag and brought to the laboratory in an icebox. Tender leaves with lesions were separated in laminar airflow. Segments of 1 × 1 cm were surface sterilized by rinsing with 0.01% mercuric chloride solution, followed by washing in sterile distilled water thrice. The direct plating method (Chowdappa *et al.*, 2014) was used to isolate the pathogen by placing the leaf segments in carrot agar medium supplemented with rifampicin (125 ppm). The inoculated samples were kept in a growth chamber with a constant temperature (25±2°C) and humidity (95%). The individual isolates obtained were characterized through morphological traits, as detailed by Gallegly and Hong (2008). Individual isolates were inoculated separately on carrot broth medium and maintained at 25±2°C to form mycelial mats. They were filtered and washed thoroughly with sterile water and dried using sterile filter paper.

#### *Molecular characterization of the pathogen*

To confirm the identity of each *Phytophthora* species, DNA was extracted from the mycelial mats of individual isolates using the DNeasy Plant Mini Kit (Qiagen, USA). The ITS6 (5'-GAAGGTGAAGTCGTAACAAGG-3') and ITS4 (5'-TCCTCCGCTTATTGATATGC-3') primer pairs (White *et al.*, 1990; Cooke *et al.*,2000) were used to amplify the pathogen. PCR, gel electrophoresis, elution of bands, sequencing and sequence analysis was conducted as described by Prathibha *et al.* (2018).

#### *Screening P. palmivora isolates for virulence levels*

*P. palmivora* isolates collected from bud rot-affected palms were initially screened for their level of virulence using the detached leaf technique (Sharadraj and Chandra Mohanan, 2014). For this, zoospore suspensions were prepared from the isolates by growing a 5 mm mycelial disc in carrot agar and incubating at 25±2°C. After

sporulation, on the 7th day, sterile distilled water (20 mL) was added and incubated at 15°C for 15 minutes. Plates were then kept at room temperature till the release of zoospores (for about 20 minutes). Zoospore suspension from each isolate was filtered through a muslin cloth, and the concentration was adjusted to $2\times10^4 mL^{-1}$.

To screen its virulence, spindle leaves, sampled from Chowghat Orange Dwarf (COD), a cultivar susceptible to bud rot, were wiped with sterile water and pricked (four times) on its dorsal side with a sterile needle to facilitate easy entry of the pathogen to the leaf and kept above sterile test tubes lying horizontally on wet cotton in a tray. Zoospore suspensions (10 µL) of each isolate were individually inoculated in the pricked region, and the inoculated area was covered with a thin layer of wet cotton. The entire set-up was covered with a polythene sheet and kept in a humid chamber at 25±2°C (Sharadraj and Chandra Mohanan, 2014; Rachana and Rajesh, 2019). Different isolates were screened for their level of virulence based on the time required for the initiation of infection and the size of the lesion formed after five days of inoculation. The highly virulent isolate of *P. palmivora* obtained from this exercise was used for the rest of the studies.

***In vitro leaf assay***

Spindle leaves, sampled from three-year-old Chowghat Orange Dwarf (COD) palm, were cleaned by swiping with 70% ethanol, and the midrib portion was removed (Figure 3.1.1.A-F). Leaf lamina was cut into segments (approx. 5 cm) aseptically under a laminar airflow chamber (Figure 3.1.1.G), surfaced sterilized with mercuric chloride (0.01%) for 10 minutes with constant shaking (Figure 3.1.1.H) and then washed 4-5 times in sterile water (Figure 3.1.1.I). These leaf segments were then placed with their dorsal side upwards in Y3 medium (Eeuwens, 1976), supplemented with sucrose (30 $gL^{-1}$), agar (6.5 $gL^{-1}$) and charcoal (0.5 $gL^{-1}$), in Petri plates (Figure 3.1.1.J). All the cultures were kept at 25±2°C and 95% humidity in a plant growth chamber (Panasonic MLR-352H-PE). Leaf lamina segments were pricked (five equal pricks) using a sterile needle (Figure 3.1.1.K) before inoculation with zoospore suspension (10 µL) of highly virulent isolate (Figure 3.1.1.L and Figure 3.1.1.M). Non-inoculated leaf segments with similar pricks served as control. Cultures were observed at regular intervals to record the initiation of infection, its advancement and other attributes, such

as the size of the lesions. Post-infection, the identity of pathogen was confirmed through morphological and molecular techniques, as described earlier.

**Fig. 3.1.1. *In vitro* inoculation assay standardized; (A) three-year-old Chowghat Orange Dwarf seedling; (B-E) collection of bud tissues from seedlings; (F) separating the leaf tissues; (G) making tissue bits; (H) surface sterilization; (I) subsequent washing; (J) inoculation of leaf bit on Y3 media; (K) pinpricking on leaf bit using a sterile syringe; (L) inoculation of *P. palmivora* zoospore suspension on leaf bit; and (M) inoculated leaf bit.**

***Leaf viability assay using Membrane Stability Index (MSI)***

The viability of the *in vitro* cultured leaf segments was assessed using the membrane stability index (Sairam *et al.*, 1997) since this parameter is negatively related to senescence or leaf death (Gupta *et al.*, 2012). Detached leaflets were taken for comparison. About 100 mg of leaf segments were taken and immersed in 10 mL distilled water, and initial electrical conductivity ($\mu Scm^{-1}$; Model PP20, Sartorius) was determined (C1) after overnight incubation at room temperature. Final electrical conductivity was determined (C2) after placing the test tubes in boiling water for 30 min. The membrane stability index (MSI) was calculated as follows:

$$MSI = \{1-(C1/C2)\} \times 100$$

***Histopathological studies using microscopy***

The histo-pathological traits were visualized using scanning electron microscopy. For scanning electron microscopy, leaf bits (1 × 1 cm) with infected portions were placed in an aluminium cylinder adhered with graphite tape and placed in a vacuum chamber. The sample was coated with a high vacuum evaporator for six minutes in an ionizing metal JEOL JFC-1100 (Fine Coat® sputter ion, JEOL Ltd., Tokyo, JP). The gold-coated samples were observed in a scanning electron microscope (JEOL-JSM-6490LV) under vacuum to get higher resolution.

***Disease assays and pathogenicity tests***

To satisfy Koch's postulate, pieces of inoculated leaf bits, showing disease lesions 36 hpi, were removed from the Petri plates, surface sterilized with 70% ethanol, plated onto carrot agar medium in Petri plates and maintained at 25+2$^{o}$C and 95% humidity in a plant growth chamber (Panasonic MLR-352H-PE). Subsequent growth of mycelia was recorded. Pathogenicity tests were conducted by detached leaf assay (Sharadraj and Chandra Mohanan, 2014), as mentioned

***RNA extraction and expression studies***

Infected leaf samples, collected for isolation of RNA, include samples 12 hours post-inoculation (12 hpi) and 12 hours un-inoculated control (12 hc), 24 hours post-inoculation (24 hpi) and 24 hours un-inoculated control (24 hc) and 36 hours post-inoculation (36 hpi) and 36 hours un-inoculated control (36 hc). Total RNA was

extracted from these samples using the NucleoSpin® RNA Plant Kit (Macherey Nagel). 260 nm/280 nm absorbance ratio was used to assess the quality and purity of the extracted RNA. RNA integrity number (RIN) was analysed using an Agilent Technologies 2100 Bioanalyzer with the Agilent RNA chip. cDNA was synthesised using the PrimeScript cDNA Synthesis Kit (Takara). The reaction mixture included 4.0 µL of 5 X PrimeScript buffer, 1 µL of PrimeScript RT enzyme mix, 1 µL of random hexamer primer and 100 ng of RNA. The reactions were incubated at 37°C for 15 min, followed by 85°C for 5 secs and then kept at 4°C. *Phytophthora* spp. are known to secrete numerous effectors into their hosts to promote infection, and therefore, the expression of effector genes is up-regulated during the infection process (Wang and Jiao, 2019). Primer pairs were designed for an RXLR effector (POM73696.1) previously reported in *P. palmivora* (Ali *et al*., 2017). Also, the 40S ribosomal gene (*G40S*) was taken as an internal control for *P. palmivora* (Ali *et al*., 2017), while eukaryotic translation initiation (*CneIF-4γ*) from coconut was taken as an internal control for coconut (Rachana and Rajesh, 2019). The details of the primers are given in Table 3.1.1.

**Table 3.1.1. Primers used for amplification of genes of host and pathogen genes via RT-PCR**

| Sl. no. | Gene name (organism) | Primer name | Primer sequence (5'-3') | Product size (bp) |
|---|---|---|---|---|
| 1. | Eukaryotic initiation factor-4γ (*Cocos nucifera*) | CneIF-4γF | CACCAGGAGACTTGGGAACT | 110 |
| | | CneIF-4γR | CAGCTTACCAACCACTTCACC | |
| 2. | 40 S rRNA (*Phytophthora palmivora*) | G40SF | AACTCTGATTGAGGCCTTCG | 243 |
| | | G40SR | AACTCTGATTGAGGCCTTCG | |
| 3. | RXLR effector (*Phytophthora palmivora*) | GRXLRF | CCTTCAAGCGGTAATCCAAA | 244 |
| | | GRXLRR | ATGACCCTTGTGGTTCTTGC | |

***Statistical analysis***

For statistical analysis, the data recorded on the size of the lesions and their relative growth rates due to infection by *P. palmivora* and the Membrane Stability Index (MSI) in *in vitro* cultured coconut leaf segments in comparison to detached leaflets were subjected to one-way analysis of variance (ANOVA) as the experiment was laid out in completely randomised design (CRD). The means obtained were compared using Duncan's Multiple Range Test (DMRT) using SPSS 15.0.

### 3.1.3. Results

***Initiation of cultures and morphological characterization***

Strains isolated from bud rot-infected palms and cultured in carrot agar medium showed similar morphological attributes like a greyish-white colony with a stellate colony pattern, the colony possessing sharp, well-defined leading edges (Figure 3.1.2.a). The growth rate of the cultures was 1-1.3 $cm^2$ $day^{-1}$, and among the isolates, TR-PP-5 recorded the maximum growth rate (1.3 $cm^2$ $day^{-1}$). The isolates showed network-like mycelia without cross walls (Figure 3.1.2.b). Also, abundant ovoid to ellipsoid sporangia, with a round base and conspicuous papilla, were produced (Figure 3.1.2.c). The sporangia of the pathogen showed sympodial arrangement and were caducous, breaking away rapidly from the sporangiophore. The average size of sporangia was found to be 59.03 × 26.63 µm with a 2.21 L/B ratio. Globose chlamydospores were found terminal as well as intercalary on the mycelia of the isolate (Figure 3.1.1.d). The average diameter of the chlamydospore was 27 µm. All the isolates were found to be A2 mating type. The oogonia were spherical, and the average size was 34 µm (Figure 3.1.2.e). All the above said morphological features are highly similar to those reported for *P. palmivora*. Challenge inoculation on the detached leaflets indicated that necrotic lesions reached a maximum size (7.11 $cm^2$) on the fifth day after inoculation (Figure 3.1.2.f). Among the isolates, TR-PP-2 showed the highest virulence under detached leaf assay. Hence this isolate was used for the rest of the study.

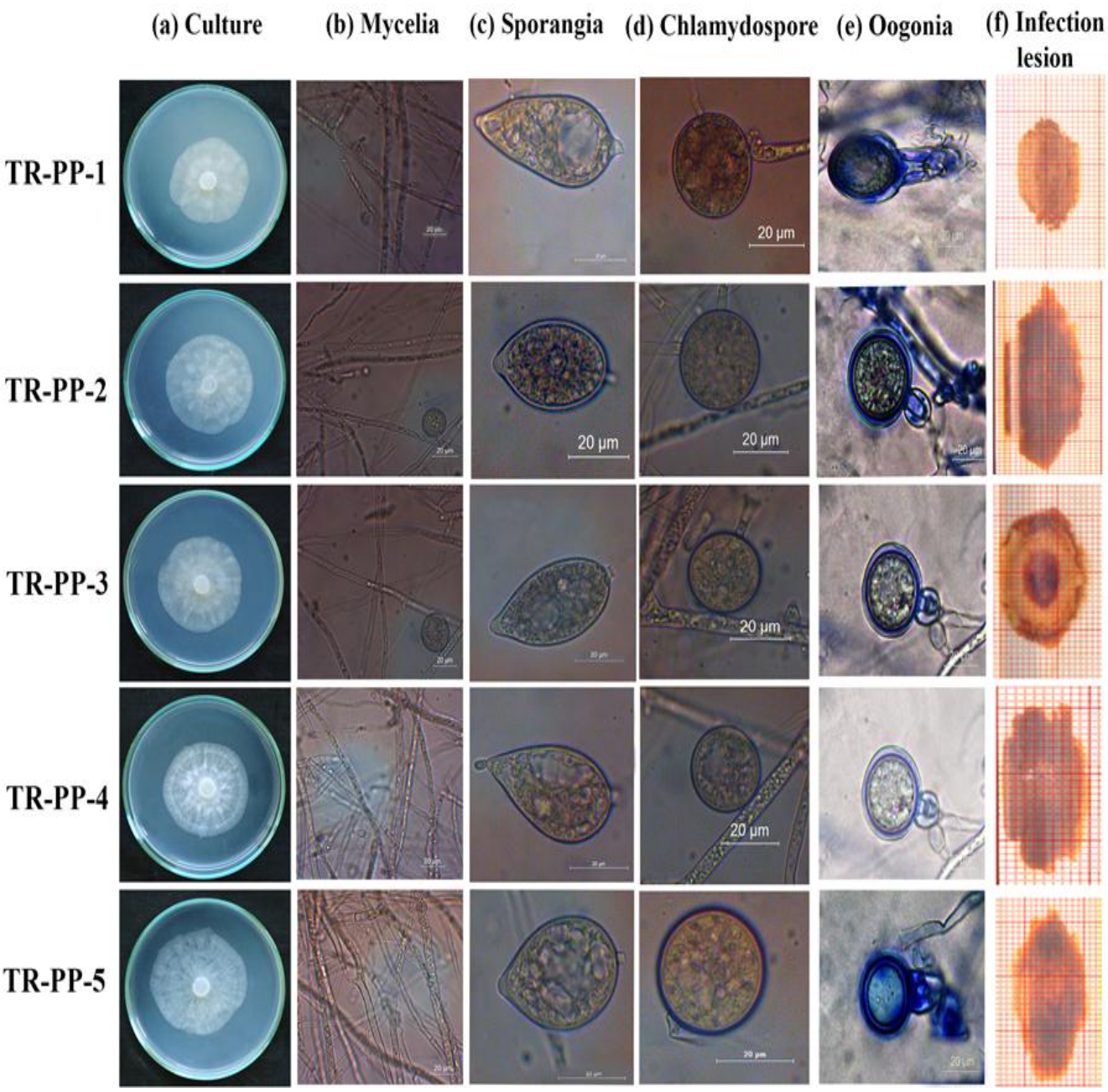


**Fig. 3.1.2. Colony morphology of different isolates (TR-PP-1 to TR-PP-1 5) and the infection lesions on the detached leaflet of coconut**

***Molecular characterization of the virulent isolate***

Molecular characterization of the isolate TR-PP-2 was undertaken using *Phytophthora*–specific *ITS* primers. The expected amplicon of around ~900 bp was obtained (Figure 3.1.3). The amplicon was sequenced, and a sequence of 846 bp (48.6 % G+C) was obtained (GenBank accession no. MK500842.1). Analysis by BLASTn revealed that the sequence was completely identical (100%) to *P. palmivora* strain TARI 28262 (GenBank accession no. GU111653) (Figure 3.1.3).

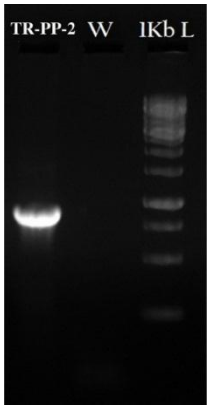


**Fig. 3.1.3. Molecular characterization TR-PP-2. Gel image of the amplicon (TR-PP-2*: P. palmivora* DNA, W: -ve control and 1 Kb L: 1 Kb ladder).**

***In vitro assay***

The morphological and molecular level characterization confirmed the causal agent as *P. palmivora,* and the challenge inoculation study verified its virulence. When the TR-PP-2 isolate was inoculated in the pricked portion of the spindle leaf segment cultured in Eeuwens Y3 medium, mild necrotic lesions were first observed after 12 hours. The lesion became more extensive and conspicuous, with an irregular pattern 48 hours after inoculation. No significant change was observed on the leaf surface of the control samples. The necrotic lesion reached an average size of 228 $mm^2$ on the fourth day after inoculation (Figures 3.1.4 and 3.1.5).

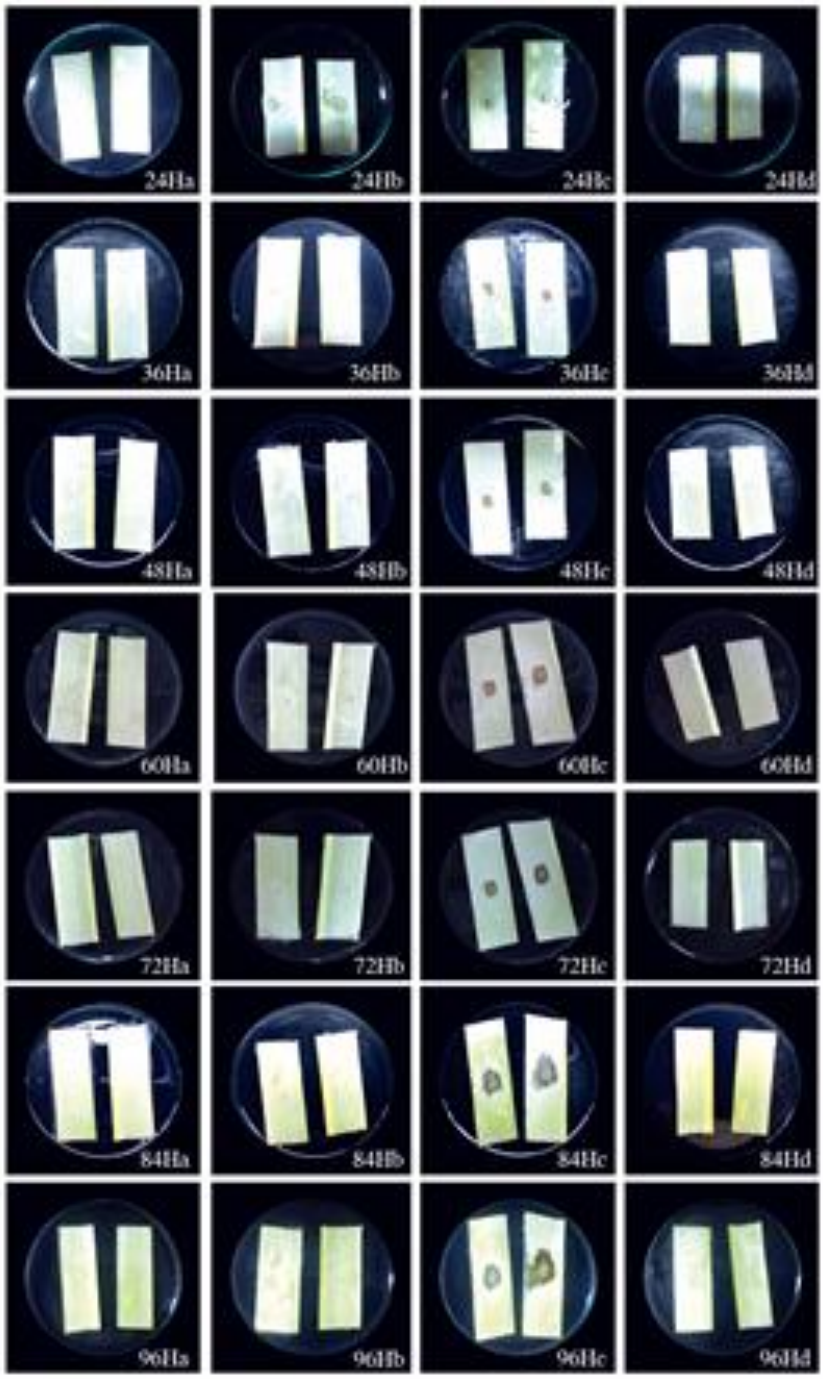


**Fig. 3.1.4. *In vitro* inoculation of *P. palmivora* on coconut spindle leaf. Ha: un-pricked and un-inoculated; Hb: pricked and un-inoculated; Hc: pricked and inoculated; and Hd: un-pricked and inoculated. Observations were taken at 24, 36, 48, 60, 72, 84 and 96 hours after inoculation.**

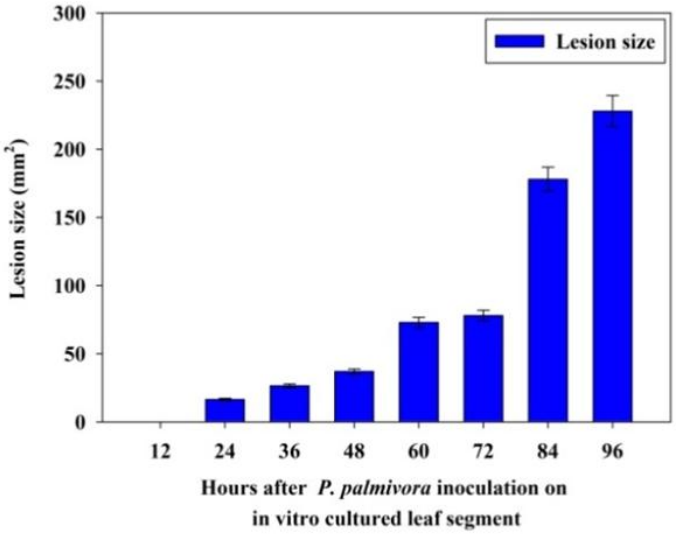


**Fig. 3.1.5. Size of the lesion and its relative growth rate caused by the *P. palmivora* on coconut leaf segments cultured *in vitro*. Observations were taken at 24, 36, 48, 60, 72, 84 and 96 hours after inoculation.**

The viability of the leaf segments cultured on *in vitro* medium was revealed through membrane stability index (MSI) assay. Preliminary observations indicate that MSI did not decrease significantly in the leaf segments even after 20 days of *in vitro* culturing in the medium, whereas it rapidly decreased in detached leaflets (Figure 3.1.6).

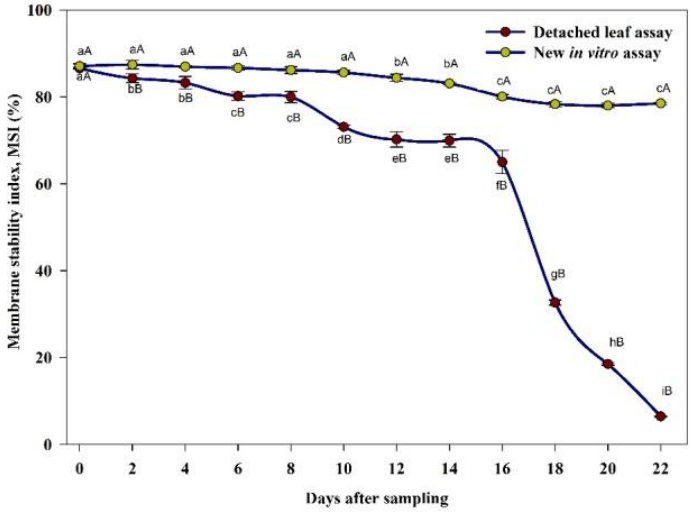


**Fig. 3.1.6. A comparison of Membrane Stability Index (MSI) in *in vitro* cultured leaf segments up to 20 days.**

### *Scanning electron microscopy*

Scanning electron micrographs of the leaf segments from this *in vitro* assay gave further evidence of the pathogen interaction. It revealed the development of hyphae along the epidermal cell surface with appressoria-like hyphae and its penetration along the walls of the trichome. Fungal hypha seems to emerge through stomata to produce sporangial structures at the surface of the epidermal layer. In the later stages of the infection, the sporangial formation and network-like hyphae on the surface seem to proliferate to form lesions (Figure 3.1.7).

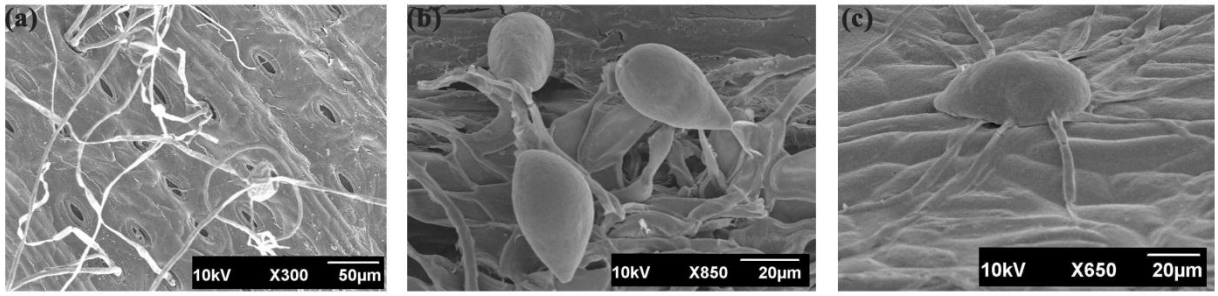


**Fig. 3.1.7. Scanning electron micrographs of the leaf segments inoculated with *P. palmivora* using the *in vitro* method. (a) mycelial growth through stomata, (d) sporangia attached in the trichome of the leaf, (c) self-emerging sporangia**

### *Pathogenicity studies*

Detached leaf inoculation experiments to complete Koch's postulates with *P. palmivora*, isolated from the *in vitro* assay, resulted in typical leaf lesions. The initial symptoms were observed at 24 hpi.

### *RT-PCR analysis*

RT-PCR analysis revealed amplification of the coconut housekeeping gene (*CneIF-4γ*) in both un-inoculated and inoculated leaf samples at all three-time points (12, 24 and 36 hpi). The expression of the *P. palmivora* housekeeping gene (*G40S*) could be observed only in inoculated leaf samples at all three-time points (12, 24 and 36 hpi) and not in un-inoculated samples. Expression of *P. palmivora* RXLR effector gene (*GRxLR*) was observed only in inoculated leaf samples at 24 and 36 hpi (Figure 3.1.8.).

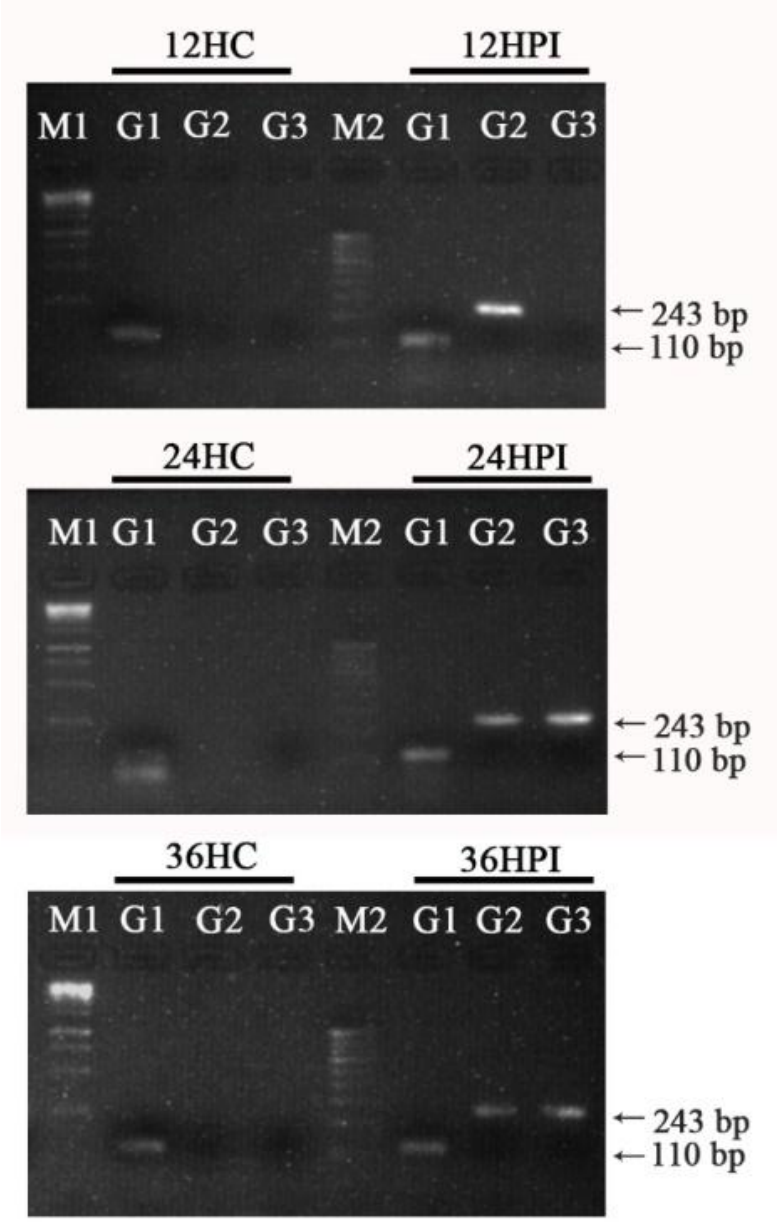


**Fig. 3.1.8. RT-PCR products after electrophoresis; M1: 1 Kb DNA ladder; M2: 100 bp DNA ladder; G1: Eukaryotic translation initiation (*CneIF-4γ*) in coconut; G2: 40S ribosomal gene (*G40S*) of *P. palmivora*; G3: *P. palmivora* RXLR effector gene (*GRxLR*)**

## 3.2. TO CARRY OUT TRANSCRIPTOME ANALYSIS OF COCONUT–*PHYTOPHTHORA PALMIVORA* INTERACTIONS USING RNA-SEQ

### 3.2.1 Introduction

RNA-sequencing (RNA-seq) has recently emerged as a powerful tool to study global changes in expression during host-pathogen interactions as it provides an unbiased, discovery-based expression profiling that is more sensitive than microarrays (Pareek *et al.*, 2011). RNA-Seq involves sequencing cDNA libraries from individuals experiencing various physiological challenges without prior knowledge of the genes' identity or sequence. Typically, methods employing RNA-seq have relied on reference genomes to assemble and quantify the millions of small sequence fragments produced by high-throughput methods. Still, bioinformatics advances now allow the *de novo* assembly of an entire transcriptome (Westermann *et al.*, 2012).

Further, it can be used to simultaneously capture host and pathogen transcriptomes, a technique commonly referred to as 'dual RNA-seq' (Westermann *et al.*, 2012). This method has been successfully used to gain novel biological insights into diverse plant-pathogen interactions. Here, we have conducted a time course experiment to comprehensively examine coconut-*Phytophthora* interactions via dual RNA-seq.

### 3.2.2. Methodology

The schematic outline of the experimental design and dual RNA-seq data analysis workflow is given in Figure 3.2.1.

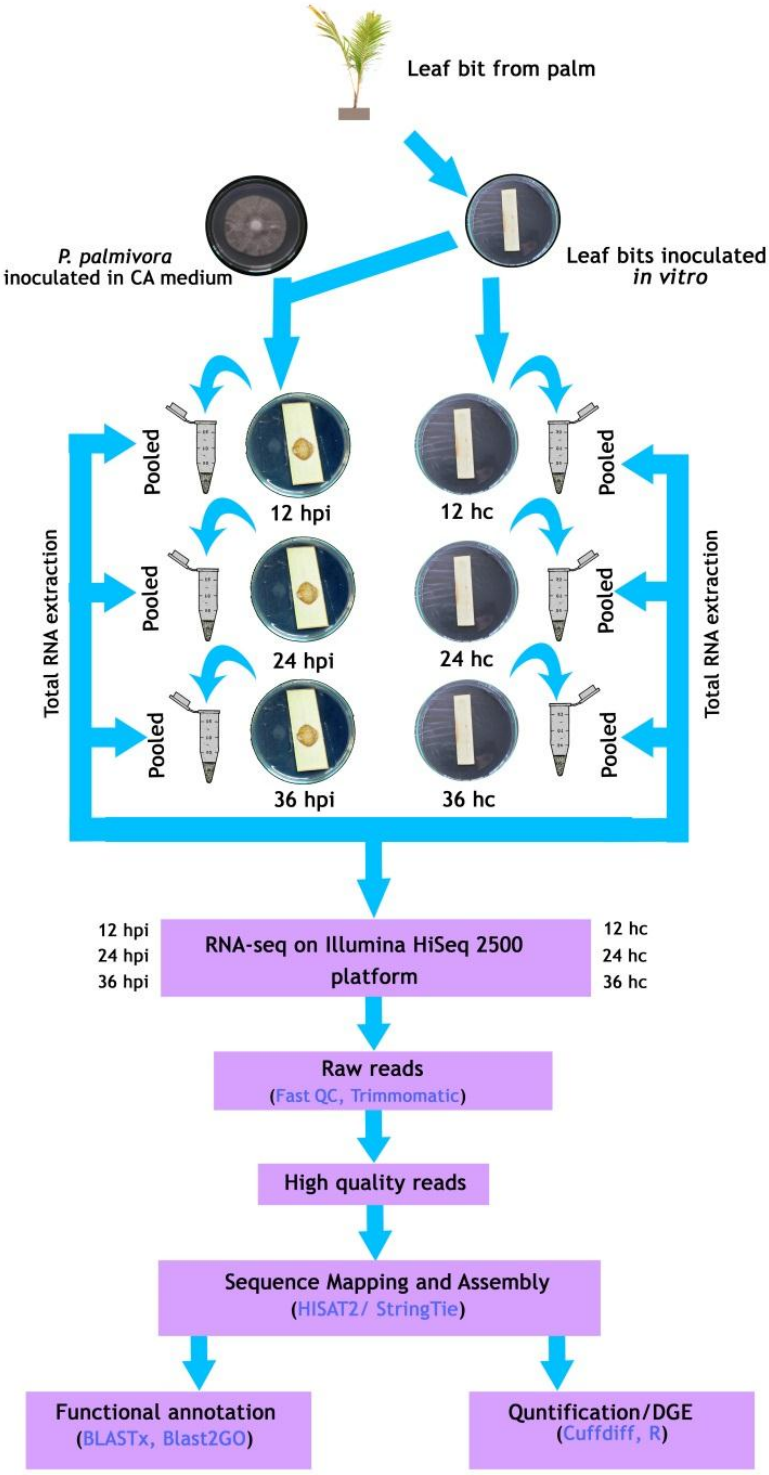


**Fig.3.2.1. Schematic outline of the experimental design and data analysis workflow**

### *Experimental design and sampling*

The *in vitro* inoculation assay standardized (described in detail in Section 3.1.) was utilized for the infection studies. Briefly, spindle leaflets from two-year-old coconut seedlings [Chowghat Orange Dwarf (COD) cultivar] were taken and inoculated in plain Y3 media (Eeuwens, 1974*)* in Petri plates. Zoospore suspension (10 µL of $2\times10^4$ $mL^{-1}$) of a virulent isolate of *P. palmivora* (GenBank accession no. MK500842.1), isolated from bud rot infected coconut palm in our laboratory and maintained in carrot agar (CA) medium, was used for the inoculation experiments. *P. palmivora* was inoculated onto pinpricked coconut leaflets. Typical necrotic lesions, indicating infection, were first observed after 12 hours post-inoculation (hpi). Samples were taken at 12, 24 and 36 hpi. Un-inoculated, but pinpricked leaflets, served as controls (hc). RNA was also extracted from fungal mycelium (M). Three biological replicates were sampled and used to isolate RNA at each time point.

To confirm the presence of the pathogen in the infection area, the infected area was wiped with alcohol, DNA was extracted from the specific area using DNeasy Plant Mini Kit (Qiagen, USA) and amplified using *Phytophthora*-specific primers (ITS6 and ITS4) (White *et al.,*1990*)*. An expected band of around ~900 bp was obtained, which was sequenced. Analysis of the sequence by BLASTn revealed complete identity to *P. palmivora* (GenBank accession no. GU111653).

### *RNA extraction and sequencing*

Total RNA was extracted from 150 mg of tissue at each specific time point [from the infection area in the case of inoculated samples and pricked area in the case of control samples] using the NucleoSpin® RNA Plant Kit (Macherey-Nagel). Total RNA was extracted from three independent biological samples per treatment. The quality and the purity of the extracted RNA were assessed by OD 260nm/280nm ratio, and RNA integrity number (RIN) was analyzed using an Agilent Technologies 2100 Bioanalyzer with the Agilent RNA chip with RIN > 8.0. The isolated RNA samples from each stage were pooled together and used for RNA-seq library construction (TruSeq RNA Sample Prep Kit, Illumina). After quality assessment, the constructed messenger RNA libraries

were subjected to paired-end sequencing on an Illumina HiSeq 2500 platform/ HiSeq 4000 platform, as per the procedure described in Rajesh *et al.* (2015).

### *Data analysis*

Raw reads, quality headed (.fastq) fasta files were subjected to quality check. Initially, the raw reads were checked for the ambiguous bases, Phred score >Q20, read length, nucleotide base content and other parameters using FastQC (https://www.bioinformatics.babraham.ac.uk/projects/fastqc/). Trimmomatic was then used to filter low-quality sequences (http://www.usadellab.org/cms/?page=trimmomatic). After trimming and filtering the low-quality reads, a QC was performed to reassess the quality of the reads. Mapping and assembly of the good quality reads to the reference genomes was performed with 'New Tuxedo Suit' (HISAT2/StringTie), using default parameters (http://daehwankimlab.github.io/hisat2/); https://ccb.jhu.edu/software/stringtie/). The coconut (NCBI Accession No. PRJNA546491) and *P. palmivora* (NCBI Accession No. PRJNA558734) reference genomes were downloaded from NCBI. Initially, indexing the coconut reference genome and alignment of reads to the coconut reference genome was done using HISAT2. The mapped reads were assembled individually with StringTie, and FPKM (Fragments Per Kilobase of transcript per Million mapped reads) was calculated for transcripts. A reference transcript was created by merging the libraries of 12 hpi, 12 hc, 24 hpi, 24 hc, 36 hpi and 36 hc prior to the different gene expression (DGE) in coconut. In comparison, 12 hpi, 24 hpi, 36 hpi and M (mycelium) were used for *P. palmivora*. The DGE analysis was undertaken using the 'cuffdiff' method in Cufflinks (http://cole-trapnell-lab.github.io/cufflinks/). The outcomes were plotted using the R software (https://rstudio.com/).

### *Transcriptome functional annotation*

Local protein databases were created for the Arecaceae family (Taxonomy ID: 4710) and *Phytophthora* spp. (Taxonomy ID: 4783). The assembled transcriptomes of both the host and the pathogen were annotated by BLASTX searches (Altschul *et al.*, 1997) against corresponding proteome databases, keeping a threshold of $1 \times 10^{-4}$ maximum e value. Blast2GO (https://www.blast2go.com/) were used to perform Gene Ontology

(GO) analysis of the assembled transcriptome and individually for *P. palmivora* and coconut.

**Validation of DEGs in coconut**

***Designing of primers***

Ten differentially expressed effectors, *viz.*, chitinase, cinnamyl alcohol dehydrogenase, WRKY transcription factor, mitogen-activated protein kinase (MAPK), transcription factor MYB2, GST6 protein, 1-aminocyclopropane-1-carboxylate oxidase, β-1,3-glucanase, calcium-dependent protein kinase and receptor-like serine/threonine-protein kinase chosen based on the enhanced expression profile for validation using quantitative real-time PCR (qRT-PCR). Gene-specific primers for the selected effectors chosen for validation were designed with Primer3 software (https://bioinfo.ut.ee/primer3-0.4.0/). Genes encoding the coconut housekeeping gene *(CneIF-4γ)* were selected as an internal control (Rachana and Rajesh, 2019).

**qRT-PCR *analysis***

Total RNA was isolated from frozen leaflets at 12, 24, and 36 hpi and from control leaflets, un-inoculated, but pinpricked leaflets, served as controls (12, 24 and 36 hc) using the RNA kit (Macherey Nagel). RNA samples were reverse transcribed to generate first-strand complementary DNA (cDNA) using the PrimeScript™ (DSS Takara Bio India Pvt. Ltd.) First Strand cDNA Synthesis Kit, according to the manufacturer's instructions. qRT-PCR tests were done with 1 µL of cDNA (50 ng) first-strand and StepOne™ Real-Time PCR System SYBR Green I Master mix, according to the manufacturer's instructions (Applied Biosystems Thermo Fisher Scientific). For statistical analysis, to compare the treatment and control groups, Student's t-test was used, with a significance level of $p < 0.05$ being reported.

**3.2.3. Results**

***RNA seq data information***

The details of RNA-seq data generated from this study, submitted to the NCBI Sequence Read Archive (SRA), are provided in Table 3.2.1. Table 3.2.2 gives an overview of the RNA-seq statistics of raw and clean reads obtained at different time intervals.

**Table 3.2.1. Details of RNA-seq data submitted to the NCBI Sequence Read Archive (SRA)**

| Library id | Sample | Accession no. | BioProject accession no. | BioSample accession no. |
|---|---|---|---|---|
| 12hcR1 | 12 hours control (R1) | SRX5914110 | PRJNA544637 | SAMN11867028 |
| 12hcR2 | 12 hours control (R2) | SRX9197107 | PRJNA544637 | SAMN16273751 |
| 12hpiR1 | 12 hours after inoculation (R1) | SRX5914109 | PRJNA544637 | SAMN11867027 |
| 12hpiR2 | 12 hours after inoculation (R2) | SRX9197106 | PRJNA544637 | SAMN16273750 |
| 24hcR1 | 24 hours control (R1) | SRX5914112 | PRJNA544637 | SAMN11867030 |
| 24hcR2 | 24 hours control (R2) | SRX9197109 | PRJNA544637 | SAMN16273752 |
| 24hpiR1 | 24 hours after inoculation (R1) | SRX5914111 | PRJNA544637 | SAMN11867029 |
| 24hpiR2 | 24 hours after inoculation (R2) | SRX9197108 | PRJNA544637 | SAMN16273752 |
| 36hcR1 | 36 hours control (R1) | SRX5914108 | PRJNA544637 | SAMN11867032 |
| 36hcR2 | 36 hours control (R2) | SRX9197111 | PRJNA544637 | SAMN16273755 |
| 36hpiR1 | 36 hours after inoculation (R1) | SRX5914107 | PRJNA544637 | SAMN11867031 |
| 36hpiR2 | 36 hours after inoculation (R2) | SRX9197110 | PRJNA544637 | SAMN16273754 |
| MR1 | Mycelia (R1) | SRX9230504 | PRJNA544637 | SAMN16331542 |
| MR2 | Mycelia (R2) | SRX9230505 | PRJNA544637 | SAMN16331543 |

**Table 3.2.2. RNA-seq statistics of raw and clean reads obtained at different time intervals**

| Sample name | Number of paired-end reads (raw reads) | Number of paired-end reads (clean reads) | Percentage of high-quality reads (%) |
|---|---|---|---|
| 12hcR1 | 64,921,052 | 64,503,262 | 99.35 |
| 12hcR2 | 91146934 | 75561988 | 82.90 |
| 12hpiR1 | 63, 662,338 | 63,090,348 | 99.10 |
| 12hpiR2 | 89235470 | 75937650 | 85.09 |
| 24hcR1 | 63,064,844 | 62,601,136 | 99.26 |
| 24hcR2 | 92164622 | 74634190 | 80.97 |
| 24hpiR1 | 67,291,090 | 66,770,394 | 99.22 |
| 24hpiR2 | 82452170 | 61507724 | 74.59 |
| 36hcR1 | 70,446,814 | 70,150,788 | 99.57 |
| 36hcR2 | 104133082 | 89001710 | 85.46 |
| 36hpiR1 | 60641514 | 57437658 | 94.71 |
| 36hpiR2 | 96660904 | 78059860 | 80.75 |
| MR1 | 152754224 | 139805622 | 91.52 |
| MR2 | 79877478 | 69183604 | 86.61 |

[12 hc: 12 hours control, 12 hpi: 12 hours post-inoculation; 24 hc: 24 hours control, 24 hpi: 24 hours post-inoculation; 36 hc: 36 hours control, 36 hpi: 36 hours post-inoculation, M: Mycelia, R1: replication 1; R2: replication 2]

***Mapping and assembly***

Mapping statistics of high-quality reads with the coconut genome and *P. palmivora* genome are given in Table 3.2.3. A total of 56901 transcripts (merged) were generated against the coconut reference genome after using StringTie merge, while 25988 transcripts (merged) were generated against the *P. palmivora* genome. The assembled transcripts of each library are provided in Table 3.2.3.

**Table 3.2.3. Summary of mapping information of pre-processed reads against *Phytophthora palmivora* genome and coconut genome separately**

| Sample name | *Phytophthora palmivora* genome | | Coconut genome | |
|---|---|---|---|---|
| | **Percentage of alignment** | **Assembled transcript** | **Percentage of alignment** | **Assembled transcript** |
| 12hcR1 | - | - | 95.48% | 38673 |
| 12hcR2 | - | - | 73.35% | 44968 |
| 12hpiR1 | 0.00% | - | 95.96% | 40649 |
| 12hpiR2 | 1.36% | 1750 | 67.82% | 48771 |
| 24hcR1 | - | - | 94.81% | 40045 |
| 24hcR2 | - | - | 83.75% | 49707 |
| 24hpiR1 | 1.28% | 6014 | 92.88% | 38958 |
| 24hpiR2 | 23.27% | 21833 | 60.98% | 36564 |
| 36hcR1 | - | - | 91.69% | 40338 |
| 36hcR2 | - | - | 69.57% | 52521 |
| 36hpiR1 | 0.95% | 4571 | 92.46% | 37154 |
| 36hpiR2 | 25.38% | 24325 | 58.51% | 38962 |
| MR1 | 94.00% | 34923 | - | - |
| MR2 | 95.17% | 34098 | - | - |

***Differential gene expression in coconut***

It was observed that 62 genes were up-regulated and eight were down-regulated at 12 hpi. 24 hpi, with 960 genes up-regulated while 505 genes were down-regulated. At 36 hpi, 411 genes were up-regulated, while 275 genes were down-regulated

***Gene ontology analysis of DGEs***

Major Gene Ontology (GO) assignments among up-regulated genes include regulation of transcription, DNA template (87), multi-organism process (68) and obsolete oxidation-reduction process (51) under Biological Process (BP); ATP binding (110), DNA-binding transcription factor activity (75) and protein binding (62) under Molecular Function (MF); and integral component of membrane (214), nucleus (176) and plasma membrane (119) under Cellular Component (CC). For down-regulated genes, they were obsolete

oxidation-reduction process (36), regulation of transcription, DNA-template (28) and multi-organism process (21) under Biological Process (BP); ATP binding (44), protein binding (33) and metal ion binding (29) under Molecular Function (MF); and integral component of membrane (134), nucleus (67) and chloroplast thylakoid membrane (66) under Cellular Component (CC) (Figure 3.2.2).

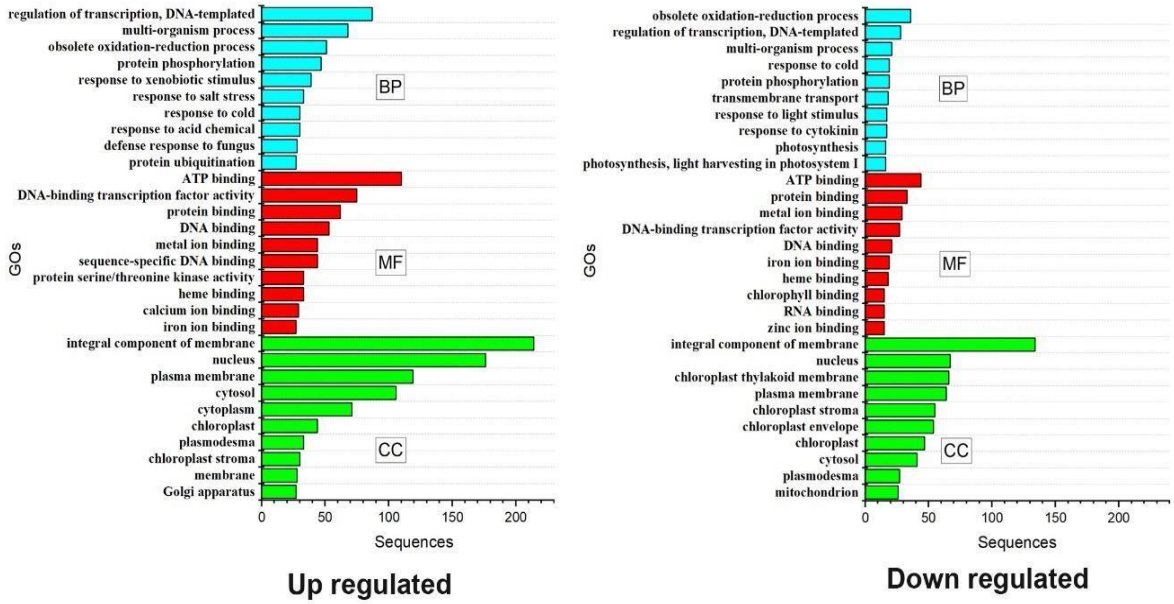


**Figure 3.2.2. Gene Ontology (GO) analysis of annotated DGEs of coconut biological process (BP), molecular function (MF), and cellular component (CC). The number of sequences can vary amongst the different classifications as numerous terms can describe a single gene product in the three classifications.**

### *Pathway analysis of differentially of DGEs*

KEGG Pathway analysis revealed pathway assignments for 1137 DGEs, which were mostly related to plant-pathogen interaction (ko04626), glycolysis/gluconeogenesis (ko00010), biosynthesis of cofactors (ko01240), pyruvate metabolism (ko00620), NOD-like receptor signalling pathway (ko04621), MAPK signalling pathway–plant (ko04016), toll and Imd signalling pathway (ko04624), plant hormone signal transduction (ko04075), toll-like receptor signalling pathway (ko04620) and phenylpropanoid biosynthesis (ko00940) among up-regulated genes. The main associated pathways for down-regulated genes are photosynthesis (ko00195), carbon fixation in photosynthetic

organisms (ko00710), photosynthesis - antenna proteins (ko00196), biosynthesis of cofactors (ko01240), plant hormone signal transduction (ko04075), NOD-like receptor signalling pathway (ko04621), porphyrin and chlorophyll metabolism (ko00860), phenylpropanoid biosynthesis (ko00940), glyoxylate and dicarboxylate metabolism (ko00630) and ribosome (ko03010).

***Primer designing***

The Primer3 software was used to design primers for qRT-PCR validation of 10 DEGs from coconut that were selected based on their expression profile (highly upregulated). These effectors included chitinase, cinnamyl alcohol dehydrogenase, WRKY transcription factor, mitogen-activated protein kinase (MAPK), transcription factor MYB2, GST6 protein, 1-aminocyclopropane-1-carboxylate oxidase, β-1,3-glucanase, calcium-dependent protein kinase and receptor-like serine/threonine-protein kinase. Details of the primers designed are provided in Table 3.2.4

**Table 3.2.4: Oligonucleotide primers designed for qRT-PCR validation of DEGs from coconut.**

| Sl.No. | Primer name | Description | Transcript ID | Primer Sequence (5'-3') | Expected amplicon size (bp) |
|---|---|---|---|---|---|
| 1. | Cn20418f | Chitinase | CNTR.20418.1 | CGAGACCGGATATCTGTGCT | 132 |
| | Cn20418r | | | TTCCAGGTCAGCTGAAGAGG | |
| 2. | Cn2426f | Cinnamyl alcohol dehydrogenase | CNTR.2426.1 | CGTCTGGCTACATTGCTTCC | 141 |
| | Cn2426r | | | AGTGCAGTCTCTCATTGGCT | |
| 3. | Cn2673f | 1-aminocyclopropane-1-carboxylate oxidase | CNTR.26738.1 | AAGAATCCCCACTCTTCGCA | 125 |
| | Cn26738r | | | TCTCCAGAACCACCTTTGCT | |
| 4. | Cn19756f | GST6 protein | CNTR.19756.1 | CTGGACGGGCAAATTTAGCA | 125 |
| | Cn19756r | | | TGCCGACGTACTCATAGACC | |
| 5. | Cn19878f | Transcription factor MYB2 | CNTR.19878.1 | CCTTGGACTGCAGAGGAAGA | 143 |
| | Cn19878r | | | GGACGGAGATAGTTGAGCCA | |
| 6. | Cn16620f | β-1,3-glucanase | CNTR.16620.3 | CCAGCAAAATGTGAAGGCCT | 145 |
| | Cn16620r | | | TTGTAGGCCAGCTGAGGAAA | |
| 7. | Cn17751f | Mitogen-activated protein kinase | CNTR.17751.1 | TGACGTTCAATCCCTCCACA | 126 |
| | Cn17751r | | | GCTGCTCAAAGTCGAAGGAG | |
| 8. | Cn5961f | Calcium-dependent protein kinase | CNTR.5961.1 | GGACTTACATGGTGCCAAGG | 122 |
| | Cn5961r | | | ATCAATGTCACGGCCCAAAC | |
| 9. | Cn27017f | WRKY transcription factor | CNTR.27017.1 | CCAGGATCGCATTCAGAACG | 111 |
| | Cn27017r | | | AGTAGTTCCTCGGGTTTGGG | |

| | | | | | |
|---|---|---|---|---|---|
| 10. | Cn15631f | Receptor-like serine/threonine-protein kinase | CNTR.15631.1 | CAGGATAGAGCCGAGGACAG | 115 |
| | Cn15631r | | | TGGCACTTCTCTCGCTACAA | |

### *qRT-PCR validation*

For quantitative real-time PCR, ten differentially expressed genes were selected (highly up-regulated) from the RNA-seq data in the hc vs. hpi group to confirm the transcriptome-based observations and the reproducibility of RNA-seq data. The expression levels of 10 chosen genes were significantly different at various phases of infection, with all of them being up-regulated. Chitinase, cinnamyl alcohol dehydrogenase, WRKY transcription factor, mitogen-activated protein kinase, and transcription factor MYB2 all showed a dynamic rise in expression with each time period. While GST6 protein showed high expression at 12 hpi, 1-aminocyclopropane-1-carboxylate oxidase, β-1,3-glucanase, calcium-dependent protein kinase, and receptor-like serine/threonine-protein kinase showed high expression at 24 hpi (Figure 3.2.3). A significant correlation was observed between qRT-PCR data (r = 0.703) and RNA-seq data (p-value = 0.023). Overall, the qRT-PCR results revealed patterns that were comparable to those seen in the RNA-seq of these genes, while the fold-change values were different.

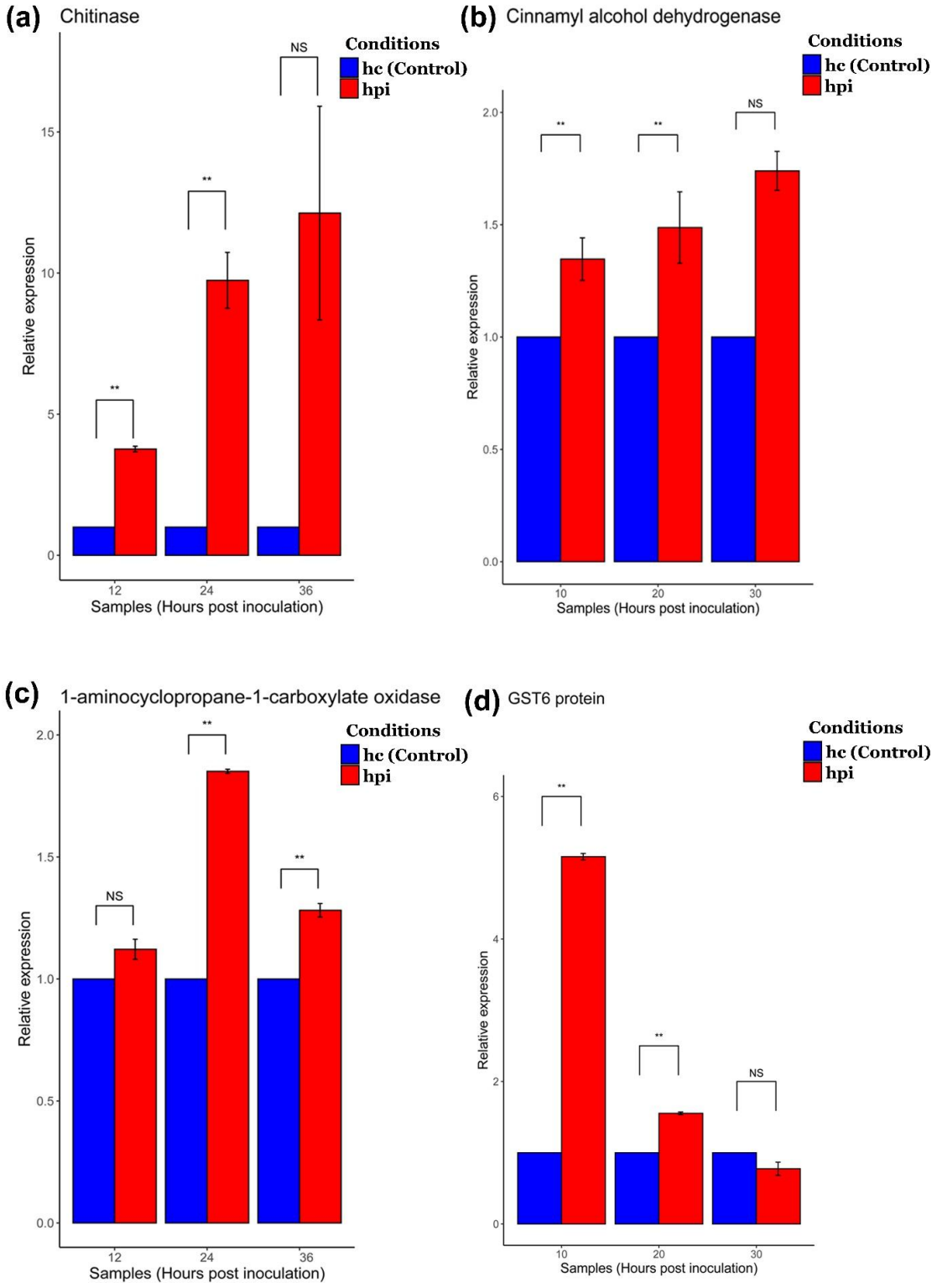
(a) Chitinase
Conditions
hc (Control)
hpi
NS
**
**
Relative expression
0
5
10
15
12
24
36
Samples (Hours post inoculation)
(b) Cinnamyl alcohol dehydrogenase
Conditions
hc (Control)
hpi
**
**
NS
Relative expression
0.0
0.5
1.0
1.5
2.0
10
20
30
Samples (Hours post inoculation)
(c) 1-aminocyclopropane-1-carboxylate oxidase
Conditions
hc (Control)
hpi
NS
**
**
Relative expression
0.0
0.5
1.0
1.5
2.0
12
24
36
Samples (Hours post inoculation)
(d) GST6 protein
Conditions
hc (Control)
hpi
**
**
NS
Relative expression
0
2
4
6
10
20
30
Samples (Hours post inoculation)

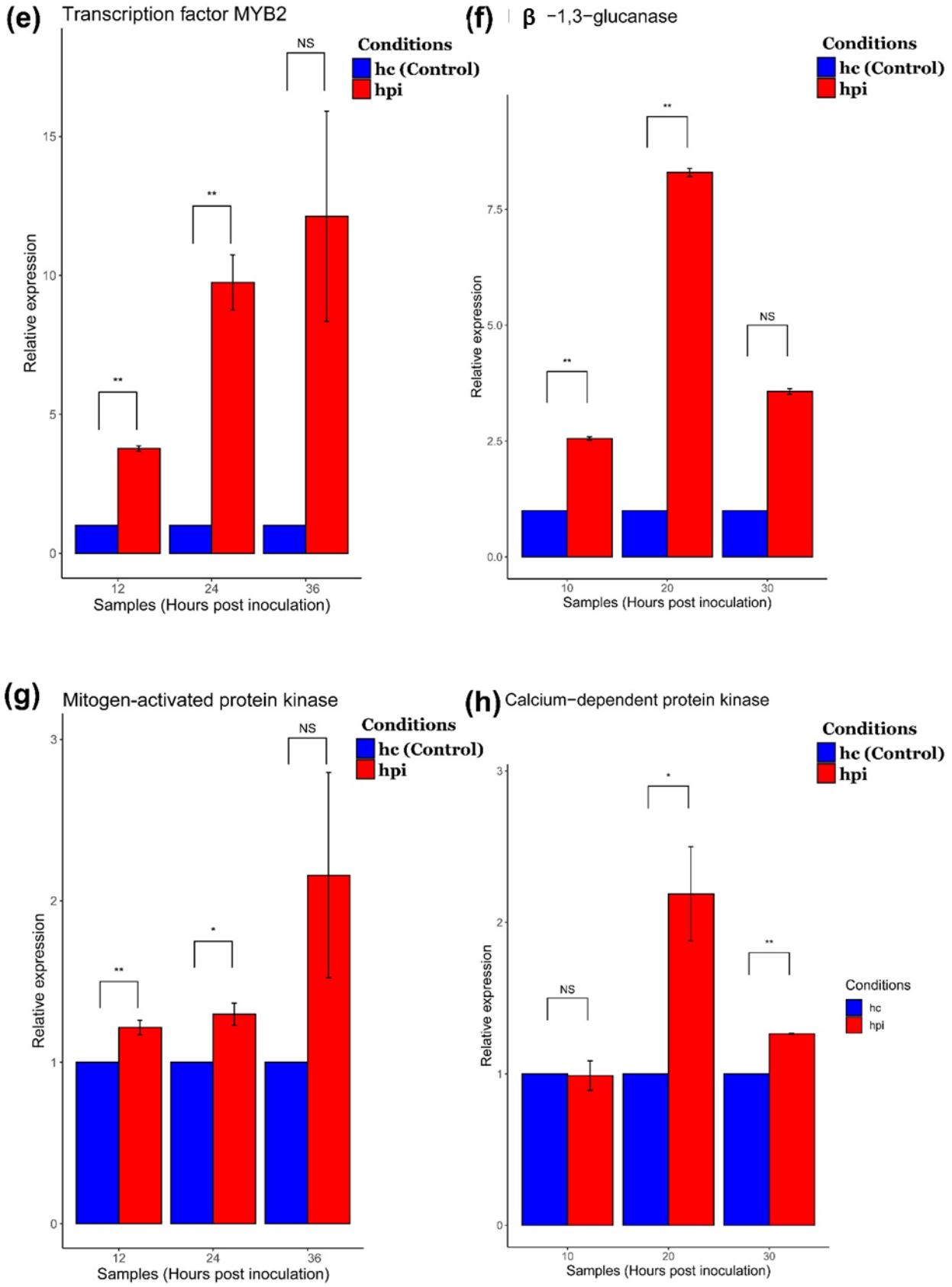
(e)
Transcription factor MYB2
Conditions
hc (Control)
hpi
NS
**
**
Relative expression
0
5
10
15
12
24
36
Samples (Hours post inoculation)
(f)
β −1,3−glucanase
Conditions
hc (Control)
hpi
**
**
NS
Relative expression
0.0
2.5
5.0
7.5
10
20
30
Samples (Hours post inoculation)
(g)
Mitogen-activated protein kinase
Conditions
hc (Control)
hpi
NS
*
**
Relative expression
0
1
2
3
12
24
36
Samples (Hours post inoculation)
(h)
Calcium−dependent protein kinase
Conditions
hc (Control)
hpi
*
NS
**
Relative expression
0
1
2
3
10
20
30
Samples (Hours post inoculation)
Conditions
hc
hpi

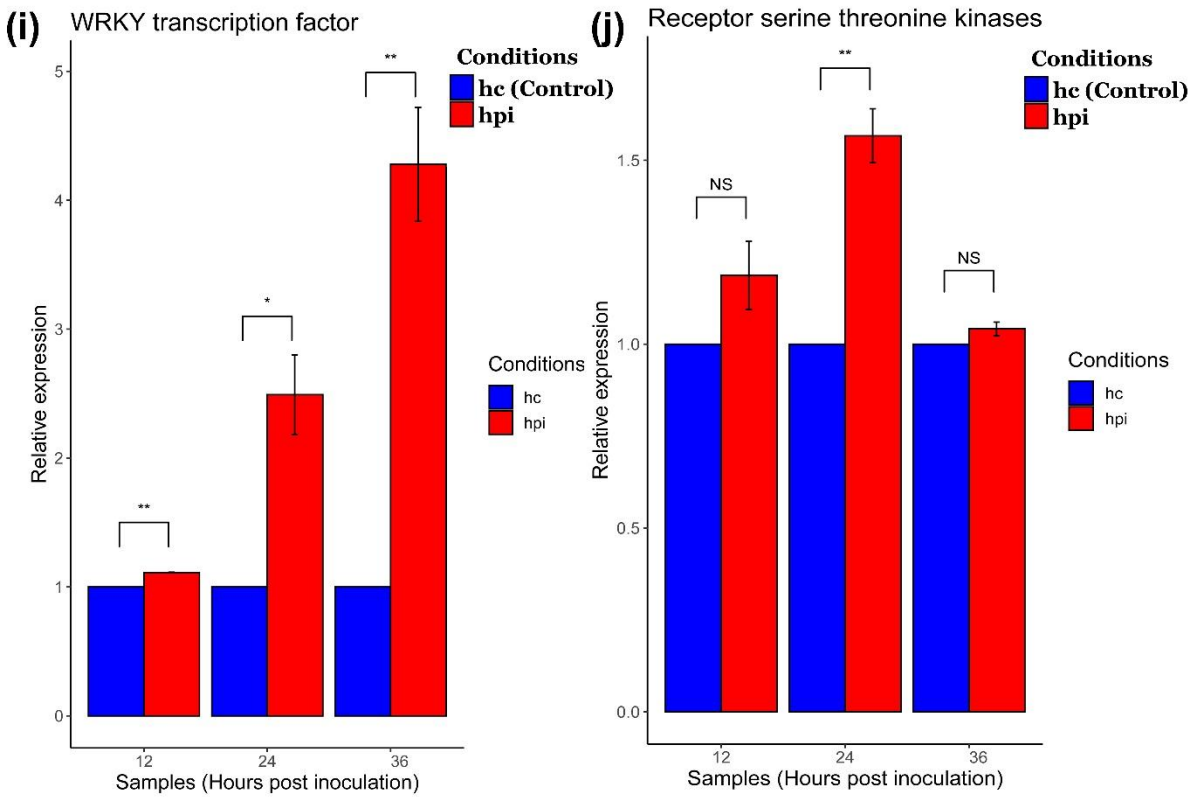


**Figure. 3.2.3. Validation of DEGs using quantitative reverse transcriptase polymerase chain reaction (qRT-PCR) (a to j); First, the relative expression values were normalised using *CneIF-4γ* as an internal reference, and the expression value of 'hc' was set to 1. The data is based on three replicates on average. For triplicates, the error bars reflect the standard error (SE). Asterisks represent significant differences in Student's t-test when compared to the inoculated sample (hpi) (* P=0.05; ** P=0.01; NS= Not statistically significant).**

### *Differential gene expression* (DEG) *in P. palmivora*

The DEG at 12 hpi in *P. palmivora* revealed that 621 genes were up-regulated and 312 were down-regulated. Twenty-four hours post-inoculation, 1754 genes were up-regulated, and 671 were down-regulated. Also, 1807 genes were up-regulated at 36 hpi, and 630 were down-regulated.

### *Gene ontology analysis of DGEs*

Major GOs assignments among up-regulated genes include transmembrane transport (227), obsolete oxidation-reduction process (190), peptide transport (174) [BP]; and ATP binding (632), protein binding (436), metal ion binding (288) [MF]; and integral component of membrane (1092) cytosol (635), nucleus (323) [CC]. For down-regulated genes, they were obsolete oxidation-reduction process (46), protein phosphorylation (36), peptide transport (33) [BP]; and ATP binding (132), protein binding (92), metal ion binding (59) [MF]; and integral component of membrane (242), cytosol (115), nucleus (68) [CC] (Figure 3.2.4).

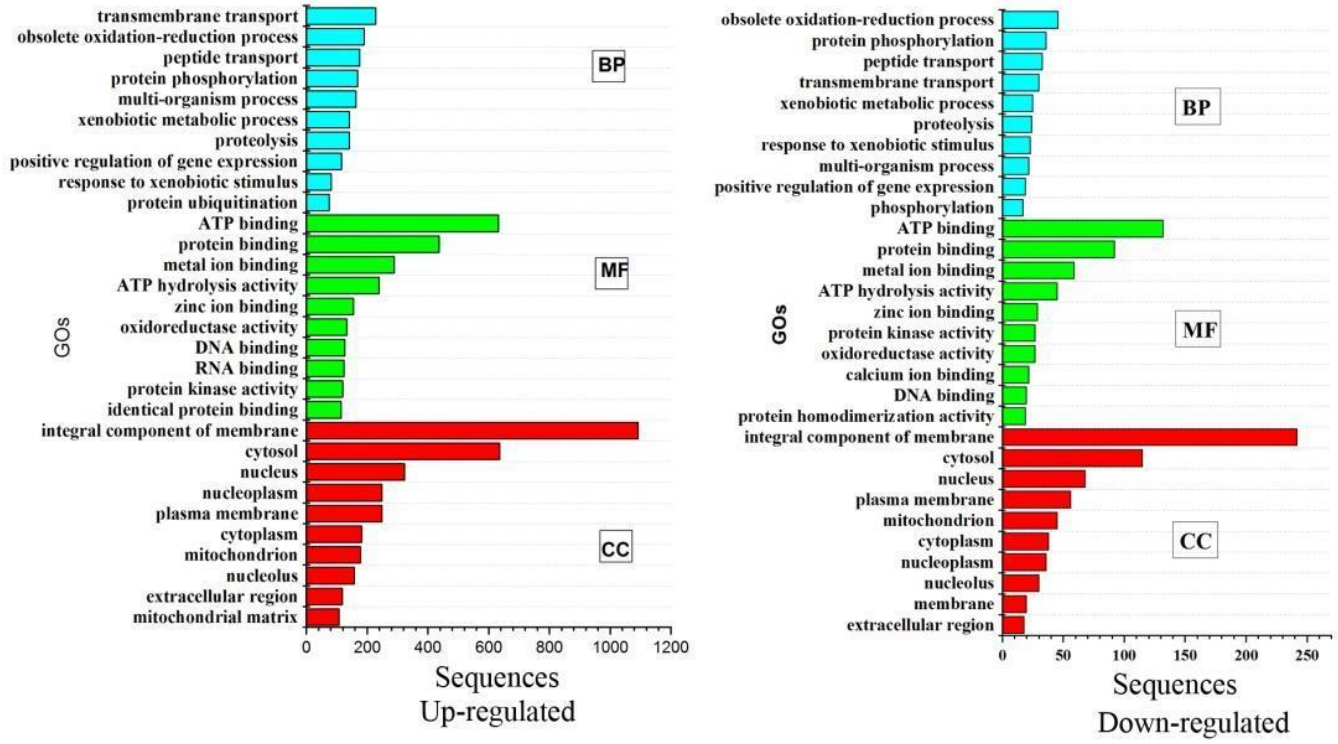


**Figure 5.3.4: Gene Ontology (GO) analysis of annotated DGEs of *P. palmivora*- biological process (BP), molecular function (MF), and cellular component (CC). The number of sequences can vary amongst the different classifications as numerous terms can describe a single gene product in the three classifications**

***Pathway analysis of DGEs***

KEGG pathway analysis revealed that 786 Up-regulated genes were linked with 280 KEGG pathways, which are mostly related to the biosynthesis of cofactors (ko01240), lysosome (ko04142), starch and sucrose metabolism (ko00500), protein processing in the endoplasmic reticulum (ko04141) and glycolysis/gluconeogenesis (ko00010) and valine, leucine and isoleucine degradation (ko00280). The down-regulated DGEs were mainly associated with the biosynthesis of cofactors (ko01240), MAPK signalling pathway (ko04010), autophagy - animal (ko04140), pyruvate metabolism (ko00620), thermogenesis (ko04714), glycolysis/gluconeogenesis (ko00010) and endocytosis (ko04144). Dioxin and xylene degradation were the most enriched KEGG pathways at 12 hpi. The three most substantially up-regulated KEGG pathways at 24 hpi were xylene, dioxine degradation, and valine leucine and isoleucine degradation. Fatty acid degradation and valine leucine and isoleucine degradation were also the top two enriched KEGG pathways at 36 hpi

## 3.3. To develop a transcriptome database of coconut-*Phytophthora palmivora* interactions

### 3.3.1. Introduction

Dual RNA-sequencing (RNA-seq) permits simultaneous analysis of host and pathogen transcriptomes and contributes to knowledge of the molecular changes occurring initially at the site of infection and during disease progression by overcoming host defence mechanisms (Attard *et al*., 2008). Genomic and transcriptome resources can provide valuable insights into the host-pathogen interaction dynamics, pathogen detection and development of reliable and sensitive disease diagnostics assays. For several *Phytophthora* spp., transcriptomes, whole genomes, and ESTs have been generated by next-generation sequencing platforms in the last decade. Dedicated databases have been developed to make the data accessible to researchers worldwide. National Center for Genome Resources, in collaboration with The Ohio State University-Ohio Agricultural Research and Development Center (OSU-OARDC), have developed a '*Phytophthora*–Plant Interaction Database (PFGD)' which contains gene expression profiles of *P. infestans* and *P. sojae* and provides functional annotation and gene expression dynamics of these two oomycetes (Gajendran *et al*., 2009). The 'Fungal

Secretome Database is a significant secretory proteins repository of fungi, including oomycetes, and provides secretome information on 525 species with 587 datasets (Choi *et al.*, 2010). Ye *et al.* (2011) analyzed the gene expression profiles in *P. sojae* and established a digital platform repository. The next-generation sequencing and EST datasets of interactions of *P. sojae* with its host soybean were made available as a database by Tripathy *et al.* (2012). 'Plant Cell Wall-Degrading Enzymes (PCWDEs) Database' contains information about plant cell wall-degrading enzymes produced by oomycetes such as *P. infestans, P. capsici, P. ramorum* and *P. sojae* (Choi *et al.*, 2013). The 'Pathogen-Host Interactions (PHI-base) database is a comprehensive storehouse of experimentally confirmed virulence/pathogenicity/effector genes from different pathogens (Urban *et al.*, 2015). Panda *et al.* (2018) established 'EumicrobeDBLite', a user-friendly extensive genomic support system and sequence analysis stage for oomycete pathogens.

Curating and establishing a coconut-*Phytophthora* interaction database, based on the results of the dual transcriptome data generated to gain insights into the coconut- *P. palmivora* interactions, will form an excellent resource for researchers working in this area to store and distribute information on host-pathogen transcriptome dynamics.

### 3.3.2. Methodology

***Design and development of the database architecture***

The web application is based on a WAMP server, comprising a Client tier (Client browser), a Middle tier (Apache webserver with PHP interpreter) and a Database tier (MYSQL DBMS). The user-friendly interface has been developed using PHP, which is an open-source server-side scripting language. The schema of database development is given in Figure 3.3.1. and database architecture in Figure 3.3.2.

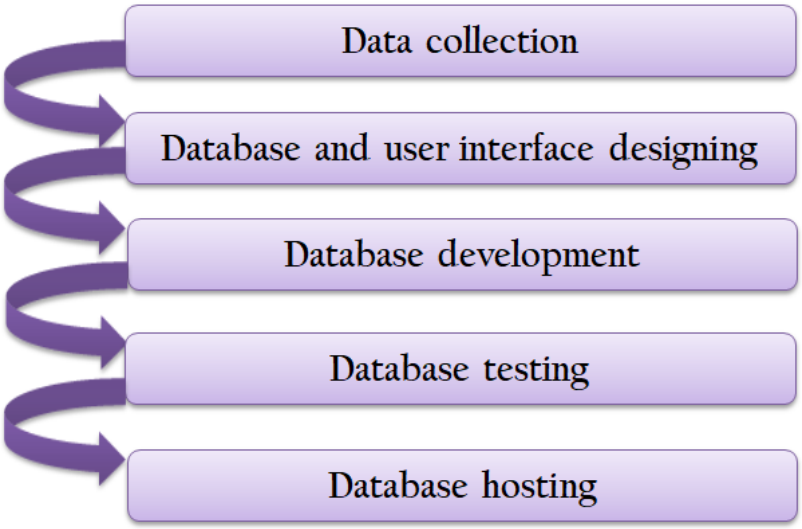


**Fig. 3.3.1. Schematic representation of database development**

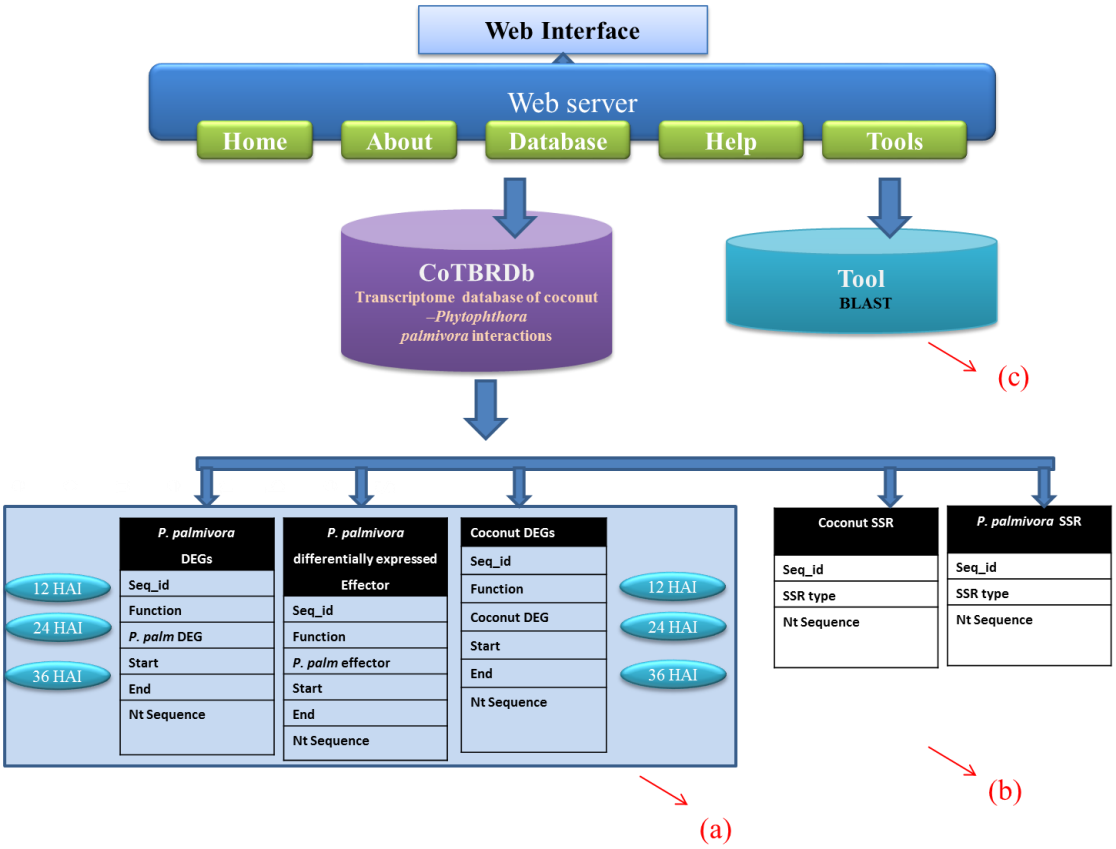


**Figure 3.3.2. Database architecture; (a) Detailed information about DEGs in coconut and *P. palmivora*; (b) information about predicted SSRs in coconut and *P. palmivora* transcriptome; (c) Alignment tool locally installed and user can search their query.**

### 3.3.3. Results

The 'Coconut Transcriptome Database for Bud Rot Disease' (available at http://14.139.181.165/cotbrdb) is an online, freely available database for research purposes and non-commercial uses to provide browsable access to the dual transcriptome data of coconut-*P. palmivora* interactions. The set of differentially expressed genes and functional SSRs (simple sequence repeats) at three phases, *viz.*, 12hpi, 24hpi and 36 hpi, are stored in the MYSQL database for custom search and retrieval of data using PHP scripts. Need-based customized queries can be generated from the web interface, allowing users to search the SSR marker information in the MySQL database.

The Coconut Transcriptome Database for Bud root disease has been organized into five tabs, *viz.*, **Home, About, Database, Help,** and **Tool**.

***Home*** tab provides brief information about the bud rot disease of coconut, the pathogen, gene expression and functional annotation of control and infected sample data at three different stages, *viz.*, 12, 24 and 36 hpi, design and development architecture of the database and purpose of database development.

***About tab*** includes detailed information about the bud rot disease, *P. palmivora* and the developed database

***Database tab*** This tab contains information about Transcripts, SSRs and Effectors. The database will provide general and statistical information (Accession id, Log2FC, p-value, Expression and Description) about the DEGs of the selected organism at a particular time of induction. Detailed information will be generated by clicking each accession id. The Database tab includes two sub-menus such as Transcript search and SSR search.

***Transcript search*** includes functional and expression-level gene annotation. Functional level gene provides information about comparative analysis of gene function at three stages. It shows the available gene information of specific genes at different points, *i.e.*, 12, 24 and 36 hpi**.**

***SSR search*** includes simple sequence repeats information of transcriptome data of coconut and *P. palmivora*. It shows gene id wise mined simple and compound SSR markers, including the Gene ids, SSR type, SSR motif, SSR kind, copy number, length, start position, and position.

The ***Help tab*** contains the exploring process of the database. The screenshot of the database home page and different tabs are given in Figure 3.3.3.

Coconut Transcriptome
Database for Bud Rot Disease
ICAR-Central Plantation Crops Research Institute
An ISO 9001:2015 Certified Institute
Home
About
Database
Help
Tool
CoTBRDb-Coconut Transcriptome Database for Bud Rot Disease
Bud rot caused by Phytophthora palmivora, is one of the most lethal diseases of coconut palm, causing decay of the terminal bud and surrounding tissues. It affects both mature and juvenile palms, with the latter being more susceptible to the disease. Phytophthora deliverseffectors, a type of secretory proteins in to the host cells, which promote the infection process. These effectors belong to different classes viz., RxLR, CRN, NLI have developed Coconut Transcriptome for the researchers.
Organism
Coconut
Feature
TRANSCRIPTS
Stage
12 HPI
24 HPI
36 HPI
Click here to view results
113 records matched
Accession id
Log2FC
pvalue
Expression
Description
CNTR.1019.1
1.644998003
0.0144
NS
Beta-1-4-xylidase
1.926310298
0.0486
Protein DETIFICATION
transcription factor WRKY24

**Fig. 3.3.3. Screenshot of the webpage and different tabs of coconut transcriptome database for coconut bud rot disease**

## 3.4. To identify effector genes involved in pathogenicity from the transcriptome data

### 3.4.1. Introduction

Phytopathogenic oomycetes are economically significant due to the immense threat they pose to the production and productivity of crops. The life cycle of pathogenic oomycetes is extremely complex- while biotrophic oomycetes colonize the living host tissues and receive nutrients from the living tissues, necrotrophic oomycetes invade and strip nutrients from dead host cells and end up consuming the host tissues. The third type, hemibiotrophic oomycetes, shows both phases during the infection process, i.e., they are biotrophic initially and later follow a necrotrophic phase (Lo *et al.*, 2015).

Oomycetes generally synthesize and secrete effector proteins during the initial phase of infection- many of the effectors are translocated to the cytoplasmic matrix of the host cells and end up modifying the host's defence. In a successful infection, effectors can suppress the immune system of the plant host. Besides, they modify the infected host tissues, turning them into a source of nutrients needed by the phytopathogen for its growth and development (Wang and Jiao, 2019). Effectors encompass a broad range of molecules possessing varied biological functions. The *Phytophthora* apoplastic effector repertoire includes cell wall-degrading enzymes, enzyme inhibitors, toxins and elicitins, unique 10-kD peptides etc. (Baillieul *et al.*, 2003). In this section, we have mined the effector transcripts, which are differentially expressed during the initial phases of coconut-*Phytophthora* interactions and validated their expression pattern via quantitative real-time PCR (qRT-PCR).

### 3.4.2. Methodology

#### *Mining of expressed effector sequences from dual RNA-seq data*

The merged transcript file, obtained in fasta format after dual RNA-seq (Section 3.2) was taken, and BLASTx analysis was performed against the *P. palmivora* proteome database (UniProt Proteome ID: UP000237271). All sequences which showed hits to identified *P. palmivora* effectors were confirmed using EffectorP, a programme that employs machine learning to predict fungal and oomycete effector proteins.

### *Differential gene expression (DGE) analysis of effectors*

The transcript levels of each gene were calculated and normalized to mapped fragments, and fragments per kilobase of exon model per million reads mapped (FPKM) to compare the gene expression level in each sample. The Cuffdiff programme (http:/cole-trapnell-lab.github.io/cufflinks/cuffdiff/) was used to classify deferentially expressed genes and apply significant fold change at P<0.005 and false discovery rate (FDR) at 0.05 % was applied. The Hemi software (http://hemi.biocuckoo.org/) was used to build a heat map from expression data.

### *Validation of differentially expression effectors*

### *Designing of primers*

Ten differentially expressed effectors viz. (four secreted RXLR effector peptide protein, two extra-cellular protease inhibitor-EPI, two Necrosis-inducing Phytophthora protein-NPP, one elicitor and one crinkler family protein-CRN) chosen at random validation using quantitative real-time PCR (qRT-PCR). Gene-specific primers for the selected effectors chosen for validation were designed with Primer3 software (https://bioinfo.ut.ee/primer3-0.4.0/). Genes encoding the *P. palmivora* 40S ribosomal subunit S3A were selected as an internal control (Evangelisti *et al*., 2017).

### *qRT-PCR analysis*

Total RNA was extracted from frozen, axenically grown *P. palmivora* mycelium with sporangia (M) and *P. palmivora* inoculated coconut leaflets harvested at 12, 24 and 36 hpi using the RNA kit (Macherey Nagel). RNA samples were reverse transcribed to generate first-strand complementary DNA (cDNA) using the PrimeScript™ (DSS Takara Bio India Pvt. Ltd.) First Strand cDNA Synthesis Kit, according to the manufacturer's instructions. qRT-PCR tests were done with 1 µl of cDNA (50 ng) first-strand and StepOne™ Real-Time PCR System SYBR Green I Master mix, according to the manufacturer's instructions (Applied Biosystems Thermo Fisher Scientific). Also, the 40S ribosomal gene (*G40S*) was taken as an internal control for *P. palmivora* (Ali *et al*., 2017), and qRT-PCR runs were conducted using three technical replicates for each sample. The 'Web Agri Stat Package (WASP)' program's completely randomised design (CRD) ANOVA technique was used to evaluate the data. The means obtained were then compared using 'Fisher's Least Significant Difference (LSD)'. The Pearson correlation

test was used to examine the correlation between the two sets of data corresponding to gene expressions acquired by RNA-seq and by RT-qPCR. R (version 4.1.2) https://www.r-project.org/; was used to generate plots.

### 3.4.3. Results

A total of 445 expressed effector transcripts were mined (Table 3.4.1.) from *Phytophthora palmivora* transcripts. The majority of the transcripts were seen to belong belonged to the RXLR class of effectors.

**Table 3.4.1. Predicted effectors in merged *P. palmivora* transcriptome**

| Sl. no. | Effector | Description | Number of transcripts |
|---|---|---|---|
| 1. | RXLR | Secreted RXLR effectors | 227 |
| 2. | NPP | Necrosis-inducing proteins | 46 |
| 3. | EPI | Extracellular protease inhibitor /Kazal-like protease inhibitor | 14 |
| 4. | CRN | Crinkler (CRN) proteins | 87 |
| 5. | ELI | Elicitor/Elicitin protein | 71 |
| | | **Total** | **445** |

A heat map comparison revealed similar effector gene expression profiles between 24 hpi and 36 hpi samples. Few effector transcripts had higher FPKM at 36 hpi when compared to the 24 hpi sample. Also, it indicates that the initial stage of infection (12 hpi) and M showing different clusters but major differences. This shows that the pathogen underwent a noticeable molecular change during the early stages of infection (Figure 3.4.1).

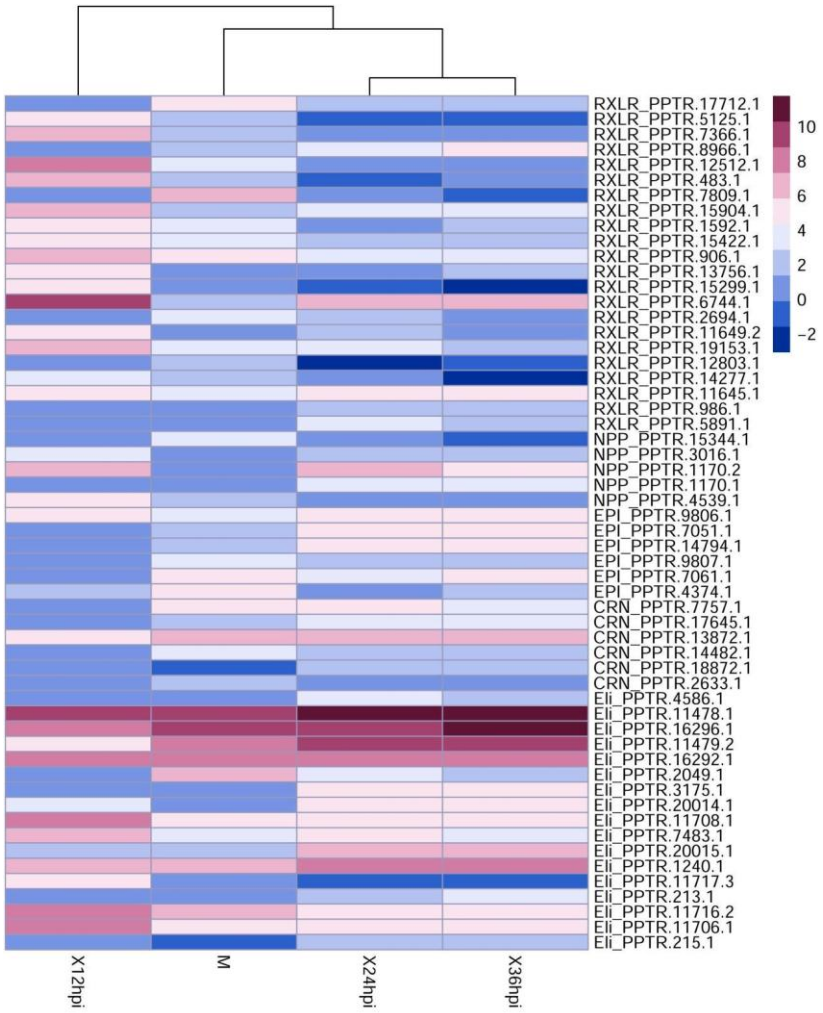


**Fig. 3.4.1. FPKM (log10) based heat map of transcripts at control (M) and 12, 24 and 36hpi**

**Differential gene expression (DGE) analysis of effectors**

DGE analysis was undertaken to identify significantly differently expressed effectors in *P. palmivora* during different times of infection in *in vitro* inoculated coconut leaflets. The Cuffdiff programme was used to detect differentially expressed genes around 12 hpi, 24 hpi, 36 hpi and M. Genes with a fold change ≥ 2 and a False Discovery Rate (FDR) < 0.05 were considered as significantly differentially expressed genes (DEGs). We observed that 21, 13 and 16 effectors were up-regulated at 12 hpi, 24 hpi and 36 hpi, respectively (Table 3.4.2).

**Table 3.4.2. Differential expressed effector transcripts in *P. palmivora***

| Effector classes | M vs 12 hpi | | M vs 24 hpi | | M vs 36 hpi | |
|---|---|---|---|---|---|---|
| | Up-regulated | Down-regulated | Up-regulated | Down-regulated | Up-regulated | Down-regulated |
| RXLR | 11 | - | 3 | 3 | 3 | 4 |
| NPP | 3 | - | 3 | - | 3 | - |
| EPI | 2 | - | 3 | 2 | 3 | 1 |
| CRN | 1 | - | 1 | - | 1 | - |
| Elicitin | 4 | - | 3 | 1 | 6 | 1 |
| **Total** | 21 | - | 13 | 6 | 16 | 6 |

### *Validation of differentially expression effectors*

### *Primer designing*

The Primer3 software was used to design primers for qRT-PCR validation of 10 effector transcripts selected based on their expression profile (highly up-regulated). These effectors included three secreted RXLR effectors (rxl6744, rxl8966 and rxl12512), two necrosis-inducing *Phytophthora* protein-NPP (npp1170 and npp4539), two extra-cellular protease inhibitors-EPI (epi14794 and epi4551), one crinkler family protein-CRN (crn18872) and two elicitors (eli11478 and eli3175). Details of the primers designed are provided in Table 3.4.3.

**Table 3.4.3. Oligonucleotide primers designed for qRT-PCR validation of differentially expressed effectors**

| Sl. no. | Primer name | Description | Transcript ID | Primer Sequence (5'-3') | Expected amplicon size (bp) |
|---|---|---|---|---|---|
| 1. | rxl6744f | Secreted RXLR effector peptide protein | PPTR. 6744.1 | TCGTCTGCGTTATTCGTCTG | 150 |
| | rxl6744r | | | CGCTGACCTTCGTCTTCTTC | |
| 2. | rxl8966f | Avr3a family secreted RXLR effector peptide protein | PPTR. 8966.1 | CGCTCCTCTGTTGAGGAAAC | 180 |
| | rxl8966r | | | GGTGGTCGCCCTATACTTTG | |
| 3. | rxl12512f | Secreted RXLR effector peptide protein | PPTR.12512.1 | CTCTTGCTTGCCTTTGTTCC | 175 |
| | rxl12512r | | | ATGACTCCGATGACCTCGAC | |
| 4. | npp1170f | Necrosis-inducing protein NPP1 | PPTR.1170.2 | GGAGTCTCTTTCCCGTAGCC | 189 |
| | npp1170r | | | CAAGGGTAGGTGGGCTATCA | |
| 5. | npp4539f | Necrosis-inducing protein NPP8 | PPTR.4539.1 | GACGCTGTACATGACCGAGA | 151 |
| | npp4539r | | | ACCCTCAAGCTACGACGAGA | |
| 6. | epi14794f | Epi6- protease inhibitor | PPTR.14794.1 | GCTTCCATTTCGCACTTGTT | 152 |
| | epi14794r | | | CGTGACAGCGACTCTAGCAA | |

| | | | | | |
|---|---|---|---|---|---|
| 7. | epi4551f | Kazal-like Extracellular Serine Protease Inhibitor | PPTR.4551.1 | GCTTGCTCCCAGCAAACTAC | 159 |
| | epi4551r | | | CCCCTCATTCACCAATAACG | |
| 8. | crn18872f | Crinkler (CRN) family protein | PPTR.18872.1 | CGATGTGCTTGGACAGAAAA | 152 |
| | crn 18872r | | | CAACTGATTCAATGCGATGG | |
| 9. | eli11478f | Elicitin | PPTR.11478.1 | TCGAAATCGGGCTACAACAT | |
| | eli11478r | | | ATTGCTGGTAGGGATGGTCA | 153 |
| 10. | eli3175f | Elicitin | PPTR.3175.1 | CTGCTGCCTCCAAGTCTAGT | 160 |
| | eli3175f | | | ACAAGGCCTACAGAGACCAC | |

The FPKM values of the selected effectors are given in Table 3.4.4

**Table 3.4.4. FPKM value of the effectors selected for validation**

| Sl. No. | Transcript ID | Effector | FPKM value | | | |
|---|---|---|---|---|---|---|
| | | | M | 12hpi | 24hpi | 36hpi |
| 1. | PPTR.6744.1 | RXLR | 3.80885 | 674.138 | 65.9915 | 65.2973 |
| 2. | PPTR.8966.1 | RXLR | 2.80474 | 0 | 15.3395 | 43.4731 |
| 3. | PPTR.12512.1 | RXLR | 12.1388 | 439.733 | 1.17724 | 1.27899 |
| 4. | PPTR.1170.2 | NPP | 1.6373 | 62.8168 | 58.2297 | 41.3364 |
| 5. | PPTR.4539.1 | NPP | 5.54403 | 38.65 | 1.63097 | 1.90353 |
| 6. | PPTR.14794.1 | EPI | 4.9703 | 0 | 41.3987 | 40.9269 |
| 7. | PPTR.4551.1 | EPI | 2.53217 | 278.523 | 31.726 | 33.4103 |
| 8. | PPTR.18872.1 | CRN | 0.398223 | 0 | 2.87702 | 3.92643 |
| 9. | PPTR.11478.1 | ELI | 923.966 | 555.79 | 2501.01 | 3495.82 |
| 10. | PPTR.3175.1 | ELI | 0.936169 | 0 | 30.4976 | 31.0843 |

***qRT-PCR analyses***

Quantitative RT-PCR was performed on 10 selected effector genes to confirm their differential expression pattern inferred from the RNA-seq data. All the genes were examined for expression analysis in three inoculation stages (12, 24 and 48 hpi), with *P. palmivora* mycelium (M) taken as control. Four of the selected effectors (rxl6744, rxl8966, rxl12512 and npp1170) showed similar expression patterns when compared with RNA-seq results with up-regulation of these effectors noticed in samples 12hpi

(Figure 3.4.3). Notably, the RXLR effector rxl6744 showed an enhanced expression pattern, which peaked at 24 hpi. In the initial stage of inoculation, necrosis-inducing effector npp1170 showed higher expression (12 hpi), with its expression decreasing at 36 hpi. Also, npp4539 showed an increasing expression pattern from 12 hpi to 36 hpi, with maximum expression at 36 hpi compared to the control. Effectors eli11706 crn18872, epi14794, and rxl8966, npp4539, epi14794 and eli3175 showed an increasing pattern of expression from 12hpi to 36 hpi. The expression of the effectors rxl12512, npp1170, and epi4551 was higher at 12 hpi. At 24 hpi, the expression of rxl6744, crn18872, and eli11478 rose. Additionally, the expression of rxl8966, npp4539, epi14794, and eli3175 peaked at 36 hpi (Figure 3.4.3**)**. The qRT-PCR data significantly correlated with the RNA-seq data. Overall, the qRT-PCR results revealed patterns that were comparable to those seen in the RNA-seq of these genes. However, the fold-change values were different.

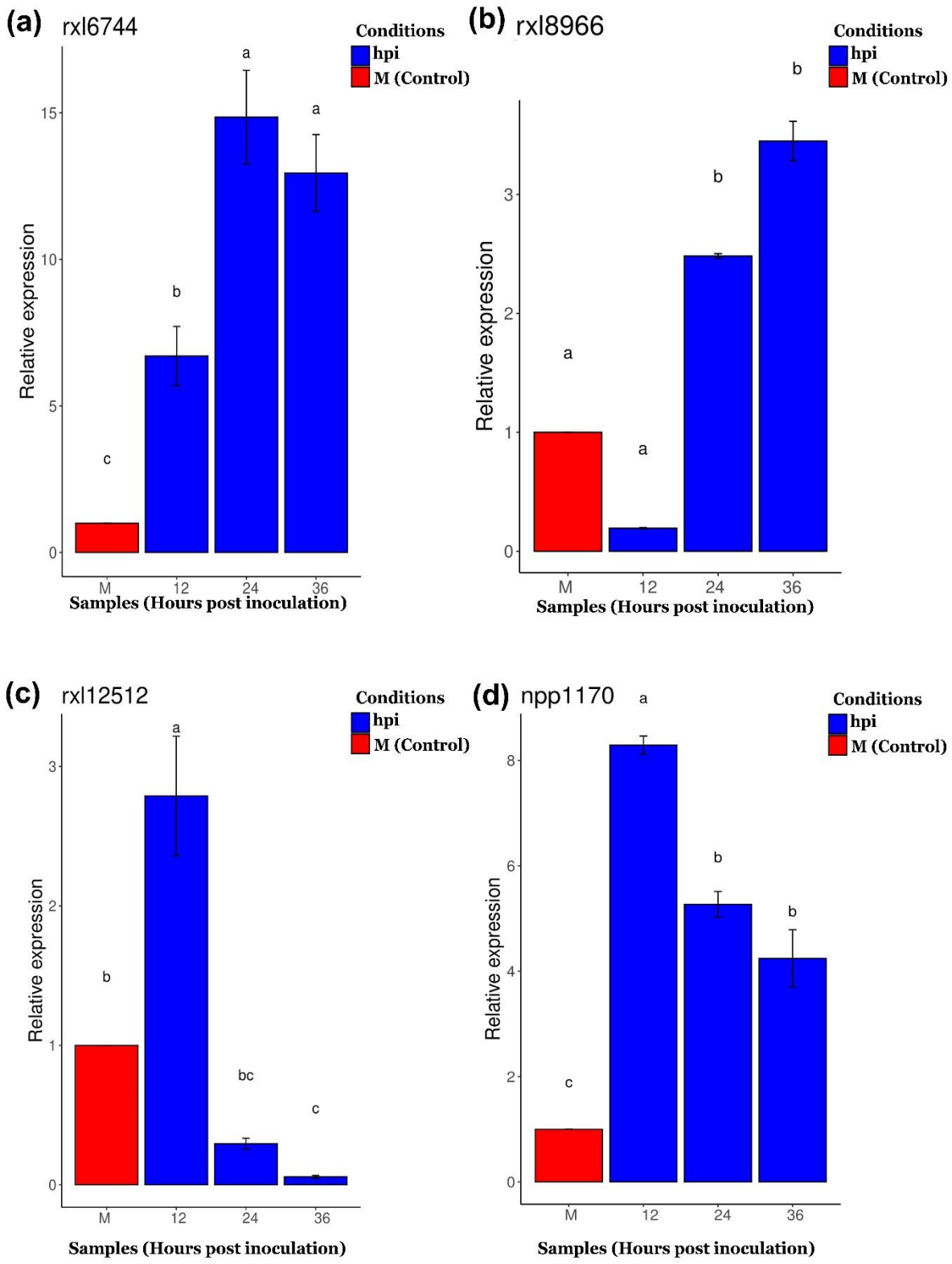
(a) rxl6744
Conditions
hpi
M (Control)
Relative expression
Samples (Hours post inoculation)
M
12
24
36
(b) rxl8966
(c) rxl12512
(d) npp1170

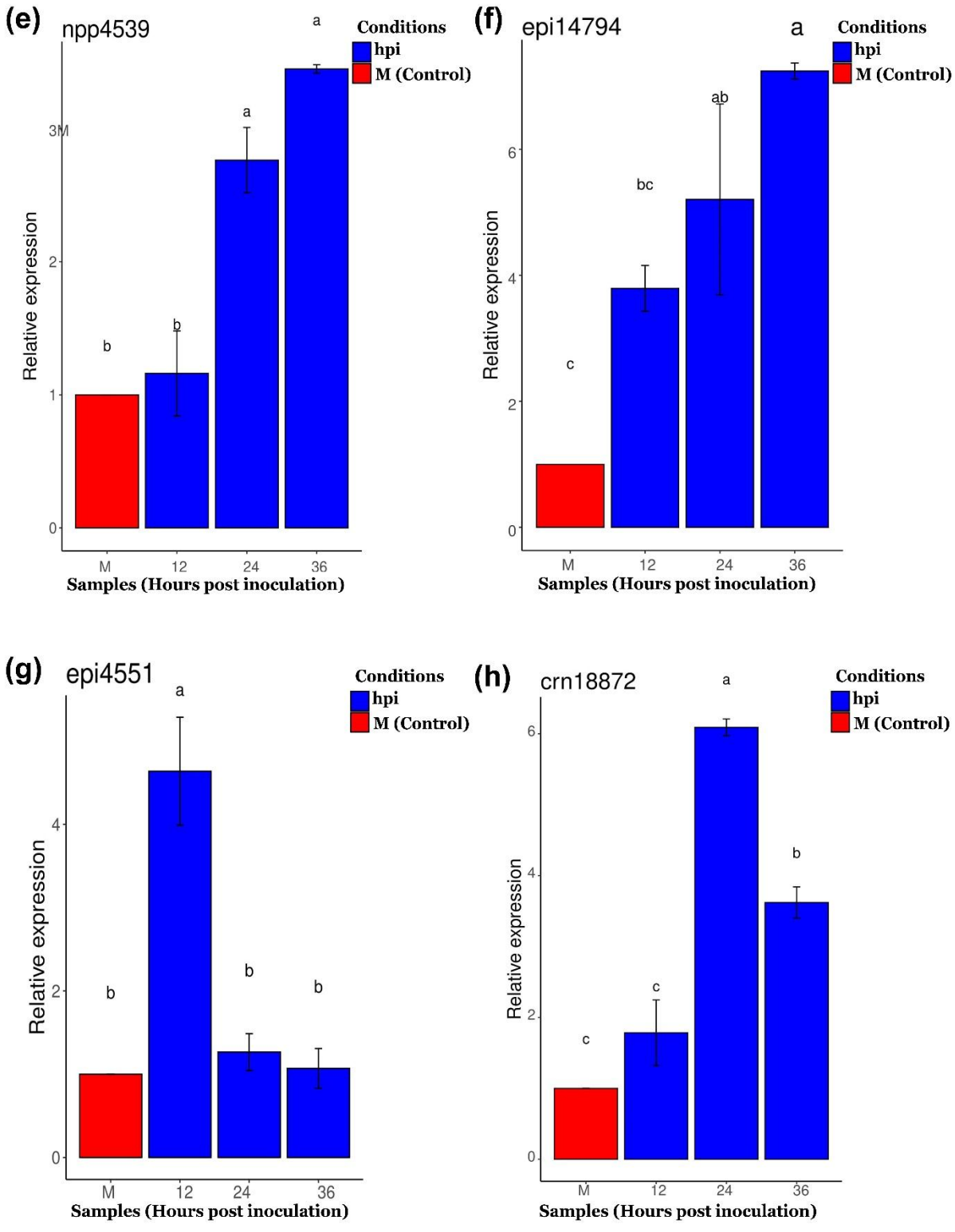
(e)
npp4539
Conditions
hpi
M (Control)
Relative expression
Samples (Hours post inoculation)
M
12
24
36
(f)
epi14794
(g)
epi4551
(h)
crn18872

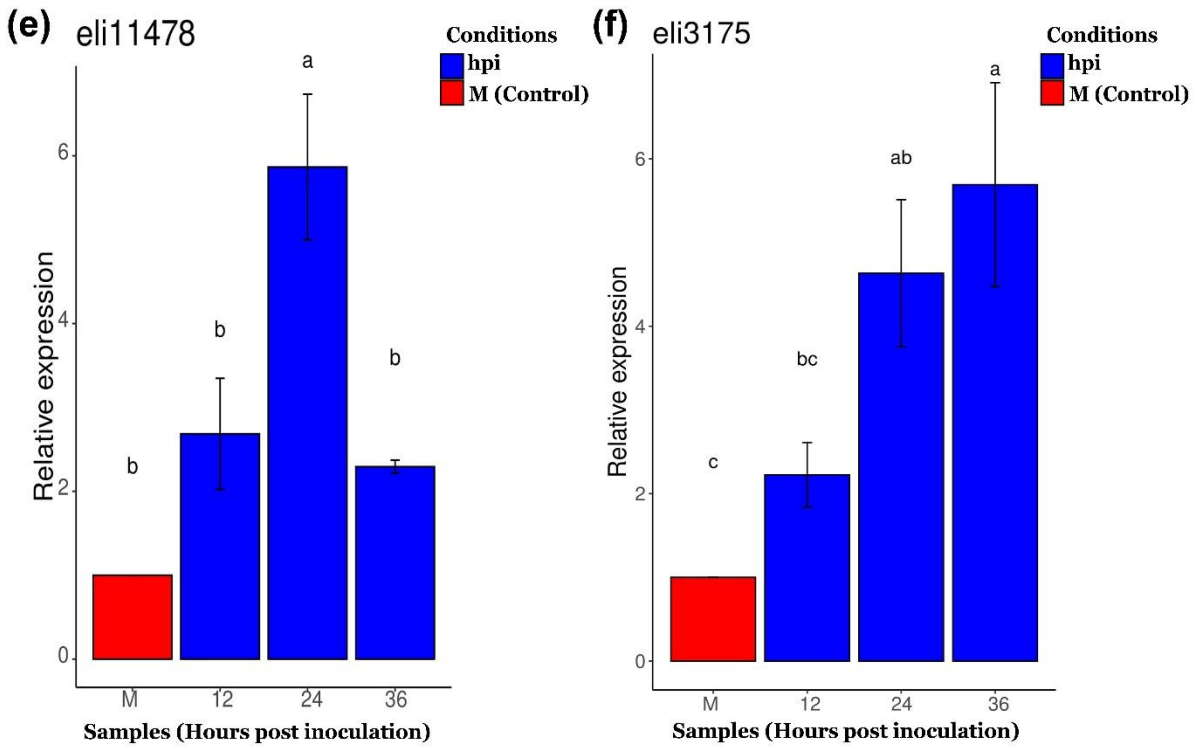


**Figure 3.4.3. qRT-PCR validation of the 10 selected effectors (a to j). The *P. palmivora* 40S ribosomal subunit S3A was selected as an internal control. The relative expression levels ($2^{-\Delta\Delta Ct}$) measured by qRT-PCR were compared to FPKM values ($Log^2FC$) from RNA-seq. One-way ANOVA and 'Fisher's Least Significant Difference (LSD)' post-hoc test for qRT-PCR data were performed, and significant differences ($P < 0.05$) are represented with a, b and c. For triplicates, the error bars reflect the standard error (SE).**

## 3.5. To identify ligands capable of targeting these pathogenicity factors by molecular docking studies

### 3.5.1. Introduction

*Phytophthora* spp. are economically significant phytopathogens as they affect the output and yield of a vast array of crops. These oomycetes secrete an arsenal of effector proteins which are known to modulate/overcome/suppress the plant's innate immunity machinery, thus facilitating the pathogen infection process (Selin *et al*., 2016). Decoding the structural and functional aspects of the effectors can enable a clear and precise understanding of how these phytopathogens can effectively colonise, infect, and replicate in their hosts. Effectors encompass a repertoire of biologically complex molecules which can function either at the host-pathogen interface ('apoplastic effectors') or inside the host cell ('cytoplasmic effectors') (Bozkurt *et al*., 2012). The latter harbour an additional host-targeting (HT) leader sequence, which is required for translocation across the host plasma membrane. The HT signal of many *Phytophthora* effectors is composed of a highly conserved N-terminal RXLR and a dEER motif further downstream, and these effectors are known as 'RXLR effectors'. The second major group of suspected cytoplasmic effectors is CRN or 'Crinkler effectors', devoid of the RXLR motif but possess a KxLFLAK motif instead (Schornack *et al*. 2010; Bozkurt *et al*. 2012).

Many bacterial phytopathogens, especially the Gram-negative bacteria, have been reported to inject effector proteins into plant cells utilizing the type3 secretion systems (T3SS). This process enables them to suppress host immunity and facilitate infection (Buttner, 2012). Therefore, disrupting these secretion systems could lead to the loss of virulence in these bacterial phytopathogens (Galan and Collmer, 1999), making them potential targets for screening and developing anti-virulence agents. Some studies targeting T3SS in bacterial phytopathogens include identifying phenolic (Khokhani *et al*., 2013) and salicylidene acyl hydrazide compounds (Yang *et al*., 2014) capable of partially or completely inhibiting T3SS in the fire blight pathogen *Erwinia amylovora*. Besides, phenolic compounds have been shown to significantly inhibit the T3SS of soft-rot pathogen *Dickeya dadantii* (Li *et al*., 2015) and the rice leaf blight pathogen *Xanthomonas oryzae* pv. *oryzae* (Fan *et al*., 2017; Tao *et al*., 2019). Zhou *et*

*al*. (2020) have recently reported the ability of small-molecule compounds to inhibit the T3SS of the crucifer black rot pathogen *Xanthomonas campestris* pv. *campestris*. Computational screening of phytochemicals from turmeric, garlic and neem for anti-fungal activities was performed against Avr3a11 effector in *Phytophthora capsici*. Alliin from garlic showed significant binding interaction with Avr3a11 (Rani *et al*., 2017). Taken together, these results provide potential leads for the development of effector targeting anti-virulence agents that could be used in disease control of the *Phytophthora palmivora*. In this section, structural studies on a few highly expressed effector proteins of *P. palmivora* were undertaken, followed by docking studies to find potential effector-targeting compounds.

### 3.5.2. Methodology

***Retrieval of nucleotide and protein sequences of selected virulence factors***

Five virulence factors of *P. palmivora*, based on their enhanced expression patterns assessed from dual RNA-seq data (Section 3.2) and qRT-PCR (Section 3.4), were used for this study. The selected proteins include (i) secreted RXLR effector protein (rxl6744), (ii) necrosis-inducing *Phytophthora* protein (npp1170), (iii) extracellular protease inhibitor (epi7051), (iv) crinkler family protein (crn18872) and (v) elicitin protein (eli11478) The effector transcript sequences were aligned with *P. palmivora* genome (NCBI ID: 66939) using BLASTn (Altschul *et al*., 1990). The aligned regions were retrieved from the *P. palmivora* genome using the 'getfasta' function in the BEDTools v2.29.2 suite. Gene prediction was carried out by using Fgenesh++ (http://www.softberry.com), and the full-length coding sequences (cds) of the selected virulence factors were retrieved.

***Protein sequence analysis of selected virulence factors***

Using the ExPASy-ProtParam tool (https://web.expasy.org/protparam/), the biochemical and biophysical properties, molecular weights (Mw), extinction coefficients, isoelectric points (pI), aliphatic indices (AI), instability indices and grand hydropathy averages (GRAVY) of the predicted protein sequences of the virulence factors were analysed. Domain similarity analysis was carried out using the Pfam 33.1 server, and GOR V (https://npsa-prabi.ibcp.fr/NPSA/npsa_gor4.html) was used to determine the secondary structure of the protein. In SignalP-5.0

(http://www.cbs.dtu.dk/services/SignalP/), predicted proteins were submitted to predict the presence and position of signal peptides. Also, TargetP 1.1 http://www.cbs.dtu.dk/services/TargetP/) was used for the prediction of the subcellular location of the six proteins. Apoplastic effector localisation was predicted using APOPLASTP (http://apoplastp.csiro.au/).TMHMM - 2.0 (http://www.cbs.dtu.dk/services/TMHMM-2.0/) was used to identify the transmembrane helices in proteins

***Three-dimensional (3-D) structure prediction of the proteins***

Determination of the 3-D structures of the six proteins was performed using the fold recognition ('threading') method since homology-based modelling could not be performed due to a lack of template structures in the Protein Data Bank (PDB). The Phyre 2 server (http://www.sbg.bio.ic.ac.uk/~phyre2/html/page.cgi?id=index) was used to predict the protein's 3D structure and ModRefiner server (https://zhanglab.ccmb.med.umich.edu/ModRefiner/) was used to optimise the structures predicted. Ramachandran plot validation was done on the predicted structure using the SAVES server (https://servicesn.mbi.ucla.edu/SAVES/) and Maestro (https://www.schrodinger.com/).

***Molecular docking studies***

Through literature searches, 14 compounds (Table 3.5.1) reported previously to possess anti-fungal properties against phytopathogens were selected for *in silico* screening against the six virulence factors. Phytochemicals from *Curcuma longa* (β-Elemene, Curcumenol, Curcumin, Curcumol, Curdione, Curzerene, Germacrone and Isocurcumenol) were studied inhibitory activity against *Fusarium graminearum* (Chen *et al*., 2018). Akter *et al*. (2019) studied and identified the antifungal action of zederone and furanodienone against *Fusarium solani*. The inhibitory activity of miconazole, ornidazole, penthiopyrad and sulfaphenazole against several fungal and microbial pathogens was analysed by Abrigach *et al*. (2018).

The structures of the 14 compounds were docked against the binding sites of the predicted structures of the virulence factors by Autodock vina (http://vina.scripps.edu/). The appropriate AutoDock-Vina input files were prepared using AutoDock software (http://autodock.scripps.edu/). File preparation by AutoDock involves removing water molecules and adding polar hydrogen atoms. The docking

results were visualised and analysed using the academic edition of the Schrödinger Maestro Suite (https://www.schrodinger.com/).

**Table 3.5.1. The 14 compounds selected for docking studies against the *P. palmivora* virulence factors**

| Sl. No. | Compound name | PubChem ID | References |
|---|---|---|---|
| 1. | β-Elemene | 6918391 | Ciqiong *et al.* (2017) |
| 2. | Curcumenol | 167812 | Ciqiong *et al.* (2017) |
| 3. | Curcumin | 969516 | Ciqiong *et al.* (2017) |
| 4. | Curcumol | 14240392 | Ciqiong *et al.* (2017) |
| 5. | Curdione | 6441391 | Ciqiong *et al.* (2017) |
| 6. | Curzerene | 572766 | Ciqiong *et al.* (2017) |
| 7. | Germacrone | 6436348 | Ciqiong *et al.* (2017) |
| 8. | Isocurcumenol | 10399139 | Ciqiong *et al.* (2017) |
| 9. | Furanodienone | 6506548 | Akter *et al.* (2019) |
| 10. | Zederone | 101286196 | Akter *et al.* (2019) |
| 11. | Miconazole | 4189 | Abrigach *et al.* (2018) |
| 12. | Ornidazole | 28061 | Abrigach *et al.* (2018) |
| 13. | Penthiopyrad | 11388558 | Abrigach *et al.* (2018) |
| 14. | Sulfaphenazole | 5335 | Abrigach *et al.* (2018) |

### 3.5.3. Results

***Primary sequence analysis***

The predicted lengths of the amino acid sequences of the five selected virulence factors ranged from rxl1612 to crn18872 (Table 3.5.2).

**Table 3.5.2. Information on the six selected virulence factors**

| Sl. No. | Transcript ID | Virulence factor | Description | *P. palmivora* genome scaffold | No. of amino acids |
|---|---|---|---|---|---|
| 1. | PPTR. 8872.1 | crn18872 | Crinkler family protein (CRN), | VOQZ01001885.1 | 459 |
| 2. | PPTR. 7051.1 | epi7051 | Necrosis-inducing *Phytophthora* protein (NLP\NPP), | VOQZ01000695.1 | 171 |
| 3. | PPTR. 1170.1 | npp1170 | Extracellular protease inhibitor (EPI), | VOQZ01000087.1 | 214 |
| 4. | PPTR.6744.1 | rxl6744 | Secreted RXLR effector protein (RXLR) | VOQZ01000706.1 | 136 |
| 6. | PPTR. 11478.1 | eli11478 | Elicitor protein (Elicitine) | VOQZ01001163.1 | 198 |

The ExPASy-ProtParam programme predicted different physic-chemical properties of the effector proteins (Table 3.5.3). The instability indices revealed that three proteins, including crn18872, epi7051, and rxl6744, whereas npp1170 and eli11478 were unstable.

**Table 3.5 3. Predicted physicochemical properties of the six selected virulence factors**

| Sl. No. | Virulence factor | Number of amino acids | Molecular weight (Da) | Theoretical pI | Total number of atoms | Instability index | Aliphatic index | Grand average of hydropathicity (GRAVY) |
|---|---|---|---|---|---|---|---|---|
| 1. | crn18872 | 459 | 51771.17 | 6.25 | 7300 | 27.61 | 86.58 | -0.303 |
| 2. | epi7051 | 171 | 18991.04 | 4.94 | 2591 | 31.19 | 49.71 | -0.793 |
| 3. | npp1170 | 214 | 23788.00 | 5.09 | 3315 | 42.74 | 80.70 | -0.243 |
| 4. | rxl6744 | 136 | 15419.42 | 9.30 | 2154 | 27.34 | 78.24 | -0.593 |
| 5. | eli11478 | 198 | 20172.54 | 3.95 | 2776 | 41.48 | 64.70 | -0.116 |

***Secondary structure prediction***

Using the GOR V online tool, the secondary structures of the five selected virulence factors were determined. The results revealed that random coils were the dominant secondary structure in all virulence factors, except in rxl1612 and rxl6744, where the predominant secondary structures were alpha-helices (Table 3.5.4).

**Table 3.5.4. GOR V predicted the secondary structure of the six selected virulence factors**

| Sl. No. | Virulence factors | Alpha-helices (Hh) | Extended-strands (Ee) | Random coils (Cc) |
|---|---|---|---|---|
| 1. | crn18872 | 176 (38.34%) | 86 (18.74%) | 197 (42.92%) |
| 2. | epi7051 | 31 (18.13%) | 25 (14.62%) | 115 (67.25%) |
| 3. | npp1170 | 80 (37.38%) | 40 (18.69%) | 94 (43.93%) |
| 4. | rxl6744 | 66 (48.53%) | 15 (11.03%) | 55 (40.44%) |
| 5. | eli11478 | 17 (8.59%) | 37 (18.69%) | 144 (72.73%) |

### *Domain analysis*

The functional domains of the *P. palmivora* virulence factors were predicted using the Pfam database. AAA ATPase domain (PF13191) was found in crn18872 with a very low E-value (0.26). Kazal-type serine protease inhibitor domain and Necrosis inducing protein domain were found in epi7051 and npp11701 proteins, respectively. RXLR phytopathogen effector protein domain was found in rxl6744. Elicitin and PT repeat domains were found in eli11478 (Table 3.5.5).

**Table 3.5.5. Pfam analysis of the virulence factors**

| Sl. No. | Proteins | Significant Pfam-A Matches | | | |
|---|---|---|---|---|---|
| | | Family | Pfam ID | Domain Description | E-value |
| 1. | crn18872 | AAA_16 | PF13191 | AAA ATPase domain | 0.26 |
| 2. | epi7051 | Kazal_2 | PF07648 | Kazal-type serine protease inhibitor domain | 9.6e-06 |
| 3. | npp1170 | NPP | PF05630 | Necrosis-inducing protein domain | 1.4e-72 |
| 4. | rxl6744 | RXLR | PF16810 | RXLR phytopathogen effector protein domain | 3.1e-19 |
| 5. | eli11478 | Elicitor | PF00964 | Elicitin domain | 5.3e-20 |
| | | PT | PF04886 | PT repeat | 2.1e-06 |

### *Characterisation of the effector proteins*

SignalP prediction of epi7051 revealed a Sec signal peptide (Sec/SPI) with a cleavage site between position 19 and 20 (THA-DN) with a high likelihood of 0.92699. Signal peptides were also detected in npp1170 [ with a probability of 0.99 with the cleavage site between 19-20 (AQA-DA)] and eli11478 [ possessing Ala20-Ala21 (SDA-AP) cleavage site, with a probability of 0.84399]. SignalP prediction of crn18872 revealed a Sec signal peptide (Sec/SPI) with a cleavage site between position 17 and 18 (AFS-VR) with a high likelihood of 0.75. The cleavage site of rxl6744 was between 25 and 26 (SNA-DQ), with a probability of 0.3502. Apoplastic localization of the effector was predicted using APOPLASTP. The proteins npp1170, epi7051 and eli11478 were found to be apoplastic effectors, while rxl6744 and crn18872 were found to be non-apoplastic effectors. Results of TMHMM prediction revealed that all proteins were localized outside the transmembrane region.

**Tertiary structure prediction and validation**

The tertiary structure prediction of the virulence proteins was carried out by Phyre 2, and the structures were refined. The refined structures were found to be stable, and >88% of amino acids were placed in favoured regions of the Ramachandran plot (Table 3.5.6.).

**Table 3.5.6. Prediction and validation of the three-dimensional structures of the five virulence factors**

| Sl. No. | Effectors | Structural details | | | Ramachandran plot validation | | |
|---|---|---|---|---|---|---|---|
| | | Helices | Strands | Turns | Favoured region | Allowed region | Disallowed region |
| 1. | crn18872 | 17 | 15 | 58 | 295 (88.7 %) | 25 (6.1%) | 21 (5.2%) |
| 2. | epi7051 | 4 | 11 | 22 | 145 (96.6%) | 1 (0.7%) | 4 (2.7%) |
| 3. | npp1170 | 5 | 15 | 23 | 169 (98.4%) | 3(1.6%) | 0 (0.0%) |
| 4. | rxl6744 | 6 | 0 | 7 | 128 (94.0%) | 6 (4.5%) | 2 (1.5%) |
| 5. | eli11478 | 8 | 3 | 24 | 155 (96.3%) | 6 (3.7%) | 0 |

| | Predicted structure | Ramachandran plot |
|---|---|---|
| crn18872 | 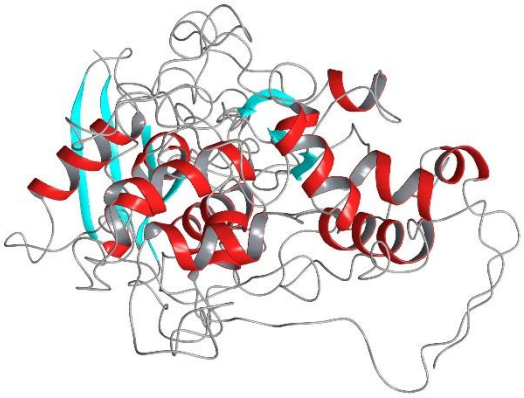 | 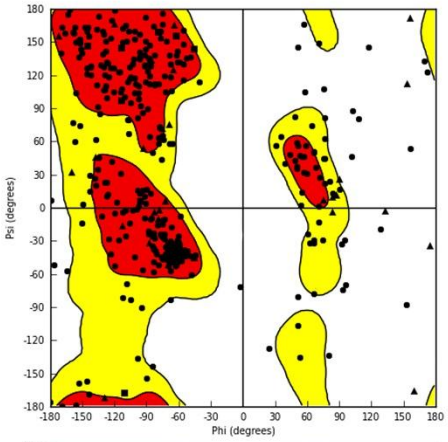 |
| epi7051 | 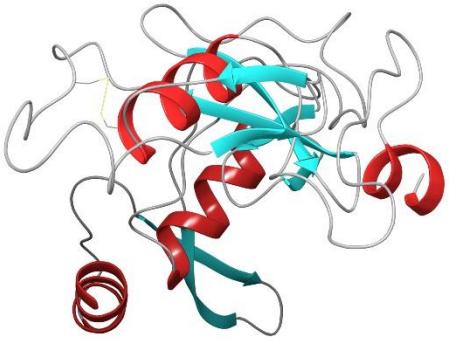 | 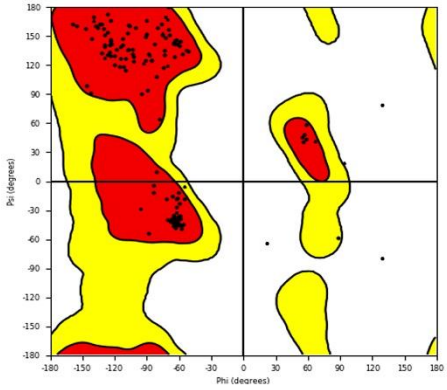 |
| npp1170 | 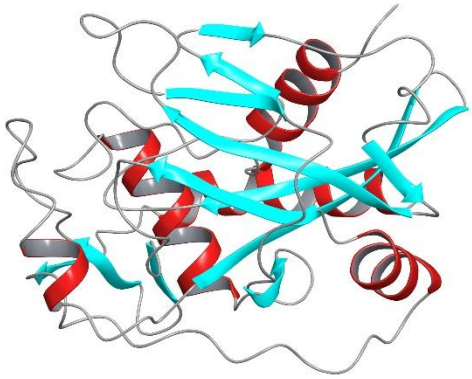 | 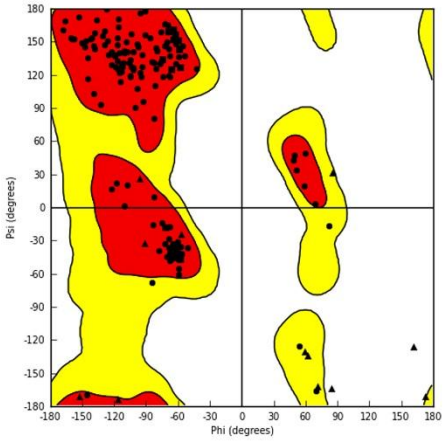 |

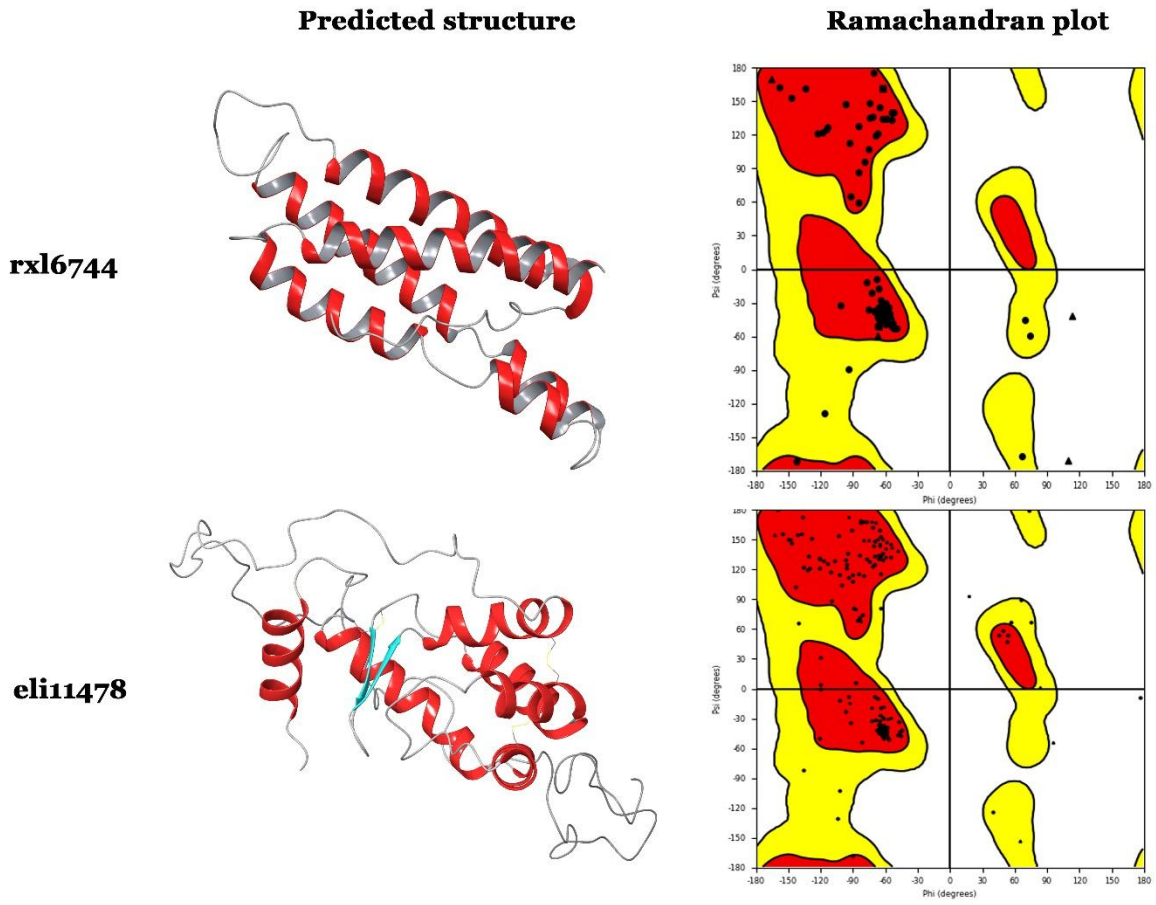


**Figure 3.5.1 Predicted structures of the five virulence factors and their Ramachandran plot validation**

## Molecular docking

The docking analysis of the five virulence factors with each of the 14 compounds revealed that curcumin and curdione showed better affinity to bind with the active site of the virulence proteins (Figure 3.5.2). The interaction of curcumin with epi7051, eli11478,rxl6744 and crn18872 proteins showed better affinity through molecular docking analysis. The best binding affinity was found to be -6.2 Kcal/mol, -7.4 Kcal/mol and -7.8 Kcal/mol. crn18872, eli11478 and epi7051 had only one hydrogen (H) bond with curcumin. Curcumin showed a good affinity with rxl6744, and binding affinity was found to be -6.2 Kcal/mol. Curdione displayed better binding energy with npp1170 (-8.4 Kcal/mol), and there was a single H bond between npp1170 and curdione (Table 3.5.7).

## Table 3.5.7. Docking analysis of virulence proteins showing best hits

| Sl. No. | Virulence proteins | Compounds showing best hits in docking | Docking score (Kcal/mol) | Hydrogen bonding | | | |
|---|---|---|---|---|---|---|---|
| | | | | No. of H bonds | Atoms in virulence protein | Atoms in compounds Used for docking | Distance (Å) |
| 1. | crn18872 | Curcumin | -7.8 | 1 | GLU145 (O) | H | 1.91 |
| 2. | epi7051 | Curcumin | -6.2 | 2 | TYR124 (H) | O | 2.32 |
| | | | | | TYR120 (H) | O | 2.21 |
| 3. | npp1170 | Curdione | -8.4 | 0 | - | - | - |
| 4. | rxl6744 | Curcumin | -6.2 | 0 | - | - | - |
| 5. | eli11478 | Curcumin | -7.4 | 1 | ARG67 (H) | O | 2.8 |

| | Interaction complex image | Ligand interaction diagram |
|---|---|---|
| **crn18872 + Curcumin** | 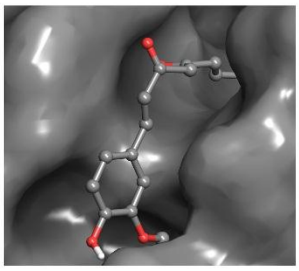 | 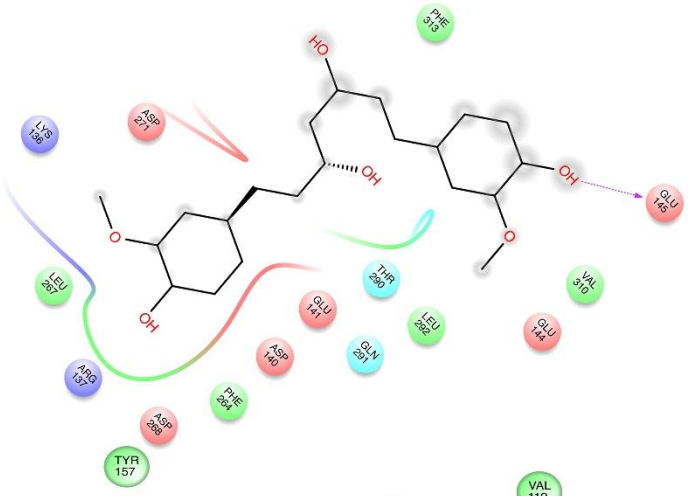 |
| **epi7051 + Curcumin** | 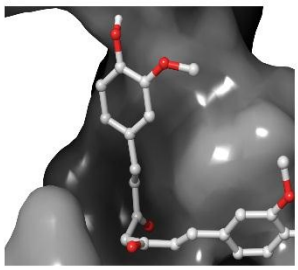 | 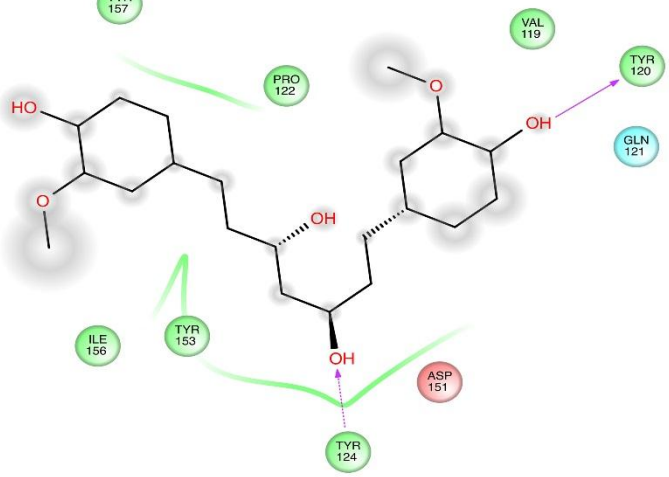 |
| **npp1170 + Curdione** | 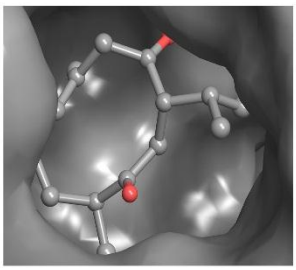 | 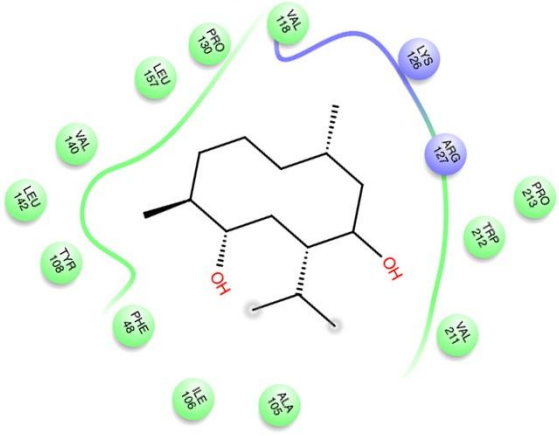 |

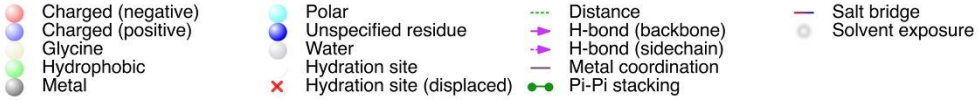

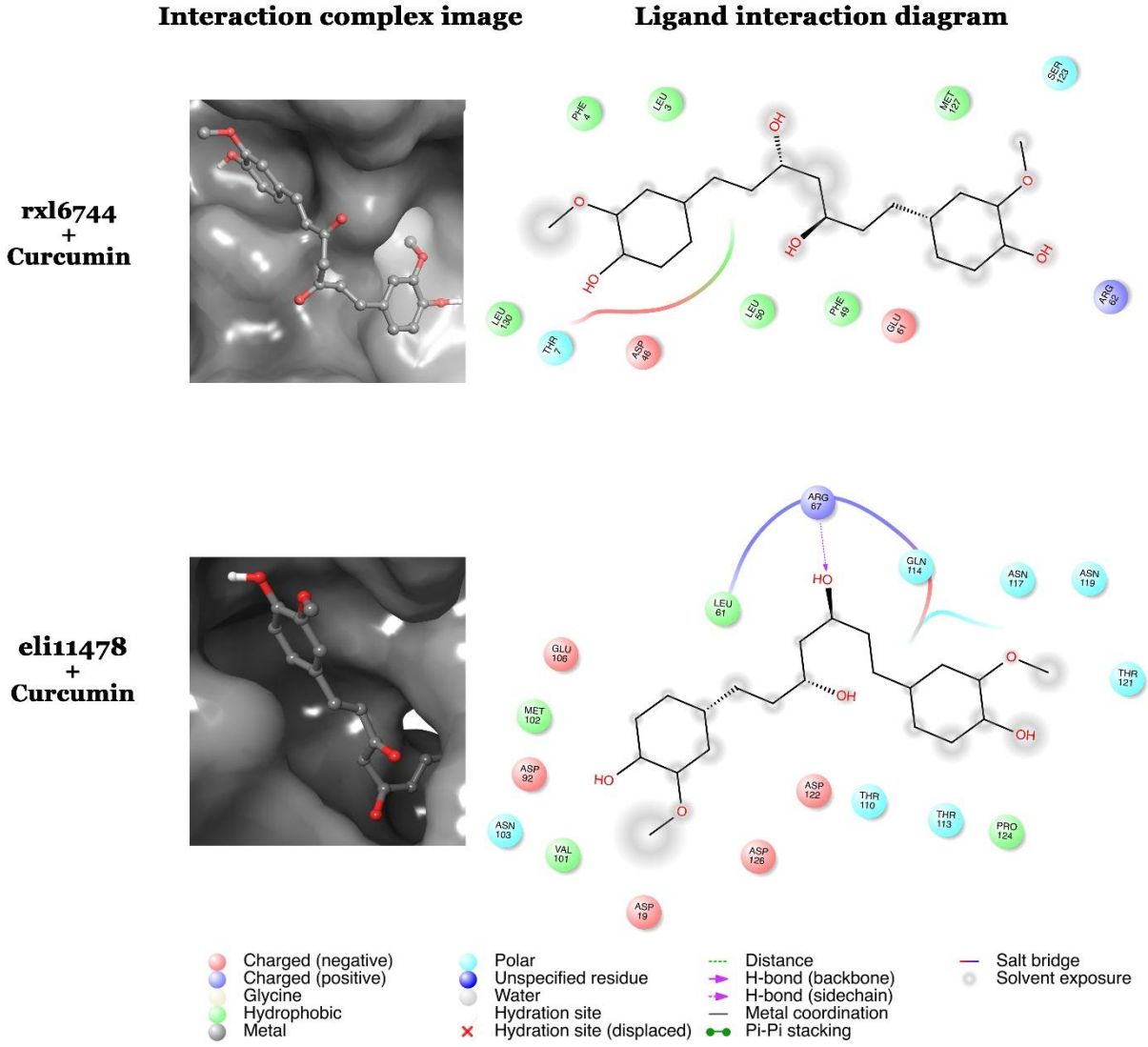


**Figure 3.5.2. Lead compounds interacting with virulence proteins and the complexes formed. Ligand interaction diagrams are shown on the right.**

## 4. SUMMARY AND CONCLUSION

Diseases are an ever-increasing threat to crops and necessitate the development of research tools for a species that often may have only a few pre-existing resources. Bud rot, caused by *Phytophthora palmivora,* is one of the major lethal diseases of the coconut palm. It is a sporadic disease but can assume epidemic proportions occasionally. High risk is involved in carrying out studies of plant-pathogen interactions through field trials, especially in coconut. We have developed an *in vitro* assay, enabling easy and close monitoring of interactions occurring between *P. palmivora* and coconut during the course of infection by recreating the field infection process in the lab. Spindle leaves from adult coconut palms were surface sterilized and inoculated in basal Y3 medium in Petri plates. After a week in culture, the surface of the leaves was pricked and inoculated with a zoospore suspension of *P. palmivora* culture. Typical lesion development was noticed on the surface of the coconut leaves 12-24 hours after inoculating the pathogen. Electrolyte leakage assays and histological studies, using light and scanning electron microscopy, were also undertaken to study the viability of the leaflets and disease progression. The pathogen could be re-isolated from the infected regions, fulfilling Koch's postulates. The presence of the pathogen in the coconut leaflets was confirmed using PCR and RT-PCR with *Phytophthora*-specific primers. The novel assay developed through this study is rapid, space-effective, precise and inexpensive and could be utilized for detailed investigations of the qualitative interactions between coconut and *P. palmivora*.

To gain novel insights into *P. palmivora* pathogenesis, a time-resolved dual RNA-seq strategy, was utilized to simultaneously capture the gene expression patterns in the infecting oomycete (*P. palmivora*) and the infected host (coconut leaflets). Samples were taken at 12, 24 and 36 hpi. Un-inoculated, but pinpricked leaflets, served as controls (hc). RNA was also extracted from fungal mycelium (M). RNA-seq and the differential gene expression (DGE) analysis of coconut transcripts revealed 62 up-regulated genes and eight down-regulated genes at 12 hpi. DGE was mostly changed at 24 hpi, with 960 up-regulated and 505 down-regulated genes. At 36 hpi, 411 genes were up-regulated, while 275 genes were down-regulated.

The DGE analysis of *P. palmivora* transcripts at 12 hpi revealed 621 genes being up-regulated and 312 genes being down-regulated. Twenty-four hours post-inoculation, 1754 genes were up-regulated, and 671 were down-regulated. Also, 1807 genes were up-regulated at 36 hpi, and 630 were down-regulated. The expression pattern of 10 differentially expressed genes in coconut, *viz.*, chitinase, cinnamyl alcohol dehydrogenase, WRKY transcription factor, mitogen-activated protein kinase (MAPK), transcription factor MYB2, GST6 protein, 1-aminocyclopropane-1-carboxylate oxidase, β-1,3-glucanase, calcium-dependent protein kinase and receptor-like serine/threonine-protein kinase were validated via quantitative real-time PCR (qRT-PCR). Chitinase, cinnamyl alcohol dehydrogenase, WRKY transcription factor, mitogen-activated protein kinase, and transcription factor MYB2 all showed a dynamic rise in expression with each time period. While GST6 protein showed high expression at 12 hpi, 1-aminocyclopropane-1-carboxylate oxidase, β-1,3-glucanase, calcium-dependent protein kinase, and receptor-like serine/threonine-protein kinase showed high expression at 24 hpi.

DGE analysis of effectors revealed that 21, 13 and 16 effectors were up-regulated at 12, 24 and 36 hpi, respectively. The expression pattern of a few differentially expressed effectors (*viz.*, necrosis-inducing protein NPP, secreted RXLR effector, elicitor, crinkler family protein-CRN, and protease inhibitor-EPI) was validated via qRT-PCR. Four of the selected effectors (rxl6744, rxl8966, rxl12512 and npp1170) showed similar expression patterns when compared with RNA-seq results with up-regulation of these effectors noticed in samples 12hpi. Notably, the RXLR effector rxl6744 showed an enhanced expression pattern, which peaked at 24 hpi. In the initial stage of inoculation, necrosis-inducing effector npp1170 showed higher expression (12 hpi), with its expression decreasing at 36 hpi.

A coconut-*Phytophthora* interaction database was also created and hosted based on the results of this study. The set of differentially expressed genes and functional SSRs (simple sequence repeats) at the three-time points, *viz.*, 12, 24 and 36 hpi, are stored in the MYSQL database for custom search and retrieval of data using PHP scripts.

Structural studies on a few highly expressed effector proteins of *P. palmivora* were also undertaken, followed by docking studies to identify potential effector-

targeting compounds. Curcumin and curdione were identified as potential lead compounds which could be utilized in future studies to target and inactivate *P. palmivora* effectors.

This study, therefore, highlights the initial processes in molecular host-pathogen interactions in coconut and provides the first comprehensive reference transcriptome for coconut-*Phytophthora* interactions, allowing the preliminary identification of *P. palmivora* effector genes. It can serve as a valuable resource that can be leveraged to improve our understanding of coconut-oomycete interactions and facilitate future work towards controlling bud rot disease.

## 5. References


1) Abrigach, F., Rokni, Y., Takfaoui, A., Khoutoul, M., Doucet, H., Asehraou, A. and Touzani, R. (2018). *In vitro* screening, homology modeling and molecular docking studies of some pyrazole and imidazole derivatives. *Biomedicine & Pharmacotherapy*, **103**: 653-661.
2) Akter, J., Takara, K., Islam, M. Z., Hossain, M. A., Sano, A. and Hou, D. X. (2019). Isolation and structural elucidation of antifungal compounds from *Curcuma amada*. *Asian Pacific Journal of Tropical Medicine*, **12**(**3**), 123.
3) Ali, S.S., Shao, J., Lary, D.J., Kronmiller, B.A., Shen, D., Strem, M.D., Amoako-Attah, I., Akrofi, A.Y., Begoude, B.D., Ten Hoopen, G.M. and Coulibaly, K. (2017). *Phytophthora megakarya* and *Phytophthora palmivora*, closely related causal agents of cacao black pod rot, underwent increases in genome sizes and gene numbers by different mechanisms. *Genome Biology and Evolution*, **9(3),** 536-557.
4) Altschul, S. F., Gish, W., Miller, W., Myers, E. W. and Lipman, D. J. (1990). Basic local alignment search tool. *Journal of Molecular Biology*, **215**(**3**), 403-410.
5) Altschul, S. F., Madden, T. L., Schäffer, A. A., Zhang, J., Zhang, Z., Miller, W. and Lipman, D. J. (1997). Gapped BLAST and PSI-BLAST: a new generation of protein database search programs. *Nucleic Acids Research*, **25**(**17**), 3389-3402.
6) Arraiano, L. S., Brading, P. A. and Brown, J. K. M. (2001). A detached seedling leaf technique to study resistance to *Mycosphaerella graminicola* (anamorph *Septoriatritici*) in wheat. *Plant Pathology*, **50**(**3**):339-346.
7) Attard, A., Evangelisti, E., Kebdani-Minet, N., Panabieres, F., Deleury, E., Maggio, C., Ponchet, M. and Gourgues, M. (2014). Transcriptome dynamics of *Arabidopsis thaliana* root penetration by the oomycete pathogen *Phytophthora parasitica*. *BMC Genomics*, **15**: 538.
8) Baillieul, F., de Ruffray, P. and Kauffmann, S. (2003). Molecular cloning and biological activity of α-, β-, and γ-megaspermin, three elicitins secreted by *Phytophthora megasperma* H20. *Plant Physiology*, **131**(**1**): 155-166.
9) Bozkurt, T. O., Schornack, S., Banfield, M. J. and Kamoun, S. (2012). Oomycetes, effectors, and all that jazz. *Current Opinion in Plant Biology*, **15**: 483-492.

10) Buttner, D. (2012) Protein export according to schedule: architecture, assembly, and regulation of type III secretion systems from plant-and animal-pathogenic bacteria. *Microbiology and Molecular Biology Reviews* **76(2)**: 262-310.

11) Chen, C., Long, L., Zhang, F., Chen, Q., Chen, C., Yu, X., Liu, Q., Bao, J. and Long, Z. (2018). Antifungal activity, main active components and mechanism of *Curcuma longa* extract against *Fusarium graminearum*. *PloS One*, **13**(**3**), e0194284.

12) Chidananda, P. and Pandurang, G. D. (2001). Bud rot management in coconut palm. Technical Folder No. 26. ICAR Research Complex for Goa, Goa. 4 p.

13) Choi, J., Park, J., Kim, D., Jung, K., Kang, S. and Lee, Y. H. (2010). Fungal secretome database: integrated platform for annotation of fungal secretomes. *BMC Genomics*, **11**(**1**), 105.

14) Choi, J., Kim, K. T., Jeon, J. and Lee, Y. H. (2013). Fungal plant cell wall-degrading enzyme database: a platform for comparative and evolutionary genomics in fungi and Oomycetes. *BMC Genomics*, **14**(**S5**): S7.

15) Chowdappa, P., Madhura, S., Kumar, B. N., Kumar, S. M. and Hema, K. R. (2014). *Phytophthora boehmeriae* revealed as the dominant pathogen responsible for severe foliar blight of *Capsicum annuum* in South India. *Plant Disease*, **98**(**1**): 90-98.

16) Cooke, D. E. L., Duncan, J. M., Williams, N. A., Weerdt, M. H. D., and Bonants, P. J. M. (2000). Identification of *Phytophthora* species on the basis of restriction enzyme fragment analysis of the internal transcribed spacer regions of ribosomal RNA. *EPPO Bulletin*, **30(3-4)**: 519-523.

17) Dhingra, O. D and Sinclair, J. B. (1995). Basic Plant Pathology Methods, 2nd edn. Lewis Publishers, Boca Raton, Florida, USA. 341p.

18) Eeuwens, C.J. (1976). Mineral requirements for growth and callus initiation of tissue explants excised from mature coconut palms (*Cocos nucifera*) and cultured *in vitro*. *Physiologia Plantarum*, **36(1)**: pp.23-28.

19) Evangelisti, E., Gogleva, A., Hainaux, T., Doumane, M., Tulin, F., Quan, C., Yunusov, T., Floch, K. and Schornack, S. (2017). Time-resolved dual transcriptomics reveal early induced *Nicotiana benthamiana* root genes and conserved infection-promoting *Phytophthora palmivora* effectors. *BMC Biology*, **15**(**1**): 39.

20) Fan, S., Tian, F., Li, J., Hutchins, W., Chen, H., Yang, F., Yuan, X., Cui, Z., Yang, C.H. and He, C. (2017). Identification of phenolic compounds that suppress the virulence of *Xanthomonas oryzae* on rice via the type III secretion system. *Molecular Plant Pathology*, **18**(**4**): 555-568.

21) Gajendran, K., Gonzales, M.D., Farmer, A., Archuleta, E., Win, J., Waugh, M.E. and Kamoun, S. (2006). *Phytophthora* functional genomics database (PFGD): functional genomics of *Phytophthora*–plant interactions. *Nucleic Acids Research*, **34**(suppl_1): D465-D470.

22) Galán, J. E. and Collmer, A. (1999). Type III secretion machines: bacterial devices for protein delivery into host cells. *Science*, **284**(5418): 1322-1328.

23) Gallegly, ME., and Hong, C. (2008). *Phytophthora*: Identifying Species by Morphology and DNA. St Paul, MN, USA, APS Press. 158 p.

24) Gupta, S. U. N. I. T. A., Gupta, N. K., Arora, A., Agarwal, V. P. and Purohit, A. K. (2012). Effect of water stress on photosynthetic attributes, membrane stability and yield in contrasting wheat genotypes. *Indian Journal of Plant Physiology*, **17**(**1**): 22-27.

25) Irwin, J. A. G., Musial, J. M., Mackie, J. M. and Basford, K. E. (2003). Utility of cotyledon and detached leaf assays for assessing root reactions of lucerne to *Phytophthora* root rot caused by *Phytophthora medicaginis*. *Australasian Plant Pathology,* **32**(**2**):263-268.

26) Jia Y, Valent B, Lee FN. (2003). Determination of host responses to *Magnaporthe grisea* on detached rice leaves using a spot inoculation method. *Plant Disease,* **87**(**2**): 129-133.

27) Khokhani, D., Zhang, C., Li, Y., Wang, Q., Zeng, Q., Yamazaki, A. and Yang, C. H. (2013). Discovery of plant phenolic compounds that act as type III secretion system inhibitors or inducers of the fire blight pathogen, *Erwinia amylovora*. *Applied and Environmental Microbiology*, **79**(**18**): 5424-5436.

28) Kovalchuk, A., Zeng, Z., Ghimire, R.P., Kivimäenpää, M., Raffaello, T., Liu, M., Mukrimin, M., Kasanen, R., Sun, H., Julkunen-Tiitto, R. and Holopainen, J.K., (2019). Dual RNA-seq analysis provides new insights into interactions between Norway spruce and necrotrophic pathogen *Heterobasidion annosum* s.l. *BMC Plant Biology*, ***19***(**1**): 2.

29)Li, Y., Hutchins, W., Wu, X., Liang, C., Zhang, C., Yuan, X. and Yang, C. H. (2015). Derivative of plant phenolic compound inhibits the type III secretion system of *Dickeya dadantii* via HrpX/HrpY two-component signal transduction and R sm systems. *Molecular Plant Pathology*, **16**(**2**): 150-163.

30) Liao, Z.X., Ni, Z., Wei, X.L., Chen, L., Li, J.Y., Yu, Y.H., Jiang, W., Jiang, B.L., He, Y.Q. and Huang, S. (2019). Dual RNA-seq of *Xanthomonas oryzae* pv. *oryzicola* infecting rice reveals novel insights into bacterial-plant interaction. *PloS One*, **14**(**4**): e0215039.

31) Lo Presti, L., Lanver, D., Schweizer, G., Tanaka, S., Liang, L., Tollot, M., Zuccaro, A., Reissmann, S. and Kahmann, R. (2015). Fungal effectors and plant susceptibility. *Annual Review of Plant Biology*, **66**: 513-545.

32)Nambiar, K.K.N. (1994) Disease and disorders of coconut. *Advances in Horticulture*. **19**: 857-882.

33)Panda, A., Sen, D., Ghosh, A., Gupta, A., Prakash Mishra, G., Singh, D., Ye, W., Tyler, B.M. and Tripathy, S. (2018). EumicrobeDBLite: a lightweight genomic resource and analytic platform for draft oomycete genomes. *Molecular Plant Pathology*, **19**(**1**): 227-237.

34)Parke, J. L., Roth, M. L., and Choquette, C. J. (2005). Detached-leaf assays with *Phytophthora ramorum*: Are they valid?. In: Sudden Oak Death Second Science Symposium: The State of Our Knowledge, 18-21 January 2005. Monterey, California, pp.535.

35)Pareek, C.S., Smoczynski, R. and Tretyn, A. (2011). Sequencing technologies and genome sequencing. *Journal of Applied Genetics*, **52**(4): 413-435.

36) Prathibha, V.H., Vinayaka Hedge, Sharadraj, K.M., Rajesh, M.K., Rachana, K.E. and Chowdappa, P. (2018). Differentiation of *Phytophthora* species associated with plantation crops using PCR and high-resolution melting curve analysis. *Journal of Plant Pathology*, **100**(**2**): 233-240.

37) Rachana, K.E and Rajesh, M.K. (2019). Selection and validation of reference genes for gene expression normalization in coconut (*Cocos nucifera* L.) under biotic stress and hormone stimuli. *Plant Gene*, **19**, 100184.

38) Radha, K. and Joseph, T. H. O. M. A. S. (1974). Investigations on the bud rot disease (*Phytophthora palmivora* Butl.) of coconut. Final Report, PL, 480, 32.

39) Rajesh, M.K., Rachana, K.E., Naganeeswaran, S.A., Shafeeq, R., Thomas, R.J., Shareefa, M., Merin, B. and Anitha, K. (2015). Identification of expressed resistance gene analog sequences in coconut leaf transcriptome and their evolutionary analysis. *Turkish Journal of Agriculture and Forestry*, ***39****(3)*: 489-502.

40) Ramesh, R. Maruthadurai and Singh, N.P. (2013). Management of bud rot disease in the coconut plantations of Goa. Extension Folder. No. 66. 1-3 pp

41) Rani, J. R., Aswathy, T. R., Kumar, M. S., Nair, A. S. and Soniya, E. V. (2017). Screening of phytochemicals from selected plants with antifungal properties against RXLR effector protein Avr3a11 in *Phytophthora capsici*. *Canadian Journal of Biotechnology*, **1**(Special): 34.

42) Sairam, R. K., Deshmukh, P. S., and Shukla, D. S. (1997). Tolerance of drought and temperature stress in relation to increased antioxidant enzyme activity in wheat. *Journal of Agronomy and Crop Science,***178**(**3**): 171-178.

43) Schornack, S., van Damme, M., Bozkurt, T. O., Cano, L. M., Smoker, M., Thines, M and Huitema, E. (2010). Ancient class of translocated oomycete effectors targets the host nucleus. *Proceedings of the National Academy of Sciences*, **107**(**40**): 17421-17426.

44) Schornack, S., van Damme, M., Bozkurt, T.O., Cano, L.M., Smoker, M., Thines, M., Gaulin, E., Kamoun, S. and Huitema, E. (2010). Ancient class of translocated oomycete effectors targets the host nucleus. *Proceedings of the National Academy of Sciences*, ***107***(**40**): 17421-17426.

45) Selin, C., de Kievit, T. R., Belmonte, M. F. and Fernando, W. G. (2016). Elucidating the role of effectors in plant-fungal interactions: progress and challenges. *Frontiers in Microbiology*, **7**: 600.

46) Sharadraj, K. M. and Chandramohanan, R. (2013). Status of bud rot disease of coconut in endemic areas of southern states of India. *Global Journal of Applied Agricultural Research*, **3**: 55-61.

47) Sharadraj, K.M. and Mohanan, R.C. (2014). A new detached coconut leaf let technique for bioassay of fungicides against *Phytophthora palmivora*–the incitant of coconut bud rot. *International Journal of Plant Protection*, **7(1)**: 161-165.

48) Srinivasulu, B. and Raghava Rao, D. V. (2009). Biocontrol of major diseases of coonut. In: P. Ponmurugan, and M. A. Deepa (Eds). Role of Biocontrol Agents for Disease Management in Sustainable Agriculture. SCITECH (India) Pvt., Chennai pp. 352–368.

49) Surin, P., Srivakorn, N., Imrie, B. and Lawn, R. (1993). A detached leaf culture technique for resistance screening against bacterial pustule in soybean. *Agriculture and Natural Resources*, **27(2)**:240-245.

50) Tao, H., Tian, H., Jiang, S., Xiang, X., Lin, Y., Ahmed, W. and Cui, Z. N. (2019). Synthesis and biological evaluation of 1, 3, 4-thiadiazole derivatives as type III secretion system inhibitors against *Xanthomonas oryzae*. *Pesticide Biochemistry and Physiology*, **160**: 87-94.

51) Toffolatti, S.L., De Lorenzis, G., Brilli, M., Moser, M., Shariati, V., Tavakol, E., Maddalena, G., Passera, A., Casati, P., Pindo, M. and Cestaro, A. (2020). Novel aspects on the interaction between grapevine and *Plasmopara viticola:* Dual-RNA-Seq analysis highlights gene expression dynamics in the pathogen and the plant during the battle for infection. *Genes*, **11(3)**: 261.

52) Tripathy, S., Deo, T. and Tyler, B. M. (2012). Oomycete Transcriptomics Database: a resource for oomycete transcriptomes. *BMC Genomics*, **13(1)**, 303.

53) Urban, M., Pant, R., Raghunath, A., Irvine, A. G., Pedro, H. and Hammond-Kosack, K. E. (2015). The Pathogen-Host Interactions database (PHI-base): Additions and future developments. *Nucleic Acids Research*, **43(D1)**: D645-D655.

54) Vawdrey, L. L., Martin, T. M. and De Faveri, J. (2005). A detached leaf bioassay to screen Durian cultivars for susceptibility to *Phytophthora palmivora*. *Australasian Plant Pathology*, **34**(**2**):251-253.

55) Wang, W. and Jiao, F. (2019). Effectors of *Phytophthora* pathogens are powerful weapons for manipulating host immunity. *Planta*, **250**:1-13.

56) Westermann, A. J., Gorski, S. A. and Vogel, J. (2012). Dual RNA-seq of pathogen and host. *Nature Reviews Microbiology*, **10**: 618-630.

57) White, T. J., Bruns, T., Lee, S. J. W. T., and Taylor, J. (1990). Amplification and direct sequencing of fungal ribosomal RNA genes for phylogenetics. In: Innis, M.A., Gelfand, D.H., Sninsky, J.J. and White, T.J. (Eds.). PCR protocols: a guide to methods and applications. Elsevier, Academic Press: New York, NY, USA. pp. 315-322.

58) Yang, F., Korban, S. S., Pusey, P. L., Elofsson, M., Sundin, G. W. and Zhao, Y. (2014). Small-molecule inhibitors suppress the expression of both type III secretion and amylovoran biosynthesis genes in *Erwinia amylovora*. *Molecular Plant Pathology*, **15**(**1**): 44-57.

59) Ye, W., Wang, X., Tao, K., Lu, Y., Dai, T., Dong, S., Dou, D., Gijzen, M. and Wang, Y. (2011). Digital gene expression profiling of the *Phytophthora sojae* transcriptome. *Molecular Plant-Microbe Interactions*, **24**(**12**): 1530-1539.

60) Zhou, L., Wang, C., Wang, G.H., Wei, Z.W., Fu, Q.X., Hang, X.H., Yang, M., Jiang, B.L. and Tang, J.L., (2020). Chemical targeting and manipulation of type III secretion in the phytopathogen *Xanthomonas campestris* for control of disease. *Applied and Environmental Microbiology*, **86**(**3**): 1-14

61) Zuluaga, A. P., Vega-Arreguín, J. C., Fei, Z., Matas, A. J., Patev, S., Fry, W. E. and Rose, J. K. (2016a). Analysis of the tomato leaf transcriptome during successive hemibiotrophic stages of a compatible interaction with the oomycete pathogen *Phytophthora infestans*. *Molecular Plant Pathology*, ***17***(**1**): 42-54.

62) Zuluaga, A. P., Vega-Arreguín, J. C., Fei, Z., Ponnala, L., Lee, S. J., Matas, A. J., Patev, S., Fry, E. W. and Rose, J. K. (2016b). Transcriptional dynamics of *Phytophthora infestans* during sequential stages of hemibiotrophic infection of tomato. *Molecular Plant Pathology*, **17(1)**: 29-41.

## 6. PUBLICATIONS

### 6.1. Publications in journals

i. **Gangaraj, K.P**., Muralikrishna K.S., Ginny Antony, Sahu B.B., Vinayak Hedge and Rajesh M.K. (2020). A rapid and reliable *in vitro* inoculation assay to investigate *Phytophthora palmivora*-coconut interactions. *Journal of Phytopathology,* **169**(5): 316-328. https://doi.org/10.1111/jph.12988.

ii. **Gangaraj, K.P** and Rajesh, M.K. (2020). Dataset of dual RNA-sequencing of *Phytophthora palmivora* infecting coconut (*Cocos nucifera* L.). *Data in Brief*, 105455. https://doi.org/10.1016/j.dib.2020.105455.

iii. **Gangaraj, K.P** and Rajesh, M.K. (2022). Characterization and structural assessment of a RxLR effector candidate from *Phytophthora palmivora*, the coconut bud rot pathogen. *Journal of Plantation Crops,* **50** (2): 100-109 https://doi.org/10.25081/jpc.2022.v50.i2.7984

### 6.2. Presentations in symposia/conferences:

i. **Gangaraj, K.P**., Santhi, C.K.V., Ginny Antony and Rajesh, M.K. (2020) Temporal gene expression patterns of coconut upon challenge by the oomycete pathogen *Phytophthora palmivora*. In: *Book of Abstracts- 29th SWADESHI SCIENCE CONGRESS*. Rishiram, R., Prasad, E., Aneesh, *et al.* (Eds.). ICAR-Central Plantation Crops Research Institute, Kasaragod. B37, p. 39.

ii. **Gangaraj, K.P**., Rajesh, M.K., Prathibha, V.H. and Vinayak Hedge (2019). Identification of RxLR effectors in coconut bud rot pathogen, *Phytophthora palmivora* though dual transcriptomics study. In:*Book of Abstracts-PLACROSYM XXIII*. Patil, S., Roobak Kumar, A., Krishna Reddy, P. *et al.* (Eds.). Central Coffee Research Institute, Coffee Research Station, Chikkamagaluru, Karnataka, India GE P37, p. 43.

iii. **Gangaraj, K.P**., Rajesh, M.K., Sharadraj, K. M., Muralikrishna K S, Prathibha, V. H. and VinayakaHegde (2016). Development of novel *in vitro* inoculation assay to investigate *Phytophthora palmivora* coconut interactions. In:*Book of Abstracts: PLACROSYM XXII*,Chowdappa, P., Muralidharan, K., Rajesh, M. K. and Ramesh, S. V. (Eds.). Central Plantation Crops Research Institute, Kasaragod, Kerala, India. B37, p. 194.

### 6.3 Sequence submitted in NCBI

- **NCBI GenBank:**
  - https://www.ncbi.nlm.nih.gov/nuccore/MK500842.1

- **NCBI Sequence Read Archive (SRA):**
  - https://www.ncbi.nlm.nih.gov/sra/SRX5914110
  - https://www.ncbi.nlm.nih.gov/sra/SRX9197107
  - https://www.ncbi.nlm.nih.gov/sra/SRX5914109
  - https://www.ncbi.nlm.nih.gov/sra/SRX9197106
  - https://www.ncbi.nlm.nih.gov/sra/SRX5914112
  - https://www.ncbi.nlm.nih.gov/sra/SRX9197109
  - https://www.ncbi.nlm.nih.gov/sra/SRX5914111
  - https://www.ncbi.nlm.nih.gov/sra/SRX9197108
  - https://www.ncbi.nlm.nih.gov/sra/SRX5914108
  - https://www.ncbi.nlm.nih.gov/sra/SRX9197111
  - https://www.ncbi.nlm.nih.gov/sra/SRX5914107
  - https://www.ncbi.nlm.nih.gov/sra/SRX9197110
  - https://www.ncbi.nlm.nih.gov/sra/SRX9230504
  - https://www.ncbi.nlm.nih.gov/sra/SRX9230505

**(Gangaraj K. P.)**
**Research Scholar**

**(M. K. Rajesh)**
**Research Supervisor**

## Appendix

# Presentations and Publications

# Abstracts

## PLACROSYM 22
## 22nd Biennial Symposium on Plantation Crops
**15-17 December 2016**

Leveraging Innovation System in Plantation Sector Through Value Addition

Indian Council of Agricultural Research -
Central Plantation Crops Research Institute

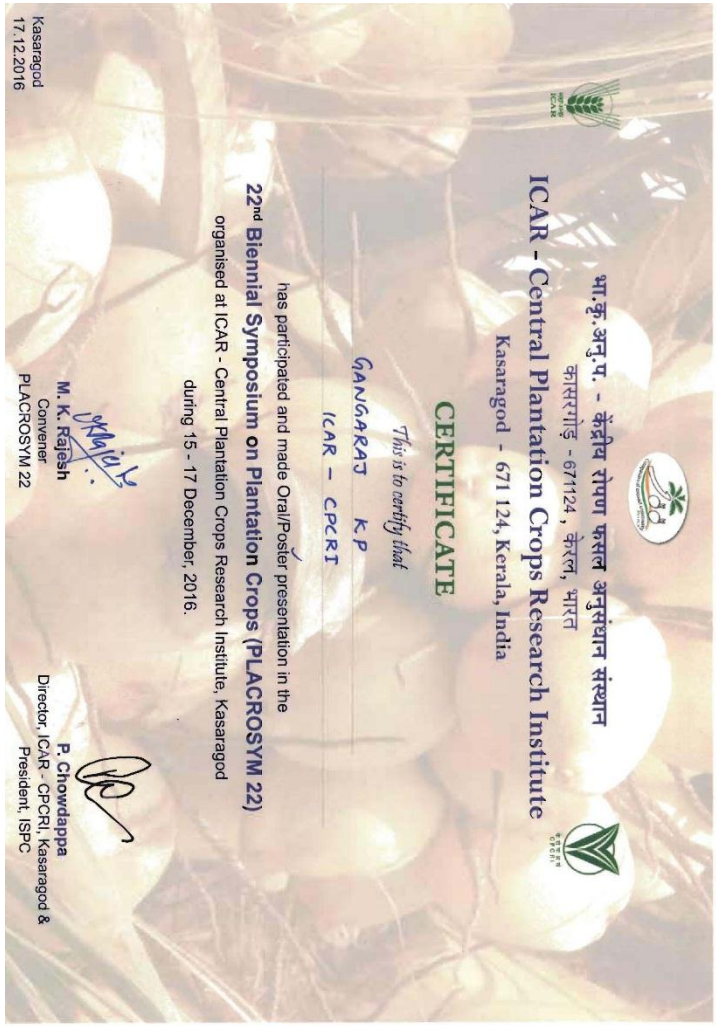
भा.कृ.अनु.प. - केंद्रीय रोपण फसल अनुसंधान संस्थान
कासरगोड़ - 671124, केरल, भारत
ICAR - Central Plantation Crops Research Institute
Kasaragod - 671 124, Kerala, India
CERTIFICATE
This is to certify that
GANGARAJ K.P
ICAR - CPCRI
has participated and made Oral/Poster presentation in the
22nd Biennial Symposium on Plantation Crops (PLACROSYM 22)
organised at ICAR - Central Plantation Crops Research Institute, Kasaragod
during 15 - 17 December, 2016.
M. K. Rajesh
Convener
PLACROSYM 22
P. Chowdappa
Director, ICAR - CPCRI, Kasaragod &
President, ISPC
Kasaragod
17.12.2016

TS3-PP28

# Development of a novel in vitro inoculation assay to investigate *Phytophthora palmivora*-coconut interactions

Gangaraj K.P.*, Rajesh M.K., Sharadraj K.M., Muralikrishna K.S., Prathibha V.H. & Vinayak Hegde
ICAR-Central Plantation Crops Research Institute, Kasaragod 671124, Kerala, India
(*gangarajkp@gmail.com)

Bud rot, caused by *Phytophthora palmivora*, is one of the major lethal diseases of coconut palm, causing decay of the terminal bud and surrounding tissues. It affects both mature and juvenile palms, with the latter being more susceptible to the disease. It is a generally a sporadic disease, but can assume epidemic proportions too. The development of novel approaches for crop protection requires a deep understanding of molecular mechanisms underlying plant-pathogen interactions. Considering the higher risks involved in carrying out studies of plant-pathogen interaction through field trials especially in a crop like coconut, we have developed an *in vitro* assay for high-throughput disease testing of *Phytophthora palmivora* in coconut. Spindle leaves from adult coconut palms were surface sterilized and inoculated in basal Y3 medium in Petri plates. After a week in culture, the surface of the leaves were pricked and inoculated with agar plugs of *P. palmivora* culture. Typical lesion development was noticed on the surface of the coconut leaves 48-72 hours after inoculation of the pathogen. The presence of pathogen in the coconut leaflets was confirmed using PCR using Phytophthora specific primers. Electrolyte leakage assays and histological studies, using light and scanning electron microscopy, were also undertaken to study the disease progression. The novel assay developed through this study is rapid, space-effective, and precise and could be utilized for detailed investigations of the qualitative interactions between coconut and *P. palmivora*.

PLACROSYM XXIII
23rd Biennial Symposium on Plantation Crops
6 - 8 March, 2019
Central Coffee Research Institute, Coffee Research Station (Post) - 577 117
Chikkamagaluru, Karnataka

**Published by**
Dr. Y. Raghuramulu
Director of Research & General Chairman, PLACROSYM XXIII
Central Coffee Research Institute, Coffee Research Station (Post) - 577 117
Chikkamagaluru, Karnataka

**Compiled and edited by**
Dr. Somashekhargouda Patil
Dr. A. Roobak Kumar
Dr. P. Krishna Reddy
Mrs. M.S. Uma
Dr. George Daniel
Dr. Jeena Devasia
Dr. Manoj Kumar Mishra
Dr. N. Surya Prakash

**ISBN No. : 978-81-932263-8-4**

**Financial support**
The financial assistance from National Bank for Agriculture and Rural Development (NABARD), Bengaluru, Karnataka towards printing of this publication is gratefully acknowledged.

**Cover page photo source**
http://homeguides.sfgate.com

**Printed at**
Omkar Offset Printers
No. 3/3, 1st Main Road, N.T. Pet, Bangalore - 560 002. Phone : 080 2670 8186
Email : omkaroffset@gmail.com Website : www.omkaroffset.com


# 23rd PLANTATION CROPS SYMPOSIUM
# (PLACROSYM XXIII)

## *Certificate*

This is to certify that, Dr / Mr / Mrs / Miss. ..... Gangaraj. K.P., CPCRI .....
has participated/presented the research paper in the 23rd Plantation Crops Symposium (Placrosym XXIII) held at Chikkamagaluru, Karnataka from 6th to 8th March 2019.

Dr. N. Surya Prakash Rao
Convener

Dr. Y. Raghuramulu
General Chairman

GE P37

## Identification of RxLR effectors in coconut bud rot pathogen, *Phytophthora palmivora* though dual transcriptomics study

**Gangaraj K.P.*, Rajesh M.K., Prathibha V.H. and Vinayak Hedge**

*ICAR-Central Plantation Crops Research Institute, Kasaragod 671124, Kerala*
***gangarajkp@gmail.com***

*Phytophthora spp.* is an oomycetes plant pathogen which causes serious damage to wide range of plants. Bud rot disease of coconut palm is caused by *P. palmivora. Phytophthora* delivers effectors, a type of secretory proteins in to the host cells, which promote the infection process. The major class of effector proteins contains the RxLR motif. Dual transcriptomic study of *Phytophthora*-coconut interactions will help in better understanding of the expression pattern and regulation of RxLR proteins. In this study, carried out using the standardized *in vitro* inoculation assay, we have found 77 RxLR proteins expressing within 24 hours of *P. palmivora* inoculation in coconut. There were 53 RxLR proteins expressing within 36 hours of *P. palmivora* inoculation in coconut. No significant effector expression of RxLR proteins could be detected in the first 12 hours after inoculation. Thirty nine RxLR candidates were found to be commonly expressed. A highly upregulated RxLR transcript was selected for further analysis. The transcript was found to encode a protein of 136 amino acids and 15.51 kDa molecular weight. Phylogenetic analysis of the protein sequence showed the sequence was closely related RXLR protein of *P. megakarya*. The candidate RxLR effectors identified in the present study would enable deciphering the disease progression machinery and use of RxLR effector candidates in coconut resistance breeding.

# 29 സ്വദേശി ശാസ്ത്ര സമ്മേളനം SWADESHI SCIENCE CONGRESS

**National Conference**

## Science and Technology for Sustainable Development

**27-29 February 2020**

**ICAR-Central Plantation Crops Research Institute, Kasaragod**

**Swadeshi Science Movement-Kerala (Vijnana Bharati)**

**ICAR-Central Plantation Crops Research Institute, Kasaragod**

**Central University of Kerala, Kasaragod**

**29th Swadeshi Science Congress**

**Organized by: SWADESHI SCIENCE MOVEMENT – KERALA**

Sastra Bhavan, B-4, 4th Floor, Mather Square, Town Railway Station Road, Kochi – 682 018

In association with:

**ICAR-Central Plantation Crops Institute, Kasaragod and Central University, Kasaragod**

**NATIONAL CONFERENCE ON SCIENCE AND TECHNOLOGY FOR SUSTAINABLE DEVELOPMENT**

## Certificate

*Certified that Mr./Ms./Dr./Prof.* Gangaraj K.P., ICAR-CPCRI, Kasaragod *has presented a paper/participated in the session on* Temporal gene expression patterns of coconut upon challenge by the acmeyte pathogen Bipolaris Palmicola *at Swadeshi Science Congress 2020 held at ICAR-CPCRI, Kasaragod during 27-29 February, 2020.*

**Dr. Anitha Karun**
Director
ICAR-CPCRI, Kasaragod

**Dr. A.R.S. Menon**
Secretary
SSM-K, Kochi

## B17. Temporal gene expression patterns of coconut upon challenge by the oomycete pathogen *Phytophthora palmivora*

**Gangaraj, K.P.** [1,3,*], **Santhi, C.K.V.** [1], **Ginny Antony**[2] **and Rajesh, M.K.**[1*]
[1] *ICAR-Central Plantation Crops Research Institute, Kasaragod*
[2]*Central University of Kerala, Periya, Kasaragod*
[3]*Mangalore University, Mangalagangotri, Mangaluru*
*E-mail: gangarajkp@gmail.com

Interactions occurring between the plant host and the phytopathogen during the early stages of infection are significant to the final outcome. *Phytophthora palmivora* causes bud rot, a major production constraint in coconut. Employing an *in vitro* assay, previously standardized in our lab, in combination with a dual RNA-sequencing (RNA-seq) strategy, we have undertaken a time-resolved (12 h, 24 h, and 36 h post-inoculation of the pathogen) genome-wide differential gene expression analysis of host genes between infected and control samples. The differential gene expression analysis revealed significant changes in the functional categories of genes related to protein kinase and phosphorylation, ATP binding, metabolism, cell wall modification and protein and DNA binding. Validation of selected transcripts, carried out by qRT-PCR, revealed that transcripts encoding serine/threonine LRR receptor-like protein kinase, endo-1, 3-β –glucosidase, lipid-transfer proteins, calmodulin, dihydroflavonol 4-reductase/flavanone 4-reductase, pectinesterase, transcription factor MYB2 and endochitinase were up-regulated in infected tissues in comparison to control. This study which combined an *in vitro* assay with RNA-Seq, revealed significant insights into the interactions between coconut and *P. palmivora* during the initial phase of infection.

Data in Brief 30 (2020) 105455

Contents lists available at ScienceDirect

Data in Brief

journal homepage: www.elsevier.com/locate/dib

Data Article

# Dataset of dual RNA-sequencing of *Phytophthora palmivora* infecting coconut (*Cocos nucifera* L.)

K.P. Gangaraj[a,b], M.K. Rajesh[a,*]

[a] *ICAR-Central Plantation Crops Research Institute, Kasaragod 671124, Kerala, India*
[b] *Mangalore University, Mangalagangotri, Mangaluru 574199, Karnataka, India*

ARTICLE INFO

*Article history:*
Received 20 February 2020
Revised 11 March 2020
Accepted 12 March 2020
Available online 18 March 2020

*Keywords:*
Dual RNA-seq
Transcriptomics
Coconut
*Phytophthora palmivora*
Gene Ontology

ABSTRACT

*Phytophthora* spp. is an oomycetes pathogen which causes serious damage to a wide range of crops. Bud rot disease of coconut palm, caused by *P. palmivora*, causes huge economic losses since it cannot be detected at an early stage. Utilizing dual RNA-sequencing (RNA-seq), we have simultaneously investigated the gene expression patterns in both, the infecting oomycete (*P. palmivora)* and infected host (coconut leaflets). Samples were collected at three time points viz., 12, 24 and 36 h, from both infected and uninfected (control) tissues and subjected to RNA-seq on an Illumina Hiseq™ 2500 sequencing platform. High quality reads obtained were subjected to mapping with corresponding reference genomes by using the HISAT2/ StringTie package. A total of 81,683 transcripts were generated against the coconut reference genome, while 9340 transcripts were generated against *P. palmivora* genome. Out of these, a total of 64,639 coconut transcripts and 9168 *P. palmivora* transcripts could be annotated using BLASTx. Gene ontology (GO) analysis, carried out using Blast2GO, resulted in 212,643 coconut and 30,736 *P palmivora* transcripts being functionally classified, with a single gene product described by numerous terms under the three classifications. The insights obtained could contribute to an understanding of pathogenesis of *P. palmivora* and inducible defense response of coconut leaves to *P. palmivora*.

* Corresponding author.
*E-mail address:* rajesh.mk@icar.gov.in (M.K. Rajesh).

https://doi.org/10.1016/j.dib.2020.105455
2352-3409/© 2020 The Author(s). Published by Elsevier Inc. This is an open access article under the CC BY license. (http://creativecommons.org/licenses/by/4.0/)

© 2020 The Author(s). Published by Elsevier Inc.
This is an open access article under the CC BY license.
(http://creativecommons.org/licenses/by/4.0/)

Specifications table

| | |
|---|---|
| Subject | Biology |
| Specific subject area | Transcriptomics |
| Type of data | Dual RNA-sequencing (RNA-seq) data |
| How data were acquired | Illumina Hiseq™ 2500 sequencing platform |
| Data format | Raw sequencing data (fastq) and analyzed data (fasta) |
| Parameters for data collection | Dual RNA-seq of coconut-*Phytophthora* interactions at different time intervals |
| Description of data collection | We employed time-resolved dual-transcriptomic approach to decipher *Cocos nucifera-Phytophthora palmivora* interactions. This approach revealed different pathogen and host transcriptome dynamics. |
| Data source location | Kasaragod, India (12°32′38.0″N; 74°57′45.7″E). |
| Data accessibility | Repository name: NCBI SRA<br>Data identification number: PRJNA544637<br>The dataset includes six records, from SRR9140949 to SRR9140954.<br>Direct URL to data: https://www.ncbi.nlm.nih.gov/sra/PRJNA544637 |

## Value of the data

- The dual RNA-seq dataset provides the first resources for coconut–*P. palmivora* interaction studies and can be leveraged in deciphering the molecular mechanisms underlying response of coconut to *P. palmivora* attack.
- The data allows further analysis to identify candidate effector genes in *P. palmivora* that possibly contribute to manipulation of host processes and promote infection.
- This data could be useful for selection of disease resistant varieties for coconut breeding programs and design of novel disease management startegies.
- It is a useful reference transcriptome to other researchers working in palm diseases caused by *Phytophthora* spp.

## 1. Data

Schematic outline of the experimental design and RNA-seq data analysis workflow is given in Fig. 1. The details of RNA-seq data submitted to the NCBI Sequence Read Archive (SRA) are provided in Table 1. Table 2 gives an overview of the RNA-seq statistics of raw read and clean reads obtained at different time intervals. Mapping statistics of high quality reads with coconut genome is given in Table 3 and with *Phytophthora palmivora* genome is given in Table 4.

**Table 1**
Details of RNA-seq data submitted to the NCBI Sequence Read Archive (SRA).

| Accession no. | Bioproject accession no. | Biosample accession no. | Library id |
|---|---|---|---|
| SRR9140951 | PRJNA544637 | SAMN11867028 | 12hc |
| SRR9140952 | PRJNA544637 | SAMN11867027 | 12hpi |
| SRR9140949 | PRJNA544637 | SAMN11867030 | 24hc |
| SRR9140950 | PRJNA544637 | SAMN11867029 | 24hpi |
| SRR9140953 | PRJNA544637 | SAMN11867032 | 36hc |
| SRR9140954 | PRJNA544637 | SAMN11867031 | 36hpi |

[12hc: 12 h control, 12hpi: 12 h post inoculation; 24hc: 24 h control, 24hpi: 24 h post inoculation; 36hc: 36 h control, 36 hpi: 36 h post inoculation].

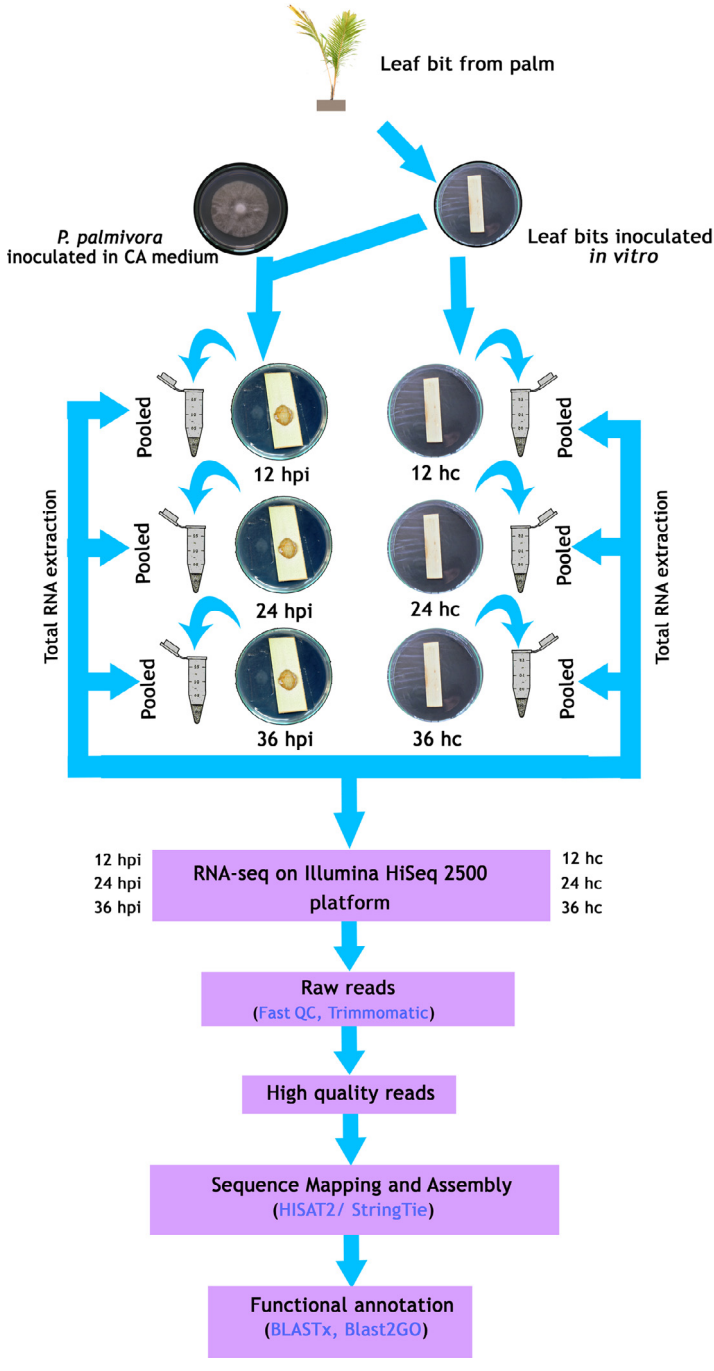


**Fig. 1.** Schematic outline of the experimental design and data analysis workflow.

**Table 2**
RNA-seq statistics of raw read and clean reads obtained at different time intervals.

| Sample name | Number of paired end reads (raw reads) | GC% | Read length (bp) | Number of paired end reads (clean reads) |
|---|---|---|---|---|
| 12hc | 64,921,052 | 47.88 | 100 × 2 | 64,503,262 |
| 12hpi | 63, 662,338 | 47.85 | 100 × 2 | 63,090,348 |
| 24hc | 63,064,844 | 47.74 | 100 × 2 | 62,601,136 |
| 24hpi | 67,291,090 | 48.53 | 100 × 2 | 66,770,394 |
| 36hc | 70,446,814 | 48.02 | 100 × 2 | 70,150,788 |

**Table 3**
Summary of mapping information of pre-processed reads against coconut genome.

| Sample name | Number of reads considered for alignment | Total number of reads aligned | Number of unaligned reads |
|---|---|---|---|
| 12hc | 64,503,262 | 62,764,100 | 3041,832 |
| 12hpi | 63,090,348 | 61,559,938 | 2583,208 |
| 24hc | 62,601,136 | 60,771,365 | 3271,750 |
| 24hpi | 66,770,394 | 63,925,486 | 4296,428 |
| 36hc | 70,150,788 | 67,896,254 | 3820,556 |
| 36hpi | 60,135,364 | 57,801,520 | 3500,526 |

**Table 4**
Summary of mapping information of unaligned reads against *P. palmivora* genome.

| Sample name | Total number of reads considered for alignment | Total number of reads aligned | Total number of unaligned reads |
|---|---|---|---|
| 12hc | 3041,832 | 1009 | 3041,784 |
| 12hpi | 2583,208 | 1499 | 2583,056 |
| 24hc | 3271,750 | 1235 | 3271,696 |
| 24hpi | 4296,428 | 855,123 | 3475,146 |
| 36hc | 3820,556 | 1077 | 3820,346 |
| 36hpi | 3500,526 | 569,557 | 2957,968 |

Figs. 2 and 3 display the functional classification of coconut and *P. palmivora* in three Gene Ontology (GO) categories viz., biological processes, molecular functions and cellular components, respectively.

A total of 81,683 transcripts were generated against the coconut reference genome, while 9340 transcripts were generated against *P. palmivora* genome. A total of 64,639 coconut transcripts and 9168 *P. palmivora* transcripts could be annotated using BLASTx program. Gene Ontology (GO) analysis, performed to assign GO identity to the annotated transcripts, revealed that 212,643 coconut transcripts could be assigned with GO terms (Biological processes = 90,956; Molecular functions = 85,563; Cellular components = 36,124) (Fig. 2). Among the *P. palmivora* transcripts, 30,736 sequences were assigned with GO terms (Biological processes = 12,634; Molecular functions = 11,706; Cellular components = 6396) (Fig. 3). We provide the first molecular resource of the interactions occurring between coconut and *P. palmivora by* simultaneously analysing the global gene expression of the oomycete and host by dual RNA-seq.

## 2. Experimental design, materials, and methods

### 2.1. Experimental design and sampling

The *in vitro* inoculation assay, standardized earlier in our laboratory [1], was utilized for the infection studies. Briefly, spindle leafles from two year old coconut seedlings [Chowghat Orange Dwarf (COD) cultivar] were taken and inoculated in plain Y3 media [2] in Petri plates. Zoospore

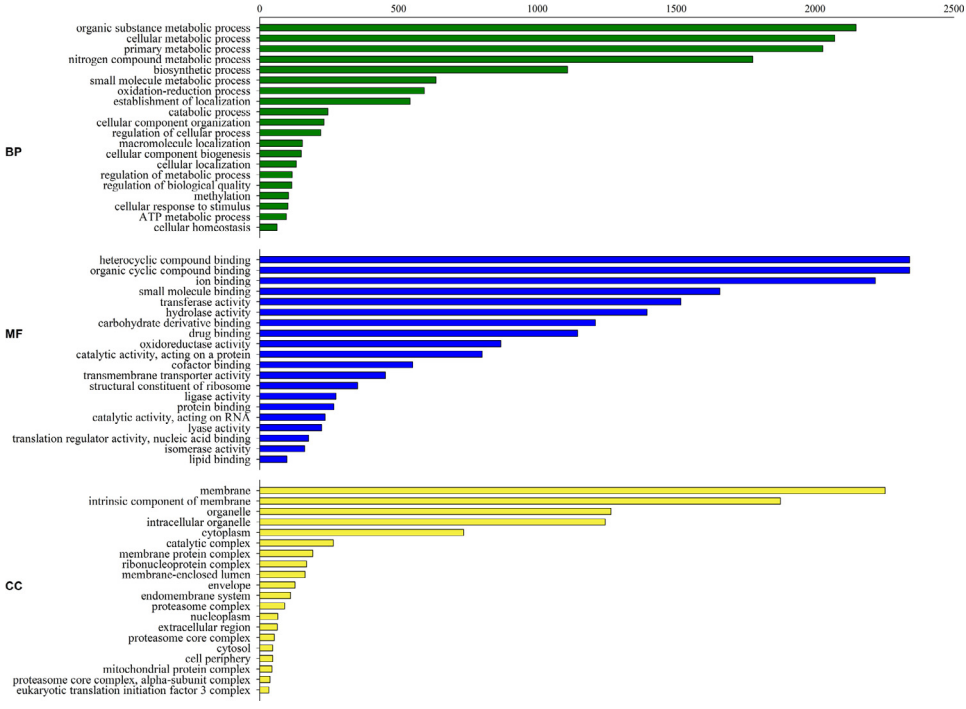


**Fig. 2.** A combined graphical representation of Gene Ontology (GO) analysis of annotated coconut transcripts- biological process (BP), molecular function (MF), and cellular component (CC). Number of sequences can vary amongst the different classifications as a single gene product can be described by numerous terms in the three classifications.

suspension (10 µl of $2 \times 10^4$ $mL^{-1}$) of a virulent isolate of *P. palmivora* (GenBank accession no. MK500842.1), isolated from bud rot infected coconut palm in our laboratory and maintained in carrot agar (CA) medium, was used for the inoculation experiments. *P. palmivora* was inoculated onto pin pricked coconut leaflets. Typical necrotic lesions, indicating infection, were first observed after 12 h post inoculation (hpi). Samples were taken at 12 hpi, 24 hpi and 36 hpi. Un-inoculated, but pin pricked leaflets, served as controls (hc). Three biological replicates were sampled at each time point and used for isolation of RNA.

To confirm the presence of the pathogen at the infection area, the infected area was wiped with alcohol, DNA was extracted from the specific area using DNeasy Plant Mini Kit (Qiagen, USA) and amplified using *Phytophthora*-specific primers (ITS6 and ITS4) [3]. An expected band of around ~900 bp was obtained, which was sequenced. Analysis of the sequence by BLASTn revealed complete identity to *P. palmivora* (GenBank accession no. GU111653).

### 2.2. RNA extraction and sequencing

Total RNA was extracted from 150 mg of tissue at each specific time points [from the infection area in case of inoculated samples and pricked area in the case of control samples] using the NucleoSpin® RNA Plant Kit (Macherey-Nagel). Total RNA was extracted from three independent samples per treatment. The quality and the purity of the extracted RNA were assessed by OD 260 nm/280 nm ratio and RNA integrity number was analyzed using an Agilent Technologies 2100 Bioanalyzer with the Agilent RNA chip with RIN (RNA Integrity Number) > 8.0. The isolated RNA samples, from each particular satge, were pooled together and used for RNA-seq library construction (TruSeq RNA Sample Prep Kit, Illumina). After quality assessment, the con-

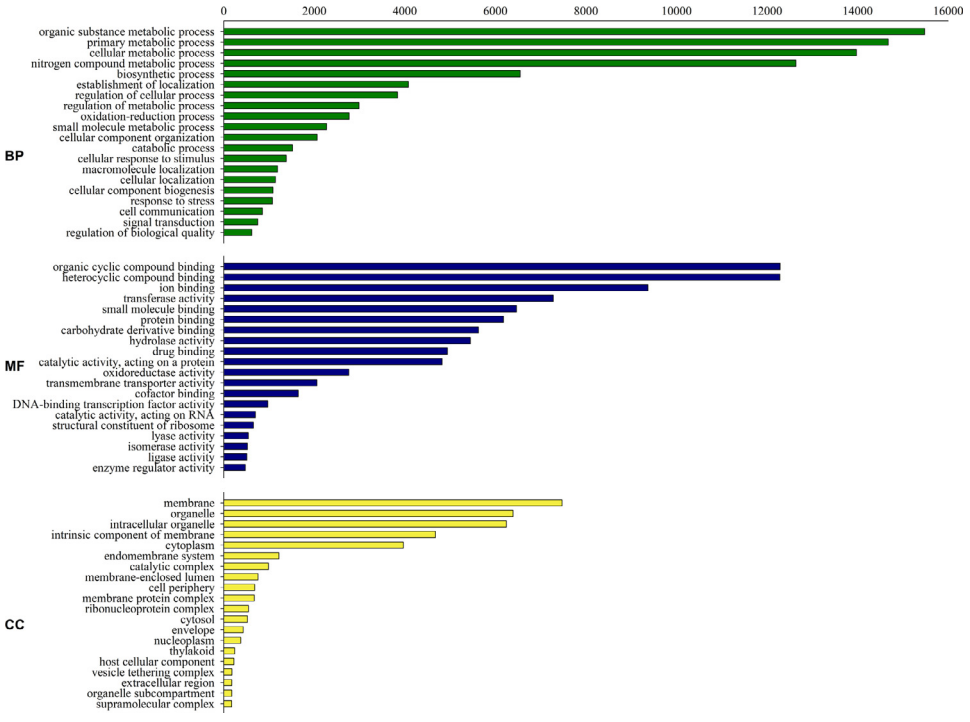


**Fig. 3.** A combined graphical representation of Gene Ontology (GO) analysis of annotated *P. palmivora* transcripts- biological process (BP), molecular function (MF), and cellular component (CC). Number of sequences can vary amongst the different classifications as a single gene product can be described by numerous terms in the three classifications.

structed messenger RNA libraries were subjected to paired-end sequencing on an Illumina HiSeq 2500 platform, as per the procdure described in Rajesh et al. [4].

### 2.3. Data analysis

Raw reads, quality headed (.fastq) fasta files were subjected to quality check. Initially, the raw reads were checked for the ambiguous bases, Phred score >Q20, read length, nucleotide base content and other parameters using FastQC [5]. Trimmomatic was then used to filter low-quality sequences [6]. After trimming and filtering of the low quality reads, a QC was performed in order to reassess the quality of reads. Mapping and assembly of the good quality reads to the reference genomes was performed with 'New Tuxedo Suit' (HISAT2/StringTie), using default parameters [7]. The reference genomes of coconut (PRJNA374600; Xiao et al. [8]) and *Phytophthora palmivora* (PRJNA318026; [9]) were downloaded from NCBI. Initially, indexing of the coconut reference genome and alignment of reads to the coconut reference genome was done using HISAT2. The aligned reads are then taken and used for the transcript assembly using the StringTie Tool. The unaligned reads were aligned with *P. palmivora* genome.

### 2.4. Transcriptome functional annotation

Local protein databases were created from five organisms viz., Phytophthora palmivora, *Phytophthora megakarya* (PRJNA318028; [9]), Hainan Tall coconut (PRJNA374600; [8]), date palm (PR-

JNA249070; [10]) and oil palm (PRJNA268357; [11]). The assembled transcriptomes, of both host and the pathogen was annotated by BLASTx search against corresponding proteome databases, keeping a threshold of $1 \times 10^{-4}$ maximum e value. Blast2GO [12] were used to perform Gene Ontology (GO) analysis of the assembled transcriptome and individually for *P. palmivora* and coconut.

## Acknowledgements

The authors would like to thank Indian Council of Agricultural Research (ICAR) and Department of Biotechnology, Government of India (Grant number: BT/BI/04/053/2002) for funding (Distributed Information sub-center).

## Conflict of Interest

The authors declare that they have no known competing financial interests or personal relationships that could have appeared to influence the work reported in this paper.

## Supplementary material

Supplementary material associated with this article can be found, in the online version, at doi:10.1016/j.dib.2020.105455.

## CRediT authorship contribution statement

**K.P. Gangaraj:** Data curation, Writing - original draft. **M.K. Rajesh:** Conceptualization, Methodology, Supervision, Writing - review & editing.

## References

[1] K.P. Gangaraj, M.K. Rajesh, K.M. Sharadraj, K.S. Muralikrishna, V.H. Prathibha, V. Hegde, Development of a novel *in vitro* inoculation assay to investigate *Phytophthora palmivora*-coconut interactions, in: P. Chowdappa, K Muralidharan, M.K. Rajesh, S.V. Ramesh (Eds.), Abstracts, 22nd Plantation Crops Symposium (PLACROSYM 22), ICAR-CPCRI, Kasaragod, India, 2016, p. 194.

[2] C.J. Eeuwens, Mineral requirements for growth and callus initiation of tissue explants excised from mature coconut (*Cocos nucifera L.*) and date (*Phoenix dactylifera L.*) palms cultured *in vitro*, Physiol. Plantarum 36 (1976) 23–28, doi:10.1111/j.1399-3054.1976.tb05022.x.

[3] T.J. White, T. Bruns, S.B. Lee, J.W. Taylor, Amplification and direct sequencing of fungal ribosomal RNA genes for phylogenetics, in: M.A. Innis, D.H. Gelfand, J.J. Sninsky, T.J. White (Eds.), PCR Protocols: a Guide to Methods and Applications, Academic Press, San Diego, USA, 1990, pp. 315–322.

[4] M.K. Rajesh, K.E. Rachana, S.A. Naganeeswaran, R. Shafeeq, R.J. Thomas, M. Shareefa, B. Merin, K. Anitha, Identification of expressed resistance gene analog sequences in coconut leaf transcriptome and their evolutionary analysis, Turk. J. Agric. For. 39 (2015) 489–502, doi:10.3906/tar-1409-75.

[5] S. Andrews, FastQC: a quality control tool for high throughput sequence data. http://www.bioinformatics.babraham.ac.uk/projects/fastqc/, 2010.

[6] A.M. Bolger, M. Lohse, M. Usadel, Trimmomatic: a flexible trimmer for Illumina sequence data, Bioinformatics 30 (2014) 2114e2120, doi:10.1093/bioinformatics/btu170.

[7] M. Pertea, D. Kim, G.M. Pertea, J.T. Leek, S.L. Salzberg, Transcript-level expression analysis of RNA-seq experiments with HISAT, Stringtie and Ballgown, Nat. Protoc. 11 (2016) 1650–1667, doi:10.1038/nprot.2016.095.

[8] Y. Xiao, P. Xu, H. Fan, L. Baudouin, W. Xia, S. Bocs, J. Xu, Q. Li, A. Guo, L. Zhou, J. Li, The genome draft of coconut (*Cocos nucifera*), Gigascience 11 (2017) 1–11, doi:10.1093/gigascience/gix095.

[9] S.S. Ali, J. Shao, D.J. Lary, B.A. Kronmiller, D. Shen, M.D. Strem, I. Amoako-Attah, A.Y. Akrofi, B.D. Begoude, G.M. Hoopen, K. Coulibaly, *Phytophthora megakarya* and *Phytophthora palmivora*, closely related causal agents of cacao black pod rot, underwent increases in genome sizes and gene numbers by different mechanisms, Genome Biol. Evol. 9 (2017) 536–557, doi:10.1093/gbe/evx021.

[10] E.K. Al-Dous, B. George, M.E. Al-Mahmoud, M.Y. Al-Jaber, H. Wang, Y.M. Salameh, E.K. Al-Azwani, S. Chaluvadi, A.C. Pontaroli, J. DeBarry, V. Arondel, De novo genome sequencing and comparative genomics of date palm (*Phoenix dactylifera)*, Nat. Biotechnol. 29 (2011) 521–527, doi:10.1038/nbt.1860.

[11] R. Singh, M. Ong-Abdullah, E.T.L. Low, M.A.A. Manaf, R. Rosli, R. Nookiah, L.C. Ooi, S.E. Ooi, K.L. Chan, M.A. Halim, N. Azizi, N. Jayanthi, B Blaire, L. Nathan, W. Steven Smith, H. Dong, H. Michael, M.A. Budiman, E.K. Lee, R. DeSalle, D. Kudrna, J.L. Goicoechea, R.A. Wing, R.K. Wilson, R.S. Fulton, M.J. Ordway, R.A. Martienssen, R. Sambanthamurthi, Oil palm genome sequence reveals divergence of interfertile species in Old and New worlds, Nature 500 (2013) 335–339, doi:10.1038/nature12309.

[12] A. Conesa, S. Götz, J.M. García-Gómez, J. Terol, M. Talón, M. Robles, Blast2GO: a universal tool for annotation, visualization and analysis in functional genomics research, Bioinformatics 21 (2005) 3674–3676, doi:10.1093/bioinformatics/bti610.

Check for updates

Received: 9 April 2020 | Revised: 2 February 2021 | Accepted: 3 February 2021

DOI: 10.1111/jph.12988

ORIGINAL ARTICLE

Journal of Phytopathology WILEY

# A rapid in vitro leaf inoculation assay to investigate *Phytophthora palmivora*–coconut interactions

Gangaraj Karyath Palliyath[1,2] | Muralikrishna Kilingar Subrahmanya[1] | Ginny Antony[3] | Sahu Binod Bihari[4] | Vinayaka Hegde[1] | Rajesh Muliyar Krishna[1]

[1]ICAR-Central Plantation Crops Research Institute, Kasaragod, India

[2]Department of Biosciences, Mangalore University, Mangalagangotri, India

[3]Central University of Kerala, Kasaragod, India

[4]National Institute of Technology, Rourkela, India

**Correspondence**
Rajesh Muliyar Krishna, ICAR-Central Plantation Crops Research Institute, Kasaragod, India.
Email: rajesh.mk@icar.gov.in

**Funding information**
Indian Council of Agricultural Research, Grant/Award Number: ICAR-CPCRI Project No. 1000765039

## Abstract

Bud rot, caused by *Phytophthora palmivora*, is one of the major lethal diseases of the coconut palm. It is a sporadic disease but can assume epidemic proportions occasionally. There is a high risk involved in carrying out studies of plant–pathogen interactions through field trials, especially in a crop like coconut. We have developed an in vitro leaf assay, which would enable an easy and close monitoring of interactions occurring between *P. palmivora* and coconut during the course of infection by recreating the field infection process in the laboratory. Spindle leaves from adult coconut palms were surface sterilized and inoculated in basal Y3 medium in Petri plates. After a week in culture, the surface of the leaves was pricked and inoculated with zoospore suspension of *P. palmivora* culture. Typical lesion development was noticed on the surface of the coconut leaves 12–24 hr after inoculation of the pathogen. Electrolyte leakage assays and histological studies using scanning electron microscopy, were also undertaken to study the disease progression. The presence of the pathogen in the coconut leaflets was confirmed using PCR and RT-PCR with *Phytophthora*-specific primers. The pathogen could be re-isolated from the infected regions, fulfilling Koch's postulates. The novel in vitro leaf assay developed through this study is rapid, space-effective, precise and inexpensive. It could be utilized for detailed investigations of the qualitative interactions between coconut and *P. palmivora*.

**KEYWORDS**
bud rot, coconut, in vitro inoculation, leaf assay, *Phytophthora palmivora*

## 1 | INTRODUCTION

*Phytophthora* spp. are notorious phytopathogens with a substantial global impact as they affect an extensive array of crops ranging from vegetables, ornamentals, plantation crops to forest trees. Placed under Stramenopiles (syn. Heterokonta; kingdom Chromista, SAR super-group), they are oomycetes which can produce hyphae (Cavalier-Smith, 2018). While some species like *P. ramorum* and *P. sojae* possess a narrow host range, others like *P. cactorum* and *P. palmivora* have a broad host range (Erwin & Ribeiro, 1996). Coconut (*Cocos nucifera* L.), eulogized as the *'Tree of Life'*, forms an essential backbone of the economies of regions along the tropics. Apart from the importance of copra and coconut oil, which is widely used as edible oil and in the manufacture of hair oils, soaps, cosmetics and other industrial products, the husk is a source of fibre which supports a sizeable coir industry. The tender nut supplies coconut water, a popular thirst quencher of health and hygienic value. *P. palmivora* and *P. katsurae* have been mainly associated with diseases of the coconut palm (Dollet et al., 2012). *P. palmivora* is the only species reported till date as a pathogen infecting coconut palms in

India and causes bud rot disease, which causes significant economic loss to the palms in states of Kerala, Karnataka, Tamil Nadu and Andhra Pradesh (Srinivasulu et al., 2008). It is usually a fatal disease of the coconut palm, characterized by the rotting of the terminal bud and surrounding tissues. Even though it affects the palms of all ages, young palms in low lying and moist situations are more susceptible to the disease. The disease is usually sporadic but has been reported to assume epidemic proportions (Srinivasulu & Raghava Rao, 2009). Climatic conditions play a significant role in the disease spread and its severity (Srinivasulu et al., 2008).

Detection of the disease in the early stages and adopting appropriate remedial measures may avert the palm's eventual loss. Integrated disease management strategies are recommended throughout the year, especially in endemic areas, for effectively managing the disease. Severely affected trees need to be removed and burnt. If disease detection is done early, the infected tissue has to be removed and the cut portion protected with Bordeaux paste (Chidananda & Pandurang, 2001; Ramesh & Maruthadurai, 2014).

Crop breeding programmes, aiming for development of disease-resistant cultivars, assume significance in a crop like coconut given the cryptic nature of the *P. palmivora* and its detection at a stage in which successful control measures can be implemented. Whole plant testing is of limited relevance for large-scale screening of bud rot disease in coconut for apparent reasons; also, studies can be restricted only to seedlings in containment/quarantine facilities or assessment in regions with a history of disease outbreaks. A deep understanding of molecular mechanisms underlying plant–pathogen interactions could enable novel approaches for crop protection. One of the techniques frequently used for investigating plant defence responses to pathogens, under laboratory conditions, is the detached leaf assay, which has been utilized in several studies such as soybean (Surin et al., 1993), wheat (Arraiano et al., 2001), alfalfa (Irwin et al., 2003), rice (Jia et al., 2003) and durian (Vawdrey et al., 2005). This laboratory assay possesses several advantages: higher reproducibility, the requirement of less space, labour, plant materials and inoculum, more consistent delivery of inoculum, uniform incubation conditions can be maintained, inoculation site can be localized to specific areas of the leaf, and more accurate quantification of disease is possible (Dhingra & Sinclair, 1995). Besides, contamination can be controlled, more replicates can be maintained, and there is no risk of spreading the phytopathogen to the environment. However, this assay also possesses disadvantages: detached leaves may not be a typical reflection of the variability of whole plants in terms of actual physical condition and age/phyllotaxy of leaves, and some of the host defence responses may be attenuated in detached leaves (Parke et al., 2005).

Histopathological and molecular events occurring during *P. palmivora* infection have not been reported in coconut. In the current study, an in vitro leaf assay was developed through challenge inoculation of *P. palmivora* on the coconut leaf segments cultured in vitro. Tracking of the infection and disease progression was undertaken using histological studies, electrolyte leakage assays, and PCR and RT-PCR with specific primers. This assay would enable detailed molecular investigations on the cascade of events during *P. palmivora* infection in coconut.

## 2 | METHODOLOGY

### 2.1 | Isolation and morphological characterization of the pathogen

Samples were collected from bud rot affected coconut palms from Kasaragod and Dakshina Kannada districts of Kerala and Karnataka state, respectively, India, during South-West monsoon season (June-July) in 2017 (Table 1). The infected palms showed typical symptoms such as decaying of the spindle leaf and its bending, commonly associated with bud rot disease (Figure 1a). The palms' infected bud region (Figure 1b) also had a characteristic foul smell and conspicuous irregular water-soaked lesions in the leaf lamina (Figure 1c).

Along with young infected leaves, the bud region was collected in an autoclaved polythene bag and brought to the laboratory in an icebox. Tender leaves with lesions were separated in laminar airflow. Segments of 1 × 1 cm size were surface sterilized by rinsing with a 0.01% mercuric chloride solution followed by washing in sterile distilled water thrice. Direct plating method (Chowdappa et al., 2014) was used to isolate pathogen by placing the leaf segments in carrot agar medium supplemented with rifampicin (125 ppm). The inoculated samples were kept in a growth chamber with a constant temperature (25 ± 2°C) and humidity (95%). The individual isolates obtained were characterized through morphological traits as detailed by Gallegly and Hong (2008). Mating or compatibility type of *P. palmivora* isolate was determined using the method adopted by Chowdappa and Chandramohanan (1997) where the isolates were paired with known *Phytophthora* isolates obtained from ICAR-Indian Institute of Spices Research (ICAR-IISR), Kozhikode, Kerala, India. Individual isolates were inoculated separately on to carrot broth medium and maintained at 25 ± 2°C for the formation of mycelial mats. They were filtered and washed thoroughly with sterile water and dried using sterile filter paper.

### 2.2 | Molecular characterization of the pathogen

To confirm the identity of each *Phytophthora* species, DNA was extracted from the mycelial mats of individual isolates using the DNeasy Plant Mini Kit (Qiagen, USA). The ITS6 (5'-GAAGGTGAAGTCGTAACAAGG-3') and ITS4 (5'-TCCTCCGCTTATTGATATGC-3') primer pairs (Cooke et al., 2000; White et al., 1990) were used to amplify the complete sequence of 5.8S ribosomal RNA gene, and I and II spacer regions completely and partial sequence of 18S ribosomal RNA gene and 28S ribosomal RNA gene regions of the pathogen. PCR, gel electrophoresis, elution of bands, sequencing and sequence analysis were conducted as described by Prathibha et al. (2018). A phylogenetic tree was

**TABLE 1** List of *Phytophthora palmivora* isolates collected in the present study

| Sl. No. | District/State | Place of collection | Isolate no. | GPS co-ordinates |
|---|---|---|---|---|
| 1. | Kasaragod/Kerala | Mannipady | TR-PP–1 | 12°32'12.1"N 74°59'55.5"E |
| 2. | Kasaragod/Kerala | Pachakkad | TR-PP–2 | 12°32'38.0"N 74°57'45.7"E |
| 3. | Dakshina Kannada/Karnataka | Kidu | TR-PP–3 | 12°42'25.1"N 75°34'27.6"E |
| 4. | Kasaragod/Kerala | Konnakkad | TR-PP–4 | 12°21'59.3"N 75°22'35.7"E |
| 5. | Kasaragod/Kerala | Elerithattu | TR-PP–5 | 12°19'54.3"N 75°18'33.0"E |

**FIGURE 1** Bud rot infection in coconut palm. (a) Bud rot-infected palm. (b) The bud region of the infected palm showing decaying. (c) Leaf lamina of the infected palm showing typical water-soaked lesions [Colour figure can be viewed at wileyonlinelibrary.com]

constructed based on ITS sequence of TR-PP-2 isolate with other *P. palmivora* isolates, including various species of *Phytophthora*, *Pythium*, *Peronospora* and *Fusarium*, sourced from GenBank, with the software MEGA -X version 10.2.0 (Kumar et al., 2018) using the neighbour-joining (NJ) method (Saitou & Nei, 1987) under 1,000 bootstrap replicates. The details of selected species for phylogenetic analysis are listed in Supplementary Table S1.

## 2.3 | Screening *P. palmivora* isolates for virulence levels

*P. palmivora* isolates collected from bud rot affected palms were initially screened for their virulence level using the detached leaf technique (Sharadraj & ChandraMohanan, 2014). For this, zoospore suspensions were prepared from the isolates by growing 5-mm mycelial disc in carrot agar and incubated at 25 ± 2°C. After sporulation at the 7th day, sterile distilled water (20 ml) was added and incubated at 15°C for 15 min. Plates were then kept at room temperature till the release of zoospores (for approximately 20 min). The concentration of zoospores was standardized based on the procedure given in Mohamed-Azni et al. (2017). A haemocytometer (Rohem, India) was utilized for the calculation of zoospore concentration. A series of inoculum concentrations, *viz*., 1, 2, 3, 4 and $5 \times 10^4$/ml, were prepared to determine the zoospore concentration capable of inducing severe infection. Based on this experiment, the zoospore concentration was fixed at $2 \times 10^4$/ml.

To screen its virulence, spindle leaves, sampled from Chowghat Orange Dwarf (COD), a cultivar susceptible to bud rot, were wiped with sterile water and pricked (four times) on its dorsal side with a sterile needle to facilitate easy entry of the pathogen to the leaf and kept above sterile test tubes lying horizontally on wet cotton in a tray. Ten microlitres of zoospore suspensions ($2 \times 10^4$/ml) of each isolate were individually inoculated in the pricked region, and the inoculated area was covered with a thin layer of wet cotton. The entire set-up was covered with a polythene sheet and kept in a humid chamber at 25 ± 2°C (Rachana & Rajesh, 2019; Sharadraj & ChandraMohanan, 2014). Different isolates were screened for its level of virulence based on the time required for the initiation of infection and the size of the lesion formed after five days of inoculation. The highly virulent isolate of *P. palmivora* obtained from this exercise was used for the rest of the studies.

## 2.4 | In vitro leaf assay

Spindle leaves, sampled from three-year-old COD palm, were cleaned by swiping with 70% ethanol, and the midrib portion was removed (Figure 2a-f). Leaf lamina was cut into segments (approx. 5 cm) aseptically under laminar airflow chamber (Figure 2g), surfaced sterilized with mercuric chloride (0.01%) for 10 min with constant shaking (Figure 2h) and then washed 4–5 times in sterile water (Figure 2i). These leaf segments were then placed with its dorsal side upwards in Y3 medium (Eeuwens, 1976), supplemented with sucrose (30 g/L), agar (6.5 g/L) and charcoal (0.5 g/L), in Petri plates (Figure 2j). All the cultures were kept at 25 ± 2°C and 95% humidity in a plant growth chamber (Panasonic MLR-352H-PE). After a week in culture, leaf

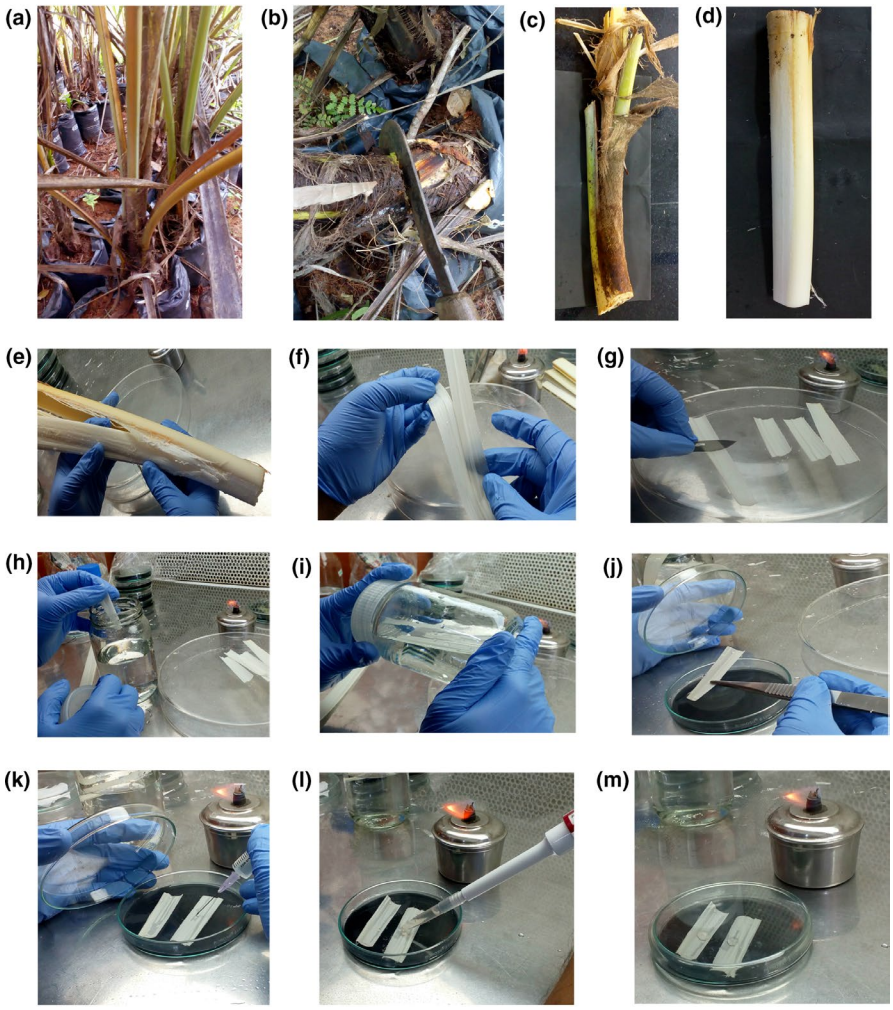


**FIGURE 2** In vitro leaf inoculation assay followed. (a) Three-year-old Chowghat Orange Dwarf seedling. (b-e) Collection of bud tissues from seedlings. (f) Separating the leaf tissues. (g) Making tissue bits. (h) Surface sterilization. (i) Subsequent washing. (j) Inoculation of leaf bit on Y3 media. (k) Pinpricking on leaf bit using a sterile syringe. (l) Inoculation of *Phytophthora palmivora* zoospore suspension on leaf bit. (m) Inoculated leaf bit [Colour figure can be viewed at wileyonlinelibrary.com]

lamina segments were pricked (five equal pricks) using a sterile needle (Figure 2k) before inoculation with zoospore suspension (10 µl) of the highly virulent isolate (Figure 2l & 2m). Non-inoculated leaf segments with similar pricks served as control. Cultures were observed at regular intervals to record the initiation of infection, its advancement and other attributes such as the size of the lesions. Postinfection, the identity of pathogen was confirmed through morphological and molecular techniques, as described earlier.

## 2.5 | Leaf viability assay using membrane stability index

The viability of the in vitro cultured leaf segments was assessed using membrane stability index (Sairam et al., 1997) since this parameter is negatively related to senescence or leaf death (Gupta et al., 2012). Detached leaflets were taken for comparison. Approximately 100 mg of leaf segments were taken, immersed in 10 ml distilled water and initial electrical conductivity ($\mu Scm^{-1}$; Model PP20, Sartorius) was determined (C1) after overnight incubation in room temperature. Final electrical conductivity was determined (C2) after placing the test tubes in boiling water for 30 min. The membrane stability index (MSI) was calculated as:

$$MSI = \{1 - (C1/C2)\} \times 100$$

## 2.6 | Histopathological studies using scanning electron microscopy

For scanning electron microscopy, leaf bits (1 x 1 cm) with infected portion were placed in aluminium cylinder adhered with a graphite tape and placed in a vacuum chamber. The sample was coated with high vacuum evaporator for six minutes in an ionizing metal JEOL JFC-1100 (Fine Coat® sputter ion, JEOL Ltd). The gold-coated samples were observed in a scanning electron microscope (JEOL-JSM-6490LV) under vacuum to get higher resolution.

## 2.7 | Disease assays and pathogenicity tests

To satisfy Koch's postulate, pieces of in vitro inoculated leaf bits, showing disease lesions at 48 hpi, were removed from the Petri

plates, surface sterilized with 70% ethanol, plated on to carrot agar medium in Petri plates and maintained at 25 + 2°C and 95% humidity in a plant growth chamber (Panasonic MLR-352H-PE). Subsequent growth of mycelia was recorded. Pathogenicity tests were conducted by detached leaf assay (Sharadraj & ChandraMohanan, 2014), as mentioned in Section 2.3.

## 2.8 | RNA extraction and expression studies

Infected leaf samples collected for the isolation of RNA, include samples 12 hr postinoculation (12 hpi) and 12 hr uninoculated control (12 hc), 24 hr postinoculation (24 hpi) and 24 hr uninoculated control (24 hc) and 36 hr postinoculation (36 hpi) and 36 hr uninoculated control (36 hc). Total RNA was extracted from these samples using the NucleoSpin® RNA Plant Kit (Macherey Nagel). The quality and the purity of the extracted RNA were assessed by observing the absorbance from$A_{260/280}$ ratio. RNA integrity number was analysed using an Agilent Technologies 2,100 Bioanalyzer with the Agilent RNA chip. cDNA was synthesized using the PrimeScript cDNA Synthesis Kit (Takara). The reaction mixture included 4.0 µl of 5 X PrimeScript buffer, 1 µl of PrimeScript RT enzyme mix, 1 µl of random hexamer primer and 100 ng of RNA. The reactions were incubated at $37^0$C for 15 min, followed by $85^0$C for 5 s and then kept at $4^0$C. *Phytophthora* spp. are known to secrete numerous effectors into their hosts to promote infection, and therefore, the expression of effector genes is up-regulated during the infection process (Wang & Jiao, 2019). Primer pairs were designed for an RxLR effector (POM73696.1) previously reported in *P. palmivora* (Ali et al., 2017). Also, 40S ribosomal gene (G40S) was taken as an internal control for *P. palmivora* (Ali et al., 2017), while eukaryotic translation initiation (CneIF-4γ) from coconut was taken as an internal control for coconut (Rachana & Rajesh, 2019). The details of the primers are given in Table 2.

After cDNA synthesis, RT-PCR was conducted on a thermal cycler (MJ Mini™, Bio-Rad). Each reaction included 1 µl of diluted cDNA (~200ng), 1 µl of forward and reverse primer (0.5 µmol), 10 µl of GeNei™ Red Dye PCR Master Mix (1X) and 6 µl distilled water. The reactions conditions were 94°C for 2 min, followed by 34 cycles of 94°C for 30 s, 55°C for 1 min, 72°C for 1 Min, and a final extension at 72°C for 10 min. Samples were visualized on 1.5% agarose gel electrophoresis (Blue Marine) in 1X TBE buffer and documented.

## 2.9 | Statistical analysis

For statistical analysis, the data recorded on the size of the lesions and their relative growth rates due to infection by *P. palmivora*, and the membrane stability index (MSI) in in vitro cultured coconut leaf segments in comparison to detached leaflets, were subjected to one-way analysis of variance (ANOVA) as the experiment was laid out in completely randomized design (CRD). The means obtained were then compared using Duncan's multiple range test (DMRT) using SPSS 15.0.

# 3 | RESULTS

## 3.1 | Initiation of cultures and morphological characterization

Strains isolated from bud rot infected palms and cultured in carrot agar medium, showed similar morphological attributes like greyish white colony, with stellate colony pattern, the colony possessing sharp well-defined leading edges (Figure 3a). The growth rate of the cultures was 1–1.3 $cm^2$/day, and among the isolates, TR-PP-5 recorded the maximum growth rate (1.3 $cm^2$/day). The isolates showed network-like mycelia without cross walls (Figure 3b). Also, abundant ovoid to ellipsoid sporangia, with a round base and conspicuous papilla were produced (Figure 3c). The sporangia of the pathogen showed sympodial arrangement and were caducous, breaking away rapidly from sporangiophore. The average size of sporangia was found to be 59.03 × 26.63 µm with 2.21 LB ratio. Globose chlamydospores were found terminal as well as intercalary on mycelia of the isolate (Figure 3d). The average diameter of the chlamydospore was 27 µm. All the isolates found to be A2 mating type. The oogonia were spherical, and the average size was 34 µm (Figure 3e). All the above said morphological features are highly similar to those reported for *P. palmivora*. Challenge inoculation on the detached leaflets indicated that necrotic lesions reached a maximum size (7.11 $cm^2$) on the fifth day after inoculation (Figure 3f). Among the isolates, the isolate TR-PP-2 showed the highest virulence in detached leaf assay. Hence, this isolate was used for the rest of the study.

**TABLE 2** Primers used for amplification of genes of host and pathogen genes via RT-PCR

| Sl. No. | Gene name (organism) | Primer name | Primer sequence (5'–3') | Product size (bp) |
|---|---|---|---|---|
| 1. | Eukaryotic initiation factor- 4γ (*CneIF–4γ*) (*C. nucifera*) | CneIF–4γF | CACCAGGAGACTTGGGAACT | 110 |
| | | CneIF–4γR | CAGCTTACCAACCACTTCACC | |
| 2. | 40 S rRNA (*G40S*) (*P. palmivora*) | G40SF | AACTCTGATTGAGGCCTTCG | 243 |
| | | G40SR | AACTCTGATTGAGGCCTTCG | |
| 3. | RxLR effector (*GRxLR*) (*P. palmivora*) | GRxLRF | CCTTCAAGCGGTAATCCAAA | 244 |
| | | GRxLRR | ATGACCCTTGTGGTTCTTGC | |

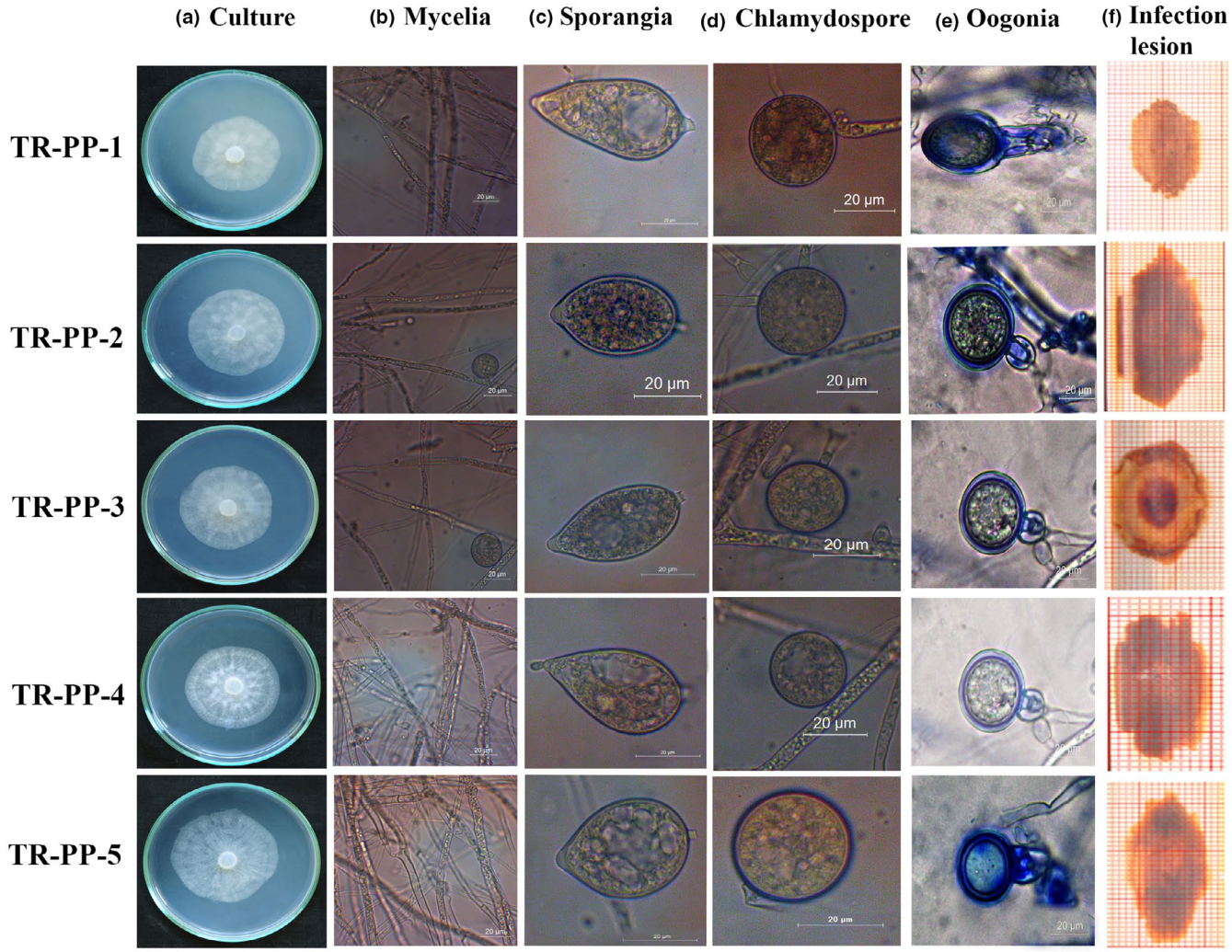


**FIGURE 3** (a-e) Colony morphology of different isolates (TR-PP-1 to TR-PP-5). (f) The infection lesions on the detached leaflet of coconut [Colour figure can be viewed at wileyonlinelibrary.com]

## 3.2 | Molecular characterization of the virulent isolate

Molecular characterization of the isolate TR-PP-2 was undertaken using *Phytophthora*-specific internal transcribed spacer (ITS) primers. The expected amplicon of around ~ 900 bp was obtained (Figure 4). The amplicon was sequenced, and a sequence of 846 bp (48.6% G + C) was obtained (GenBank accession no. MK500842.1). The phylogenetic tree constructed, based on NJ method, based on 23 ITS regions of the different *Phytophthora* spp. and other phytopathogens, revealed two main clusters (Figure 5). Within the first main cluster, the isolate TR-PP-2 formed a separate sub-cluster with other *P. palmivora* isolates from coconut, cocoa and oil palm. Also, TR-PP-2 isolate was genetically closest to a *P. palmivora* isolate from coconut from India (GenBank accession no. AM422704). *P. megakarya* represented the closest group to other *P. palmivora* isolates. The second sub-cluster within the first main cluster was formed by *Peronospora* spp. and *Pythium* spp. formed the third sub-cluster. *Fusarium* isolates formed the second main cluster.

## 3.3 | In vitro leaf assay

The morphological and molecular level characterization confirmed the causal agent as *P. palmivora* and challenge inoculation study verified its virulence. When the TR-PP-2 isolate was inoculated in the pricked portion of the spindle leaf segment cultured in Eeuwens Y3 medium, mild necrotic lesions were first observed by 24 hpi. The lesion became more extensive and more conspicuous with an irregular pattern 48 hpi. No significant changes were observed on the leaf surface of the control samples. The necrotic lesion reached an average of 228 $mm^2$ on the fourth day after inoculation (Figures 6 and 7).

Viability of the leaf segments cultured on in vitro medium was revealed through membrane stability index (MSI) assay. Preliminary

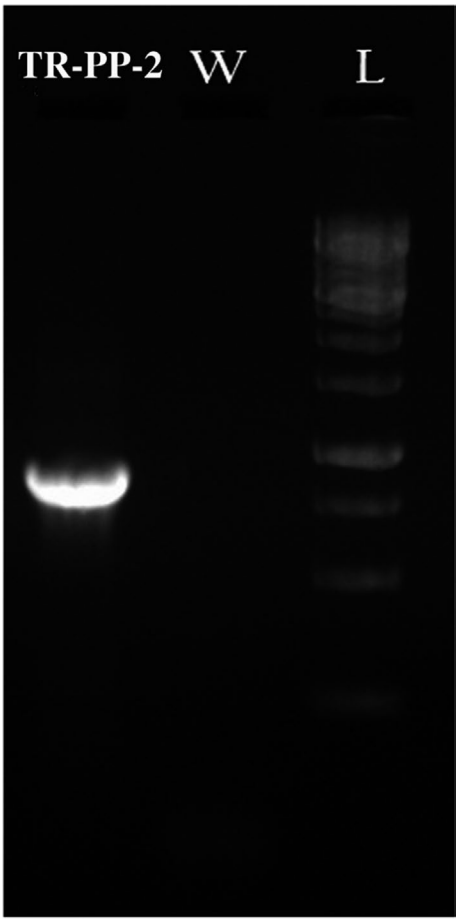


**FIGURE 4** Molecular characterization of the isolate TR-PP-2. Gel image of the amplicon (TR-PP-2: *Phytophthora palmivora* DNA, W: -ve control and 1Kb L: 1Kb Ladder)

observations indicate that MSI did not decrease significantly in the leaf segments even at 20 days of in vitro culturing in the medium, whereas it rapidly decreased in detached leaflets (Figure 8).

### 3.4 | Assessment of infection by scanning electron microscopy

Scanning electron micrographs of the leaf segments from this in vitro leaf assay gave further evidence on the pathogen interaction. It revealed the development of hyphae along the epidermal cell surface with an appressoria like hyphae and its penetration along the walls of the trichome. Fungal hypha seems to emerge through stomata to produce sporangial structures at the surface of the epidermal layer. In the later stages of the infection, the sporangial formation and network like hyphae on the surface seem to proliferate to form lesions (Figure 9).

### 3.5 | Pathogenicity studies

Re-isolation of the pathogen from the lesions in the leaflets (48 hpi), of in vitro leaf assay, fulfilled Koch's postulates. When cultured in carrot agar medium, the pathogen exhibited similar morphological characteristics like greyish white colony, with stellate colony pattern, with sharp well-defined leading edges. Detached leaf inoculation experiments, with zoospores derived from the mycelia, resulted in typical lesions in the leaves, with initial symptoms being observed at 24 hpi.

### 3.6 | RT-PCR analysis

RT-PCR analysis revealed amplification of coconut housekeeping gene (CneIF-4γ) in both uninoculated and inoculated leaf samples at all the three time points (12, 24 and 36 hpi). The expression of *P. palmivora* housekeeping gene (G40S) could be observed only in inoculated leaf samples at all the three time points (12, 24 and 36 hpi) and not in uninoculated samples. Expression of *P. palmivora* RxLR effector gene (*GRxLR*) was observed only in inoculated leaf samples at 24 and 36 hpi (Figure 10).

## 4 | DISCUSSION

*Phytophthora palmivora* infects approximately 170 different plant species in the tropics. The management of this destructive phytopathogen has been dependent on various cultural and chemical techniques and resistance breeding. Standard screening protocols for crops, for assessing resistant/susceptible plantlets against phytopathogens, include spraying plants with conidial suspensions of pathogen isolates (Xu & Ko, 1998) under greenhouse or field condition. However, these strategies are challenging to adopt in a crop like coconut. Interaction studies of this pathogen with coconut have been challenging due to the lack of an easy, reliable and practical assay method for extensive screening. The palm structure and the long life cycle limit the feasibility of whole plant pathogenicity tests in coconut. Therefore, in this study, we have attempted to mimic the infection progression, occurring in actual field conditions, under in vitro conditions in the laboratory.

We have initially screened multiple isolates of *P. palmivora* collected from various regions of Kerala and Karnataka States, India, during the peak monsoon season, for their virulence using the detached leaf technique. We have undertaken primary identification of these isolates utilizing morphological characteristics. All the isolates exhibited morphological traits similar to those reported previously for *P. palmivora* (Erwin & Ribeiro, 1996; Martin et al., 2012; Martínez et al., 2010). The mycelia are network-like and without any cross walls, while the sporangia are ovoid and ellipsoid, possessing a round base and conspicuous papilla. Among the four isolates, TR-PP-2 was identified as the most virulent among the isolates based on the lesion size (Figure 4). The most virulent isolate's identity was further validated by identifying the ITS sequence data via BLASTN and phylogenetic analysis. Phylogenetic analysis, undertaken using ITS sequence data, clustered the *P. palmivora* TR-PP-2 isolate with other *P. palmivora* isolates and *P. megakarya* (Figure 5); both these species have been

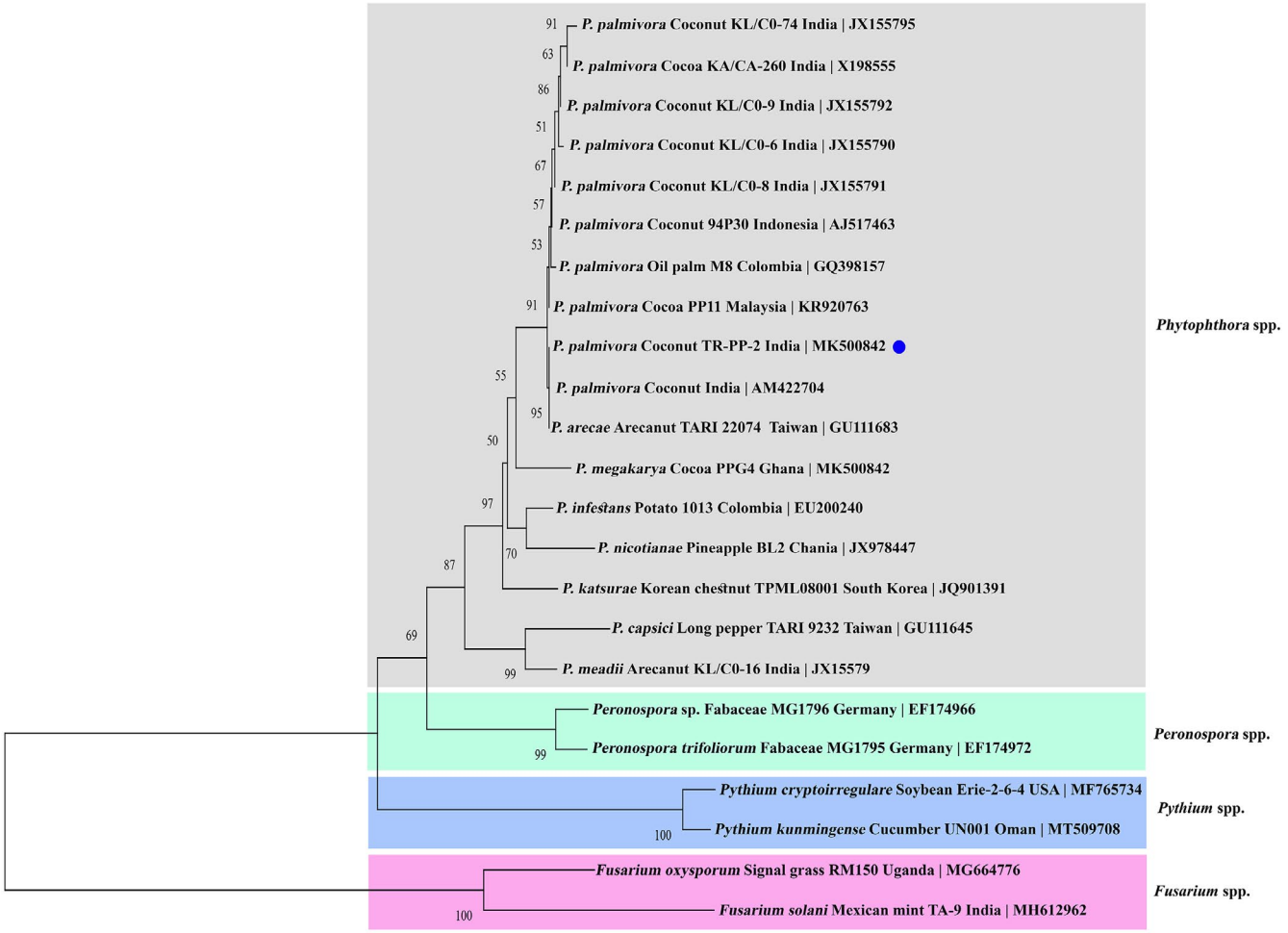
91 P. palmivora Coconut KL/C0-74 India | JX155795
63 P. palmivora Cocoa KA/CA-260 India | X198555
86 P. palmivora Coconut KL/C0-9 India | JX155792
51 P. palmivora Coconut KL/C0-6 India | JX155790
67 P. palmivora Coconut KL/C0-8 India | JX155791
57 P. palmivora Coconut 94P30 Indonesia | AJ517463
53 P. palmivora Oil palm M8 Colombia | GQ398157
91 P. palmivora Cocoa PP11 Malaysia | KR920763
P. palmivora Coconut TR-PP-2 India | MK500842
55 P. palmivora Coconut India | AM422704
95 P. arecae Arecanut TARI 22074 Taiwan | GU111683
50 P. megakarya Cocoa PPG4 Ghana | MK500842
97 P. infestans Potato 1013 Colombia | EU200240
70 P. nicotianae Pineapple BL2 Chania | JX978447
87 P. katsurae Korean chestnut TPML08001 South Korea | JQ901391
69 P. capsici Long pepper TARI 9232 Taiwan | GU111645
99 P. meadii Arecanut KL/C0-16 India | JX15579
Phytophthora spp.
Peronospora sp. Fabaceae MG1796 Germany | EF174966
99 Peronospora trifoliorum Fabaceae MG1795 Germany | EF174972
Peronospora spp.
Pythium cryptoirregulare Soybean Erie-2-6-4 USA | MF765734
100 Pythium kunmingense Cucumber UN001 Oman | MT509708
Pythium spp.
Fusarium oxysporum Signal grass RM150 Uganda | MG664776
100 Fusarium solani Mexican mint TA-9 India | MH612962
Fusarium spp.

**FIGURE 5** Phylogenetic tree, constructed from 23 ITS sequence data, depicting the evolutionary relationships of *Phytophthora palmivora* isolates. Numbers at nodes indicate the bootstrap values in percentage (%) [Colour figure can be viewed at wileyonlinelibrary.com]

placed together in Clade 4 based on comprehensive phylogenetic studies undertaken by Yang et al. (2017).

The TR-PP-2 isolate was further used for standardizing the in vitro leaf assay. This isolate caused necrotic lesions on all treated samples, and lesions were first observed 12 hr postinoculation, after which it increased in size (Figure 5). Under field conditions, as the infection progresses, sunken leaf spots are visible on leaves, the spot margins being irregular in shape and are water-soaked (Srinivasulu et al., 2008). The symptom development and its characteristics under in vitro leaf assay were consistent with the symptoms occurring under natural conditions in the field.

The membrane stability index (MSI) of in vitro cultured leaf segments did not change significantly for up to 20 days in the media suggesting that the medium used (Y3) keeps the leaf healthy and turgid till the symptoms develop and most importantly this method did not affect the virulence of the pathogen *P. palmivora* (Figure 7). The consistent MSI indicates the viability as this parameter is negatively related to senescence or leaf death (Gupta et al., 2012). However, the MSI of the detached leaflets showed a rapid decrease indicating loss of viability of leaves. This indicates that actual molecular mechanisms underlying pathogen–host interactions cannot be studied in the detached leaves.

Further, the detection of the pathogen could be performed successfully, and the symptom of the spread of the mycelia and secondary growth assessment was substantiated by SEM (Figure 8). The growth of the lesion size over time and the scanning electron micrographs suggest that the detached in vitro leaf assay is reliable and the interaction between the pathogen and the host proceeds normally akin to field conditions. Also, the conditions of incubation have minimal effect on disease development. The pathogenicity of isolates was investigated by detached leaf assay. Zoospores, derived from mycelia from isolated regions of in vitro infected leaves, could further infect the leaves in detached leaf assays, fulfilling Koch's postulates.

*Phytophthora* spp. secrete several effector proteins into plants, to suppress the basal plant immunity and promote infection (Wang & Jiao, 2019). To confirm the interaction at the molecular level, we used RT-PCR to detect the secretion or presence of effectors in the inoculated leaves. *P. palmivora* effector gene, *GRxLR*, was detected at 24 hpi and 36 hpi (Figure 10). The internal control for *P. palmivora*

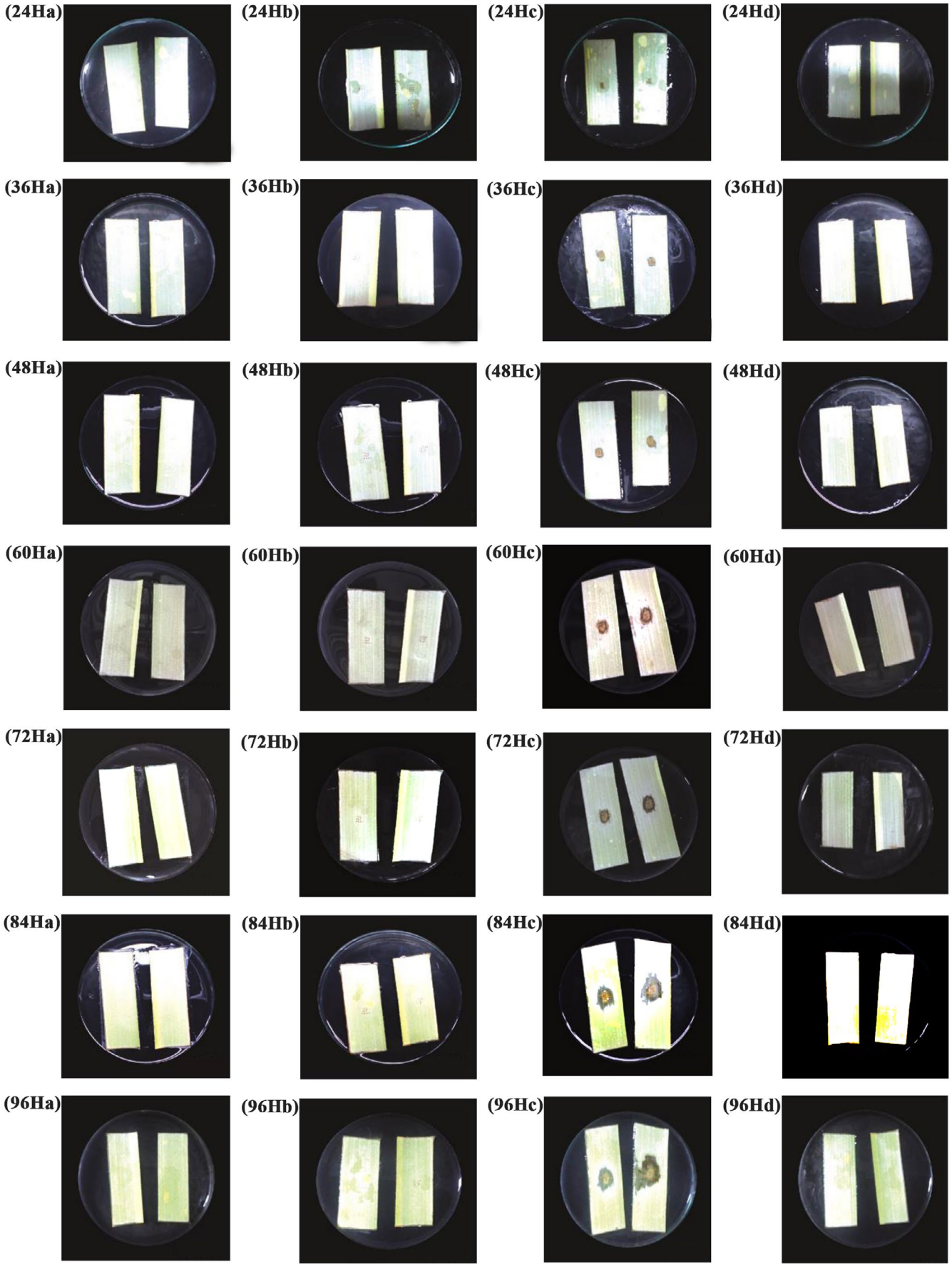


**FIGURE 6** In vitro inoculation of *Phytophthora palmivora* on coconut spindle leaf. Ha: un-pricked and uninoculated; Hb: pricked and uninoculated, Hc: pricked and inoculated and Hd: un-pricked and inoculated. Observations were taken at 24, 36, 48, 60, 72, 84 and 96 hr postinoculation (hpi) [Colour figure can be viewed at wileyonlinelibrary.com]

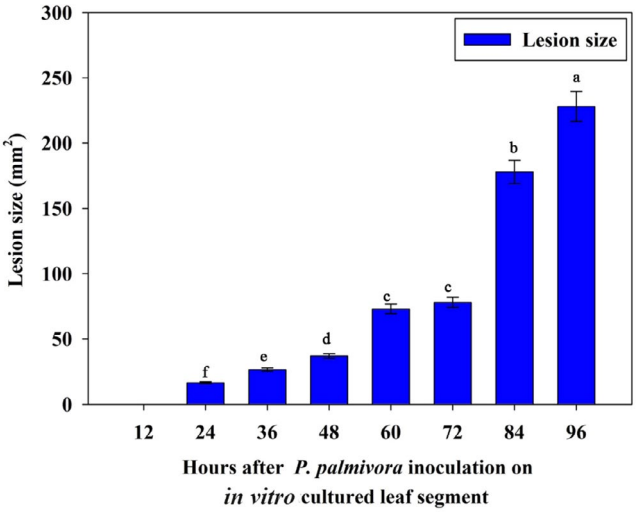


**FIGURE 7** Size of the lesions and their relative growth rate caused by the *P. palmivora* on coconut leaf segments cultured in vitro. Observations were taken at 24, 36, 48, 60, 72, 84 and 96 hr after inoculation [Colour figure can be viewed at wileyonlinelibrary.com]

G40S was detectable at 12 hpi (Figure 10). The detection of effector in the in vitro leaf assay suggests the feasibility of using this method to map and study finer aspects of host-pathogen interactions, especially identification of specific effectors.

In our study, we observed that wounding was required for producing localized lesions using the in vitro leaf assay in coconut, which corroborates the previous report of Sharadraj and ChandraMohanan (2014) who had reported the same observation using detached leaflets. One reason could be the presence of epicuticular wax (Escalante et al., 2002; Riedel et al., 2009) and phenols in mature coconut leaflets (Jay et al., 1989) could form barriers to infection. Under natural conditions in the field, *P. palmivora* is known only to attack the single terminal bud or 'cabbage' of coconut, which consists of several folded embryonic leaves, but is devoid of sufficient epicuticular wax and phenols. Sarria et al. (2016) and Mohamed-Azni et al. (2019) had reported the development of typical infection in un-wounded, immature leaflets of oil palm inoculated with zoospores of *P. palmivora*. Also, the study by Mohamed-Azni et al. (2019) revealed differences in cross pathogenicity of *P. palmivora* isolates from Malaysia, on different crops. While infection was observed, either directly or via

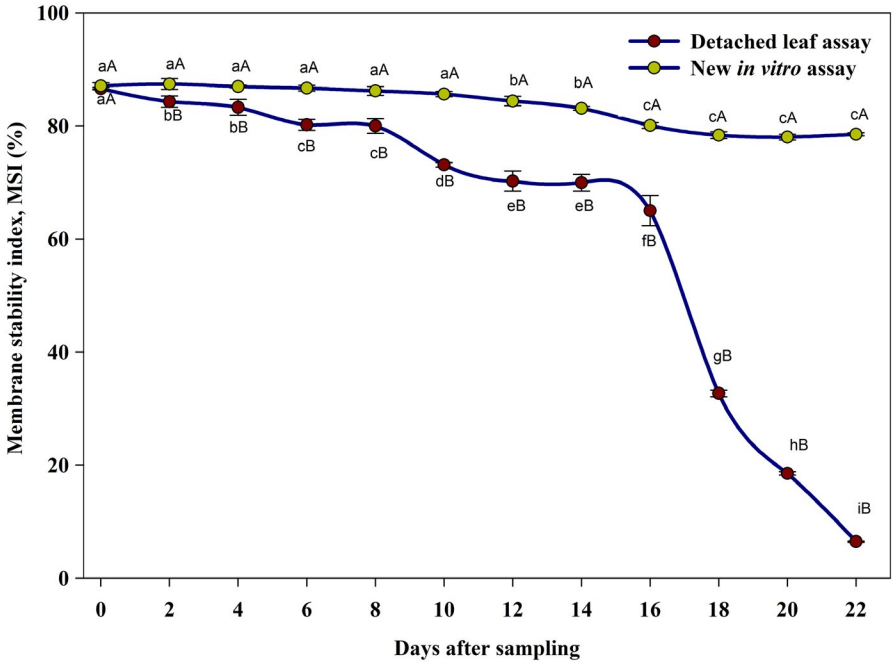


**FIGURE 8** A comparison of membrane stability index (MSI) in in vitro cultured leaf segments up to 20 days [Colour figure can be viewed at wileyonlinelibrary.com]

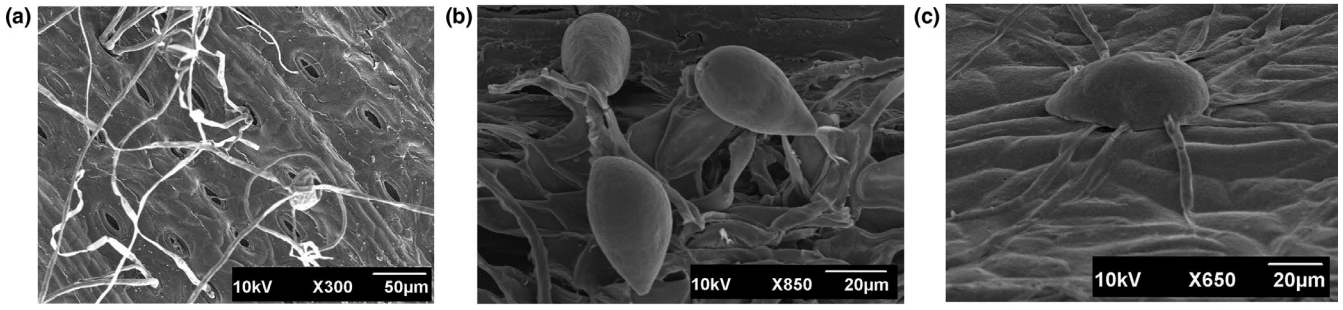


**FIGURE 9** Scanning electron micrographs of the leaf segments inoculated with *P. palmivora* using the in vitro method. (a) Mycelial growth through stomata, (b) Sporangia attached in trichome of the leaf and (c) Self-emerging sporangia

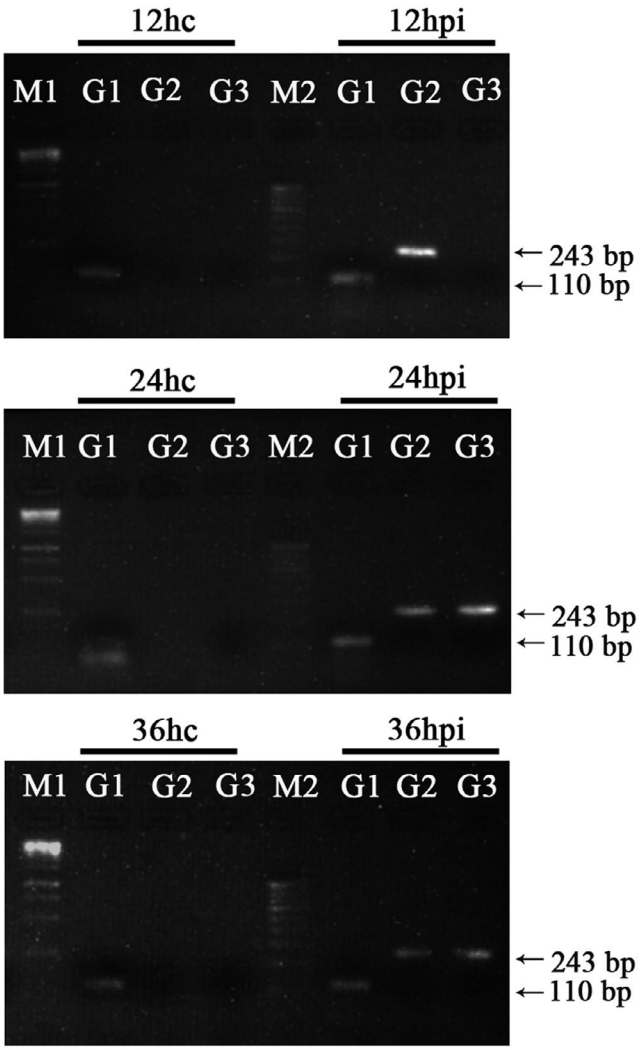


**FIGURE 10** RT-PCR products after electrophoresis; M1: 1 Kb DNA ladder; M2: 100 bp DNA ladder; G1: eukaryotic translation initiation (CneIF-4γ) in coconut; G2: 40S ribosomal gene (G40S) of *Phytophthora palmivora*; and G3: *P. palmivora* RxLR effector gene (*GRxLR*)

wounding, on cocoa, durian and rubber seedlings, it did not result in severe bud rot symptoms in oil palm. Freeman and Beattie (2008) reported that disease progression is prevented if the plant's external barriers were not damaged.

The in vitro leaf assay developed in this study requires less human resources and time for screening coconut accessions worldwide for their resistance/susceptibility to *P. palmivora*. The molecular basis underlying the pathogenesis in *P. palmivora*–coconut interaction remains unclear. This assay would be a very useful tool for the detailed examination of the repertoire of potential pathogenic molecules possessing the capacity to induce disease symptoms. This assay would also facilitate studies of the kinetics of the regulatory partners in the disease biology in coconut. The causative elements that regulate programmed cell death, and more specifically, interacting molecules in coconut can also be addressed by using the in vitro infection assay experiments.

## 5 | CONCLUSION

*P. palmivora*–coconut interaction is less studied partly due to the logistics and lack of suitable assay method. In this study, we have developed a rapid, efficient, reliable and economical method to study the pathogenicity of *P. palmivora*, which could be performed under controlled conditions and can be used to determine the effectors from *P. palmivora*. The advantage of in vitro leaf screening methods is that despite providing favourable disease expression conditions if the cultivar is identified as resistant to disease, the cultivar can further be considered for breeding programmes. Also, this method reduces the risk of the pathogen spreading to the surrounding. This method is a useful tool for epidemiological studies and beneficial for laboratories and research centres with limited plant growth facilities and minimal budget.

## ACKNOWLEDGEMENTS

The authors would like to thank the Indian Council of Agricultural Research (ICAR) for funding (ICAR-CPCRI Project No. 1000765039).

## CONFLICT OF INTEREST

The authors declare no conflict of interest.

### Peer Review

The peer review history for this article is available at https://publons.com/publon/10.1111/jph.12988.

## DATA AVAILABILITY STATEMENT

The data that support the findings of this study are openly available in NCBI at https://www.ncbi.nlm.nih.gov/nuccore/MK500842.1/

## ORCID

*Rajesh Muliyar Krishna* https://orcid.org/0000-0003-3815-0365

## REFERENCES

Ali, S. S., Shao, J., Lary, D. J., Kronmiller, B. A., Shen, D., Strem, M. D., Amoako-Attah, I., Akrofi, A. Y., Begoude, B. A. D., ten Hoopen, G. M., Coulibaly, K., Kebe, B. I., Melnick, R. L., Guiltinan, M. J., Tyler, B. M., Meinhardt, L. W., & Bailey, B. A. (2017). *Phytophthora megakarya* and *Phytophthora palmivora*, closely related causal agents of cacao black pod rot, underwent increases in genome sizes and gene numbers by different mechanisms. *Genome Biol and Evol*, *9*(3), 536–557. https://doi.org/10.1093/gbe/evx021

Arraiano, L. S., Brading, P. A., & Brown, J. K. (2001). A detached seedling leaf technique to study resistance to *Mycosphaerella graminicola* (anamorph *Septoria tritici*) in wheat. *Plant Pathology*, *50*(3), 339–346.

Cavalier-Smith, T. (2018). Kingdom Chromista and its eight phyla: A new synthesis emphasising periplastid protein targeting, cytoskeletal and periplastid evolution, and ancient divergences. *Protoplasma*, *255*(1), 297–357. https://doi.org/10.1007/s00709-017-1147-3

Chidananda, H. R., & Pandurang, G. D. (2001). *"Bud Rot Management in Coconut Palm"*. Technical Folder No.26, ICAR Research Complex for Goa (Indian Council of Agricultural Research), Old Goa-403 402, Goa, India.

Chowdappa, P., & Chandramohanan, R. (1997). Occurrence and distribution of mating types of *Phytophthora* species causing black pod disease of cocoa. *Indian Phytopathology*, *50*(2), 256–260.

Chowdappa, P., Madhura, S., Kumar, B. N., Kumar, S. M., & Hema, K. R. (2014). *Phytophthora boehmeriae* revealed as the dominant pathogen responsible for severe foliar blight of *Capsicum annuum* in South India. *Plant Disease*, *98*(1), 90–98.

Cooke, D. E. L., Drenth, A., Duncan, J. M., Wagels, G., & Brasier, C. M. (2000). A molecular phylogeny of *Phytophthora* and related oomycetes. *Fungal Genetics and Biology*, *30*, 17–32. https://doi.org/10.1006/fgbi.2000.1202

Dhingra, O. D., & Sinclair, J. B. (1995). *Basic plant pathology methods*, 2nd ed. (p. 341). Lewis Publishers, Boca Raton, Florid.

Dollet, M., De Franqueville, H., & Ducamp, M. (2012). *Bud rot and other major diseases of coconut, a potential threat to oil palm.4th IOPRI-MPOB International Seminar*, 13-14 December 2012, Bandung, Indonesia.

Eeuwens, C. J. (1976). Mineral requirements for growth and callus initiation of tissue explants excised from mature coconut palms (*Cocos nucifera*) and cultured *in vitro*. *Physiologia Plantarum*, *36*(1), 23–28.

Erwin, D. C., & Ribeiro, O. K. (1996). *Phytophthora Diseases Worldwide*. : APS Press.

Escalante, F., Gamboa, M. R., Lecher, J. G., Arroyo, G. A., Zizumbo, D., Oropeza, C., & Peña-Rodríguez, L. M. (2002). Major components from epicuticular wax of *Cocos nucifera*. *Rev Soc Quím Méx*, *46*, 247–250.

Freeman, B. C., & Beattie, G. A. (2008). *"An Overview of Plant Defenses against Pathogens and Herbivores"*. The Plant Health Instructor. Plant Pathology and Microbiology Publications. 94. DOI: 10.1094/PHI-I-2008-0226-01

Gallegly, M. E., & Hong, C. (2008). *Phytophthora: Identifying Species by Morphology and DNA*. : APS Press.

Gupta, S., Gupta, N. K., Arora, A., Agarwal, V. P., & Purohit, A. K. (2012). Effect of water stress on photosynthetic attributes, membrane stability and yield in contrasting wheat genotypes. *Indian Journal of Plant Physiology*, *17*(1), 22–27.

Irwin, J. A. G., Musial, J. M., Mackie, J. M., & Basford, K. E. (2003). Utility of cotyledon and detached leaf assays for assessing root reactions of lucerne to *Phytophthora* root rot caused by *Phytophthora medicaginis*. *Australasian Plant Pathology*, *32*(2), 263–268. https://doi.org/10.1071/AP03006

Jay, M., Bourdeix, R., Potier, F., & Sanslaville, C. (1989). *Premiers Résultats De L'étude Du Polymorphisme Des Polyphénolsfoliaires Du cocotier*. Oléagineux, *44*, 151–161.

Jia, Y., Valent, B., & Lee, F. N. (2003). Determination of host responses to *Magnaporthe grisea* on detached rice leaves using a spot inoculation method. *Plant Disease*, *87*(2), 129–133.

Kumar, S., Stecher, G., Li, M., Knyaz, C., & Tamura, K. (2018). MEGA X: Molecular evolutionary genetics analysis across computing platforms. *Molecular Biology and Evolution*, *35*(6), 1547–1549. https://doi.org/10.1093/molbev/msy096

Martin, F. N., Abad, Z. G., Balci, Y., & Ivors, K. (2012). Identification and detection of *Phytophthora*: Reviewing our progress, identifying our needs. *Plant Disease*, *96*(8), 1080–1103.

Martínez, G., Sarria, G. A., Torres, G. A., Varon, F., Romero, H. M., & Sanz, J. I. (2010). Advances in research on *Phytophthora palmivora*, causal agent of bud rot of oil palm in Colombia. *Palmas*, *31*, 55–63.

Mohamed-Azni, I. N. A., Sundram, S., & Ramachandran, V. (2019). Pathogenicity of Malaysian *Phytophthora palmivora* on cocoa, durian, rubber and oil palm determines the threat of bud rot disease. *Forest Pathology*, *49*(6), e12557. https://doi.org/10.1111/efp.12557

Mohamed-Azni, I. N. A., Sundram, S., Ramachandran, V., & Seman, I. A. (2017). An *in vitro* investigation of Malaysian *Phytophthora palmivora* isolates and pathogenicity study on oil palm. *Journal of Phytopathology*, *165*(11–12), 800–812.

Parke, J. L., Roth, M. L., & Choquette, C. J. (2005). *Detached-Leaf Assays With Phytophthora ramorum: Are They Valid?*. In: Sudden Oak Death Second Science Symposium: The State of Our Knowledge, 1821 January 2005. Monterey, California, pp 535.

Prathibha, V. H., Hedge, V., Sharadraj, K. M., Rajesh, M. K., Rachana, K. E., & Chowdappa, P. (2018). Differentiation of *Phytophthora* species associated with plantation crops using PCR and high-resolution melting curve analysis. *Journal of Plant Pathology*, *100*(2), 233–240.

Rachana, K. E., & Rajesh, M. K. (2019). *Selection and validation of reference genes for gene expression normalization in coconut (Cocos nucifera L.) under biotic stress and hormone stimuli*. Plant Gen 19:100184.

Ramesh, R., & Maruthadurai, R. (2014) *"Manual on Diagnosis of Insect Pests and Diseases of Plantation and Spice Crops of Goa"*. Technical Bulletin No. 38. Old Goa, India, ICAR RC for Goa.

Riedel, M., Riederer, M., Becker, D., Herran, A., Kullaya, A., Arana-López, G., Peña-Rodríguez, L., Billotte, N., Sniady, V., Rohde, W., & Ritter, E. (2009). Cuticular wax composition in *Cocos nucifera* L.: Physicochemical analysis of wax components and mapping of their QTLs onto the coconut molecular linkage map. *Tree Genetics and Genomes*, *5*(1), 53.

Sairam, R. K., Deshmukh, P. S., & Shukla, D. S. (1997). Tolerance of drought and temperature stress in relation to increased antioxidant enzyme activity in wheat. *Journal of Agronomy and Crop Science*, *178*(3), 171–178. https://doi.org/10.1111/j.1439-037X.1997.tb00486.x

Saitou, N., & Nei, M. (1987). The neighbor-joining method: A new method for reconstructing phylogenetic trees. *Molecular Biology and Evolution*, *4*(4), 406–425.

Sarria, G. A., Martinez, G., Varon, F., Drenth, A., & Guest, D. I. (2016). Histopathological studies of the process of *Phytophthora palmivora* infection in oil palm. *European Journal of Plant Pathology*, *145*(1), 39–51. https://doi.org/10.1007/s10658-015-0810-9

Sharadraj, K. M., & ChandraMohanan, R. (2014). A new detached coconut leaf let technique for bioassay of fungicides against *Phytophthora palmivora*–the incitant of coconut bud rot. *International Journal of Plant Pathology*, *7*(1), 161–165.

Srinivasulu, B., Gaautam, B., Sujatha, A., Kalpana, M., Vijayalakshmi, P., Pavanirani, A., Chandran, B. S. R. S., & Ramakrishna, Y. (2008). *Bud rot disease of coconut*. Technical Bulletin, AICRP on palms, Horticultural Research Station, Andhra Pradesh Horticultural University, Ambajipeta, pp 1-24.

Srinivasulu, B., & Raghava Rao, D. V. (2009). Biocontrol of major diseases of coconut. In P. M. Ponmurugan, & A. Deepa (Eds.), *Role of Biocontrol Agents for Disease Management in Sustainable Agriculture* (pp. 352–368). : Scitech Pvt.

Surin, P., Srivakorn, N., Imrie, B., & Lawn, R. (1993). A detached leaf culture technique for resistance screening against bacterial pustule in soybean. *Kasetsart Journal-Natural Science*, *27*, 240–250.

Vawdrey, L. L., Martin, T. M., & De Faveri, J. (2005). A detached leaf bioassay to screen Durian cultivars for susceptibility to *Phytophthora palmivora*. *Australasian Plant Pathology*, *34*(2), 251–253.

Wang, W., & Jiao, F. (2019). Effectors of *Phytophthora* pathogens are powerful weapons for manipulating host immunity. *Planta*, *250*, 413–425. https://doi.org/10.1007/s00425-019-03219-x

White, T. J., Bruns, T., Lee, S. J. W. T., & Taylor, J. (1990). Amplification and direct sequencing of fungal ribosomal RNA genes for phylogenetics applications. In N. Innis, D. Gelfand, J. Sninsky, & T. White (Eds.). *PCR Protocols: A Guide to Methods and Applications* (pp 315-322). : Academic Press, Inc.

Xu, X. L., & Ko, W. H. (1998). A quantitative confined inoculation method for studies of pathogenicity of fungi on plants. *Botanical Bulletin of Academia Sinica*, *39*, 187–190.

Yang, X., Tyler, B. M., & Hong, C. (2017). An expanded phylogeny for the genus *Phytophthora*. *IMA Fungus*, *8*(2), 355–398. https://doi.org/10.5598/imafungus.2017.08.02.09

## SUPPORTING INFORMATION

Additional supporting information may be found online in the Supporting Information section.

**How to cite this article:** Karyath Palliyath G, Kilingar Subrahmanya M, Antony G, Binod Bihari S, Hegde V, Muliyar Krishna R. A rapid in vitro leaf inoculation assay to investigate *Phytophthora palmivora*–coconut interactions. *J Phytopathol*. 2021;169:316–328. https://doi.org/10.1111/jph.12988

Research Article

doi:10.25081/jpc.2022.v50.i2.7984
Journal of Plantation Crops, 2022, 50(2): 100-109

# Molecular characterisation and structural assessment of an RXLR effector from *Phytophthora palmivora*, the coconut bud rot pathogen

**K.P. Gangaraj[1,2] and M.K. Rajesh[1,*]**

[1]*ICAR-Central Plantation Crops Research Institute, Kasaragod- 671124, Kerala, India*
[2] *Mangalore University, Mangalagangotri, Mangaluru-574199, Karnataka, India*

*(Manuscript Received: 18-05-2020, Revised: 04-09-2020, Accepted: 15-04-2022)*

## Abstract

*Phytophthora* species are phytopathogenic oomycetes that damage a wide variety of crops. *Phytophthora* delivers effectors, which are secretory proteins, into the host cells. Effectors promote infection by reprogramming the host cellular machinery and are key determinants of oomycete virulence. The major class of *Phytophthora* effector proteins contains the RXLR motif. In this study, we have carried out the molecular and structural characterisation of an *RXLR* effector *(RXLR6744)* from a virulent *P. palmivora* isolated from bud rot disease-affected coconut palm. The open reading frame (ORF) of the *RXLR6744,* amplified using RT-PCR, had a length of 411 bp. The gene was found to encode a predicted protein of 136 amino acids and had a molecular weight of 15.52 kDa. Phylogenetic analysis of the amino acid sequence revealed that it was closely related to RXLR proteins from *P. palmivora* (causing black pod disease in cocoa) and related species *P. megakarya*. Topology analysis revealed that the protein was composed of six α-helices. The structural prediction was undertaken by computer-aided homology modelling. From the Ramachandran plot analysis, it could be observed that the majority (96.3%) of amino acids were present in the preferred region, 3.7 per cent of amino acid residues were present in the allowed region, and no residues were observed in the disallowed region. The structure showed an average quality of 94.4 per cent, indicating it to be a high-quality structure. This study provides the detailed characterisation of an RXLR effector from *P. palmivora*. It will aid the elucidation of its role in pathogenesis and facilitate further refined investigations of the structure/function relationships of oomycete effectors.

***Keywords*:** Effectors, homology modelling, *Phytophthora palmivora,* RXLR

## Introduction

Plant diseases are a significant yield and quality constraint for plantation crops. Phytopathogens can be fungal, bacterial, viral or phytoplasma and can damage plant parts above or below the ground. Among phytopathogenic oomycetes, *Phytophthora* is a major genus responsible for impairment for economically important crops worldwide and inflicting serious damage to natural ecosystems (Erwin *et al*., 1996). More than 200 species of *Phytophthora* have been identified; prominent members include *P. infestans*, *P. sojae, P. ramorum* and *P. cinnamomi* (Riolo *et al*., 2020; Scanu *et al*., 2021). The Great Irish Famine, which occurred due to late blight disease in potatoes caused by *P. infestans,* resulted in the loss of millions of lives in Ireland from 1845 to 1852 (Yoshida *et al.*, 2013). A tropical relative of *P. infestans*, with its origins in south-eastern Asia, is *Phytophthora palmivora* (McHau and Coffey, 1994), with international trade aiding in its spread world over (Scott, 2013).

The host range of *P. palmivora* is wide, and virulence has been established in the roots and leaves of both monocotyledons and dicotyledons (Rey *et al*., 2015). It causes root/bud/fruit rot diseases in many important tropical fruits, spices and oil seeds (Drenth and Sendall, 2004). As a hemibiotroph, *P. palmivora* first parasitises living

**Corresponding Author: rajesh.mk@icar.gov.in*

tissues; it grows and sporulates in dead tissues. Motile zoospores infect plants when they come into contact with plant surfaces; they encyst, germinate and form appressoria, which aid penetration of the plant surface (Judelson and Blanco, 2005). Once the pathogen has gained access to plant tissues, it develops 'digit-like' haustoria that protrude into living plant cells and release virulent effector proteins that cause the plant to be infected. A necrotrophic stage follows, characterised by necrosis of host tissue and the release of zoospores from sporangia (Zuluaga *et al*., 2016).

*Phytophthora* spp. secrete many effector proteins, and these proteins have specific sites of action. Apoplastic effectors enter the extracellular spaces of plants, while cytoplasmic effectors are translocated into the plant's cells and target sub-cellular regions (Birch *et al*., 2006; Kamoun, 2006; Hunziker *et al*., 2021). By inhibiting host proteases and glucanases, which accumulate in response to pathogen infection, apoplastic effectors contribute to counter-defence (Rose *et al*., 2002; Tian *et al*., 2004, 2005). Contrary to this, cytoplasmic effectors are poorly understood in terms of their biochemical activities. The RXLR family of *Phytophthora* cytoplasmic effectors was discovered through their avirulence (*Avr*) function, *i.e.,* their ability to trigger hypersensitive cell death on genotypes with corresponding disease resistance genes (*R*) (Armstrong *et al*., 2005; Rehmany *et al*., 2005; Chepsergon *et al*., 2021).

As the infection progresses through the biotrophic phase, phytophthoral cytoplasmic effectors play a crucial role in virulence. An RXLR effector consists of a secretion signal peptide followed by a conserved N-terminal domain with the RXLR consensus sequence (Arg-Xaa-Leu-Arg). The translocation of these effectors inside plant cells depends on the RXLR domain (Whisson *et al*., 2007). C-terminal regions of these effectors appear to be involved in their biochemical activity (Schornack *et al*., 2009). The N-terminal part of Avr1b contains a signal peptide (SP) and the RXLR-dEER domain, which contains the RXLR motif and the dEER motif. RXLR proteins display a high degree of sequence diversity in their effector domains. However, it is important to note that despite this diversity, there are some recognisable sequence relationships within the C-terminal regions of RXLR effectors and some repeating sequence motifs such as 'W', 'Y', and 'L' (Jiang, 2008). Nearly half of RXLR effectors possess the W, Y, and L motifs. In contrast to the RXLR motif, the 'dEER' motif has a stretch of primarily acidic amino acids (Shan *et al.,* 2004; Kamoun, 2006; van Poppel *et al*., 2008).

Despite the economic impact and widespread distribution of *P. palmivora* in coconut and other palms, no studies have been undertaken on the characterisation of the effector protein repertoire of *P. palmivora*. In the present study, we have amplified the full-length coding sequence of a highly expressed *RXLR (RXL6744)*, identified from our previous coconut-*P. palmivora* interaction studies undertaken using dual RNA-sequencing (dual RNA-seq) (Gangaraj and Rajesh, 2020). We have also predicted the three-dimensional structure (3-D) of the RXLR protein. The findings could help us understand how the RXLR proteins function as an effector to aid oomycete pathogenesis and establish target molecules to control *P. palmivora*.

## Materials and methods

### Primer designing

We have selected a highly expressed RXLR transcript *(RXLR6744)*, identified from dual RNA-seq data generated in-house (Gangaraj and Rajesh, 2020). Enhanced expression of this transcript was observed at 24 hours post inoculation (hpi) of pin-pricked coconut leaflets with the virulent *P. palmivora* TR-PP-2 isolate (Gangaraj *et al*., 2021). The full-length coding sequence (cds) was picked up from the genome sequence of the *P. palmivora*, incitant of oil palm disease (isolate ZC01), which is available in NCBI (Genome ID: 66939; GenBank assembly accession: GCA_008079305.1; Sequence ID: VOQZ01000128.1: 107016-107426). The full-length *RXLR* gene was retrieved from NCBI-Genbank (Sequence ID: VOQZ01000128.1: 106805-107448) through BLAST analysis. Primer3 (v. 0.4.0) (http://bioinfo.ut.ee/primer3-0.4.0/) programme was utilised to design primers to amplify the full-length coding sequence of the RXLR effector.

### *In vitro* inoculation assay and RNA isolation

This study used a previously isolated and characterised virulent strain of *P. palmivora*

(TR-PP-2) (Gangaraj and Rajesh, 2020; Gangaraj *et al*., 2021). Using the *in vitro* inoculation assay developed (Gangaraj and Rajesh, 2020; Gangaraj *et al*., 2021), seven-day-old culture disks of the TR-PP-2 isolate were inoculated onto *in vitro* maintained and pin-pricked coconut leaflets of Chowghat Orange Dwarf cultivar. Total RNA was extracted 24 h post-inoculation (hpi) utilising the NucleoSpin RNA Plant and Fungi kit (Macherey Nagel, Germany). The OD 260 nm/280 nm ratio was used to evaluate the RNA quality and purity. The RNA Integrity Number (RIN) was determined using an Agilent 2100 Bioanalyzer (Agilent Technologies) and was observed to be >8.0. The high-quality RNA was stored at -80 °C until it was used in the next step of the process.

**RT-PCR analysis**

RNA samples were reverse transcribed to generate first-strand complementary DNA (cDNA) using the PrimeScript™ 1st strand cDNA Synthesis Kit (DSS Takara). GRXLRM-forward (5'-GGGATA CTCGAGACGCCAAG-3') and GRXLRM reverse (5'-GAGGCGATAGAGCACCTCAC-3') primers were used for amplifying the full-length cds of the RT-PCR analysis. The RT-PCR reaction mix consisted of 0.3 µL of *Taq* polymerase (1U/µL;), 2 µL of 10x *Taq* Buffer A (GeNei™), 0.8 µL of 10 mM dNTP mix (GeNei™), 0.2 µM each of forward and reverse primer (Eurofins Genomics) and 1 µL (~200 ng) of synthesised cDNA, in a total volume of 20 µL. The reaction conditions were initial denaturation at 95 °C for 5 minutes and then 94 °C for 35 seconds, 55 °C for 1 minute, 72 °C for 1 minute for about 35 cycles, and a final extension at 72 °C for about 10 minutes (MyCycler™ Thermal Cycler; Bio-Rad). The amplicon was cloned in a T/A cloning vector (pTZ57R/T; InsTAclone™ PCR Cloning Kit; Thermo Fisher Scientific). Colony PCR was carried out using GRXLRM-forward and GRXLRM-reverse primers. Plasmid DNAs from positive clones were extracted with plasmid purification kits (QIAprep Spin Miniprep Kit; Qiagen). The inserts were sequenced, in an ABI Prism 377 automated DNA sequencer, by Sanger's method.

**Sequence analysis of RXLR effector**

The sequence was processed using BioEdit 7.2 (http://en.bio-soft.net/format/BioEdit.html) and CAP3 (http://doua.prabi.fr/software/cap3) programmes. The open reading frame (ORF) was predicted with ORF Finder (https://www.ncbi.nlm.nih.gov/ orffinder/) and compared to other *Phytophthora* spp. using Basic Local Alignment Search Tool (BLAST) analysis in National Center for Biotechnology Information (NCBI), http://www.ncbi.nlm.nih.gov/). With 1,000 bootstrap replicates, phylogenetic relationships of protein sequence were inferred using the Neighbor-Joining (NJ) approach (MEGA X version 10.2.4; https://www.megasoftware.net/). ProtParam (http://web.expasy.org/protparam/) was used to compute the theoretical pI, molecular weight and amino acid composition. SignalP-5.0 (http://www.cbs.dtu.dk/services/SignalP/) was used to determine the presence of signal peptides and their cleavage sites based on the predicted amino acid sequence of the effector protein. TargetP 1.1 (http://www.cbs.dtu.dk/services/TargetP-1.1/index.php) was used to predict the subcellular location of eukaryotic proteins, and TMHMM-2.0 (http://www.cbs.dtu.dk/services/TMHMM/) were used to identify the transmembrane helices in proteins. The secondary structure information was predicted using Sopma (https://npsa-prabi.ibcp.fr/cgi-bin/npsa_automat.pl?page=/NPSA/npsa_sopma.html) and Jpred 4 (http://www.compbio.dundee.ac.uk/jpred/).

**Three-dimensional structure prediction of RXLR protein**

Prediction of the three-dimensional (3D) structure of the RXLR protein was made by using the fold recognition ('threading') method since homology-based modelling could not be performed due to the lack of template structures in the Protein Data Bank (PDB). Two different servers, *viz*., Phyre2 (http://www.sbg.bio.ic.ac.uk/~phyre2/html/page.cgi?id=index) and SPARKS-X (https://sparks-lab.org/server/sparks-x/), were used to predict the 3D models. Ramachandran plot validation was done on the predicted structure by utilising the SAVES server (https://saves.mbi.ucla.edu/). ModRefiner (https://zhanglab.ccmb.med.umich.edu/ModRefiner/) was used for high-level refinement of the predicted structure. The refined model was further validated through the SAVES server and ProSA-web (https://prosa.services. came.sbg.ac.at/prosa.php). PDBsum server (http://www.ebi.ac.uk/thornton-srv/databases/cgi-bin/pdbsum/

GetPage.pl?pdbcode=index.html) was used to study the topology.

## Results and discussion

### Amplification of RXLR region

A sequence of 411 bp length was obtained using GRXLRM-forward and GRXLRM-reverse primers. A standalone BLAST sequence search against the *P. palmivora* (isolate) was performed and showed maximum similarity. The complete cds were translated, and 136 amino acid length RXLR effector was identified without any introns. The sequence was deposited in NCBI (Accession no. MW768152).

### Primary sequence analysis

Sequence alignment analysis of the sequenced product indicated perfect identity with secreted RXLR effector sequences from *P. palmivora* available in the Genbank database. The BLAST analysis showed 99.26 per cent homology with the subject sequence (GenBank accession no: POM73696.1) (Supplementary File 1). According to phylogenetic analysis, RXLR protein (coconut bud rot) was genetically similar to RXLR protein from *P. palmivora* isolate (cocoa) (GenBank accession no. POM73696) and closely related to RXLR protein (GenBank accession no: OWZ10115) from *P. megakarya* (Fig. 1); the detailed information is available in Supplementary File 2. The primary sequence analysis, using ProtParm, showed that the predicted molecular weight of RXLR protein was 15518.56 Da. The total number of negatively charged residues (*viz*., Asp + Glu) and positively charged residues (*viz.,* Arg + Lys) was 16 and 20, respectively. The instability index (II) is computed as 29.52; this classified the protein as stable. An analysis of the atomic composition of the protein sequence revealed 675 carbon atoms, 1079 hydrogen atoms, 207 nitrogen atoms, 204 oxygen atoms and five sulphur atoms. The grand average of hydropathicity (GRAVY) was -0.623, which indicates hydrophilicity.

### Characteristics of RXLR effector

The SignalP 5.0 server predicted the presence of signal peptides (1-25 amino acid regions) and the location of their cleavage sites (25 and 26) in the RXLR protein. The TargetP predicted protein analysis indicates the protein located in the 'secretory pathway', and the signal peptide found in the sequence showed the highest score (0.928). Transmembrane analysis was carried out through an HMM-based method using TMHMM; the analysis revealed that RXLR was an extracellular

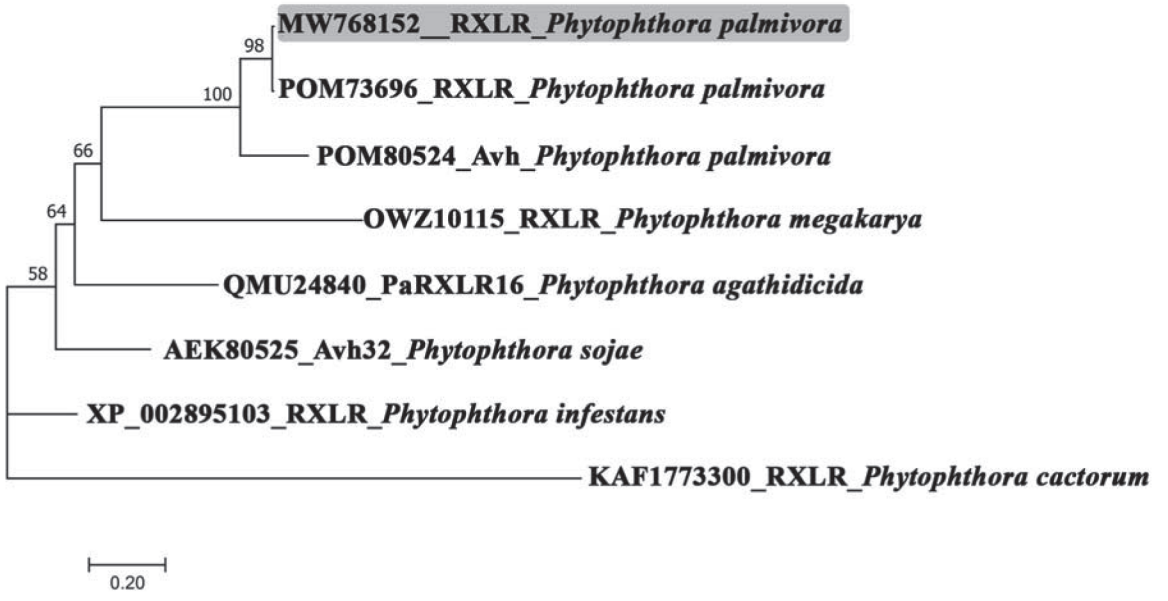


**Fig. 1. Phylogenetic analysis of the protein sequence showed that the selected RXLR sequence was closely related to the RXLR protein sequence of *P. palmivora* and *P. megakarya***

protein. InterProScan explained that the protein was a modular protein comprising of a signal peptide domain (1-25), RXLR domain (47-51) and effector domain (62-136). The CDD analysis showed that the sequence contained the RXLR domain with a threshold of 1.66 $e^{-13}$. Sequence modules (W, Y, and L) were observed in the C-terminal domain of RXLR (Fig. 2).

The MEME predicted motifs in protein sequence showed the presence of RXLR and dEER motifs. The conserved RXLR motif (Arg-Xaa-Leu-Arg) is followed by a high proportion of acidic residues (D/E). Analysis of the secondary structure, using JPred 4, showed that the protein contains five helical regions (Fig. 2). The SOPMA secondary structure prediction indicated that the *P. palmivora* RXLR protein sequence contained 52.94 per cent (72) of alpha-helices (Hh), 6.62 per cent (9) of beta-turns (Tt), 9.56 per cent (13) of extended strands (Ee) and 30.88 per cent (42) of random coils (Cc).

**Structural prediction of RXLR protein**

SPARKS-X and Phyre 2 programmes were used to predict the 3D structure of RXLR *via* threading processes, and the Ramachandran plot was utilised to evaluate the overall quality of the structure. While the structure predicted by SPARKS-X contained more than 90 per cent residues in the favoured region, the structure predicted by Phyre 2 showed less than 80 per cent residues in the favoured region. The predicted structure generated by SPARKS-X was therefore used for further study. SAVES analysed the Ramachandran plot of 'model.4.pdb' with 94.0 per cent amino acid residues in the favoured region, 4.5 per cent in the allowed region and just 1.5 per cent in the outer layer, respectively (Table 1). As approximately 94 per cent of the residues fall in the favoured region, the model was found to be good and reliable, and this model was selected for model refinement.

ModRefiner server has been used to reduce energy for the predicted structure's refinement. Once again, quality evaluation using SAVES was performed in the refinement model. The structure showed the highest percentage (96.3%) of amino acid in the favoured region, five (3.7%) amino acid residues in the allowed and no residue was observed in the disallowed region. The structure showed an overall quality of 94.4 per cent and was considered a high-quality structure. The ProSA score (Z-Score) of -4.02 for the model indicates that the energetic architecture of the predicted structure was good (Fig. 3). PDBsum server was used to study the topology of the refined structure. The findings revealed that the structure consisted of six alpha helices, eight helix-helix interactions, and three each of beta and gamma turns.

The structural topology revealed that the signal peptide was obtained in a single helical unit. The effector domain is composed of two alpha-helical units;

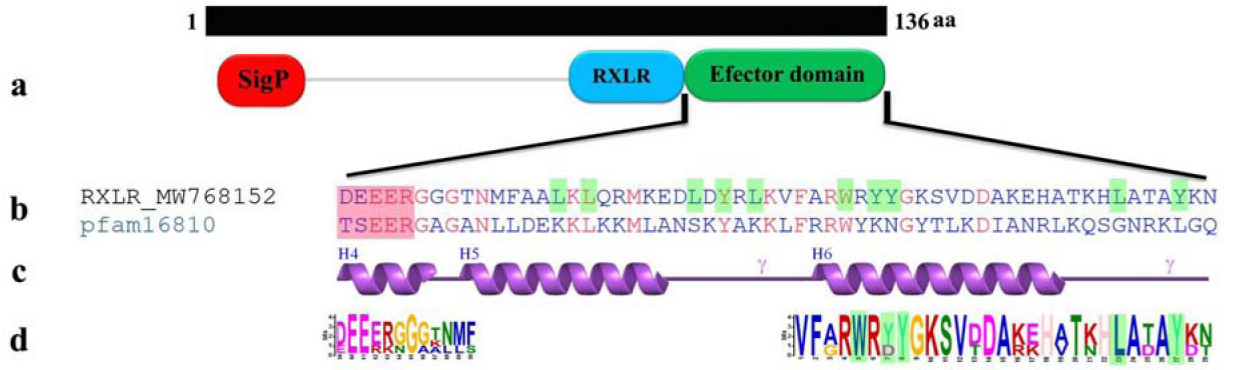


**Fig. 2. Characteristics of RXLR protein. (a) Domain representation of RXLR protein. (b) Effector domain sequence analysis- the red boxes represent the dEER motif, and the green boxes represent the Tryptophan (W), Tyrosine (Y), and Leucine (L) positions. (c) Secondary structural elements of the effector domain. (d) MEME motif identification of effector domain; MEME sequence motifs define connected 'W-Y-L' modules**

**Table 1. Structural summary and Ramachandran plot validation details of predicted structures of RXLR using SPARKS-X server**

| Model | Z score | Structural details | | | | Ramachandran plot validation | | |
|---|---|---|---|---|---|---|---|---|
| | | Group | Helices | Strands | Turns | Favoured region (%) | Allowed region (%) | Outlier region (%) |
| Model.1 .pdb | -2.82 | 136 | 8 | 0 | 12 | 91.8 | 4.5 | 3.7 |
| Model.2 .pdb | -5.06 | 136 | 7 | 0 | 10 | 91.8 | 6.7 | 1.5 |
| Model.3 .pdb | -3.8 | 136 | 6 | 0 | 15 | 93.3 | 5.2 | 1.5 |
| Model.4 .pdb | -3.05 | 136 | 6 | 0 | 8 | 94.0 | 4.5 | 1.5 |
| Model.5 .pdb | -3.8 | 136 | 6 | 0 | 9 | 91.0 | 4.5 | 4.5 |
| Model.6 .pdb | -3.84 | 136 | 5 | 2 | 16 | 90.3 | 4.5 | 5.2 |

the region is the major functional unit of the RXLR effector. The targeting region is mainly composed of four alpha helical units; this region contains RXLR and dEER motifs.

Plant pathogens secrete effectors, which enable host invasion by overcoming the plant immune responses (Petre *et al.*, 2020). *Phytophthora* spp. ubiquitously secrete RXLR proteins onto host cell surfaces or into host cells; these proteins play a significant and integral role in pathogenesis (Chepsergon *et al*., 2021). Characterisation of RXLR effectors has been reported in *P. infestans* (Wang *et al*., 2019), *P. parasitica* (Huang *et al*., 2019) and *P. sojae* (Wang *et al*., 2019). To resolve the effector structure characteristics of a highly expressed RXLR effector from *P. palmivora* incitant of coconut bud rot, we have sequenced the cds of *RXLR (RXl6744)* from *P. palmivora* and translated it into protein for structure prediction.

The sequenced product had a length of 411 bp, and a BLAST search revealed a perfect match with *P. palmivora* RXLR sequences. The translated RXLR was a 136 amino acid long effector, without any introns, as translated from the ORF Finder from NCBI. Wide variations have been reported in the size of the RXLR protein, with the length ranging

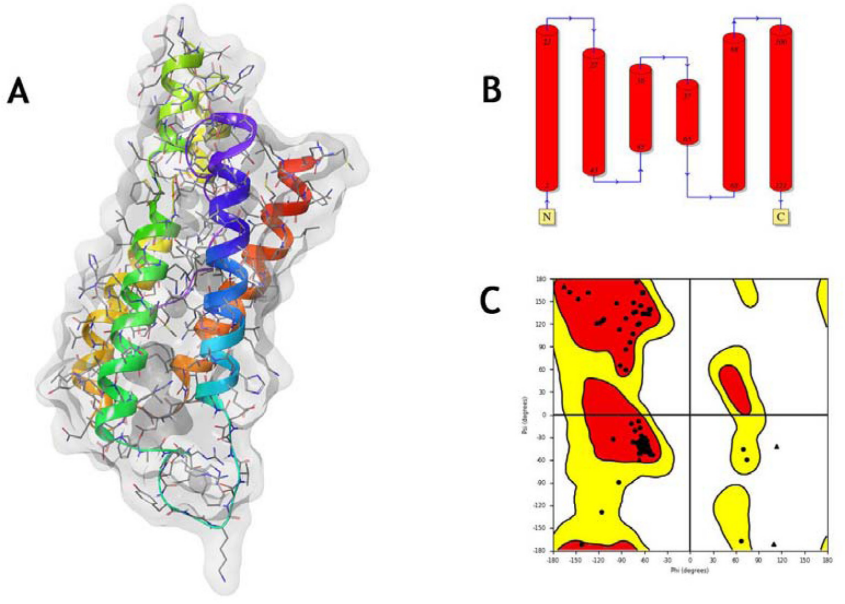


**Fig. 3. Predicted 3D structure of RXLR effector. A. Predicted three-dimensional structure; B. Structural topology of the predicted model; C. Ramachandran plot validation of predicted model 4**

from 84-381 amino acids (Petre *et al*., 2020). The RXLR gene investigated here did not have introns, a feature shared by many oomycete RXLR effectors (Jiang *et al.*, 2008; Ai *et al*., 2020). For the effectors of the RXLR family to be translocated into the plant cell, the RXLR motif appears to be essential; however, it is not essential for the biochemical activity of RXLR effectors (Zhao *et al*., 2018).

The probed C-terminal domain of the current study contained Tryptophan (W), Tyrosine (Y), and Leucine (L). However, domain analysis did not reveal any repetitions of the WY domain, which are characteristic of most RXLR proteins in the C-terminal regions (Anderson *et al*., 2015). In different effectors, the WY domain is found singly or as divergent tandem repeats (Zhao *et al*., 2018). Goss *et al*. (2013) have reported that RXLR genes from *P. ramorum* show variation in the copy number of the WY domain. As observed within regions containing WY, the WY domain may represent a platform capable of supporting polymorphism in surface residues, variation in the copy number of repeats, insertions within these repeats, and oligomerisation (Anderson *et al*., 2015). According to Win *et al*. (2012), the WY domains appear to be a feature which is unique to *Phytophthora* and downy mildew causing phytopathogens, indicating that the WY fold could have played an important role during the evolution of RXLR effectors (Anderson *et al*., 2015).

Various physicochemical properties of the RXLR protein were assessed using the ProtParam tool. The predicted molecular weight of RXLR protein was 15.52 K Da. Several phytopathogens, including bacteria, fungi, and oomycetes, secrete several low molecular weight protein effectors, which are believed to modulate plant immune responses and enhance pathogenicity (Liu *et al*., 2018). The instability index estimates the protein's stability- a protein whose instability index is below 40 is estimated to be stable, while the protein is projected to be unstable at a value above 40 (Guruprasad *et al.*,1990; Gamage *et al*., 2019). The RXLR effector protein investigated in the current study was stable since it had an instability index of 29.52. As increasing GRAVY scores suggest greater hydrophobicity, the negative GRAVY indices of all proteins tested demonstrated their affinity with water (Chang and Yang, 2013; Magdeldin *et al*., 2012). We observed that the RXLR protein was less charged and lower in GRAVY, suggesting that the protein was hydrophilic (Tyler, 2009; Singh *et al*., 2017; Yang *et al*., 2020). These findings suggest that the RXLR protein possessed the properties needed to act extra-cellularly.

The secretory protein features were identified using TargetP, SignalP and TMHMM servers, similar to the analysis carried out earlier in *P. sojae*, *P. ramorum*, *P. capsici*, and *P. infestans* (Ye *et al*., 2015). Three domains: the signal peptide domain, RXLR domain, and effector domain, were predicted by InterProScan. Related domain patterns have been reported for RXLR effectors from oomycetes like *P. infestans*, *P. capsici* and *P. sojae* (Birch *et al*., 2009; Boutemy *et al.*, 2011; Win *et al*., 2012). We found the presence of the RXLR-dEER motif in the RXLR effector, which was in line with the previous studies of Jiang *et al*. (2008), Boutemy *et al*. (2011) and Guo *et al*. (2020). A central alpha-helical fold is formed at both the N and C termini of the WY-domain, which is capable of tolerating significant plasticity. Furthermore, it promotes amino acid substitutions in surface residues and oligomerisation as additional alteration mechanisms (Boutemy *et al*., 2011). By using JPred 4, the secondary structure of the RXLR protein was predicted. The analysis revealed that the protein contained five helical regions, which concur with Ye *et al*. (2015). They reported that short alpha-helices were a typical structural feature of oomycete RXLR effector proteins.

All 3D models were predicted by SPARKS-X and Phyre2 servers. The Ramachandran plot constructed validated that the structure predicted by SPARKS-X was better, with more than 90 per cent residues in the favoured region. After refinement of the models by the ModRefiner server, Model 4 showed a better ProSA score (Z-Score) of -4.02, indicating that the quality of the structure was good (Wiederstein and Sippl, 2007). The refined 3D structure of RXLR protein satisfied all the validation criteria based on the Ramachandran plot analysis (Fig. 3). According to the Ramachandran plot analysis of the predicted structure, 94.0 per cent residues of Φ/Ψ angles are in the most favoured regions, 4.5 per cent residues in the allowed region

and just two residues (1.5%) in the disallowed region. In addition, the structure's overall quality factor was 94.4, which indicates that the structure is of high quality. Generally, high-quality protein structures generate values greater than 50 (Messaoudi *et al.*, 2013). The structural topology revealed that the signal peptide was obtained in a single helical unit and the N-terminal region was a four-helical bundle of abundance as observed in RXLR protein in *P. infestans* (Yaeno *et al*., 2011; Maqbool *et al*., 2016).

The present study describes the molecular and structural characterisation of a highly expressed RXLR effector protein from *P. palmivora*, incitant of coconut bud rot disease. To analyse structure-function relationships more precisely, it is necessary to determine the three-dimensional structures of the RXLR protein family from *P. palmivora*. Correlating their structural determinants with their biological activities requires further research.

## Acknowledgement

The authors thank the Indian Council of Agricultural Research (ICAR), New Delhi, India, for funding (ICAR-CPCRI Project no. 1000761030).

## References

Ai, G., Yang, K., Ye, W., Tian, Y., Du, Y., Zhu, H., Li, T., Xia, Q., Shen, D., Peng, H. and Jing, M. 2020. Prediction and characterisation of RXLR effectors in *Pythium* species. *Molecular Plant-Microbe Interactions* **33**: 1046-1058.

Anderson, R.G., Deb, D., Fedkenheuer, K. and McDowell, J.M. 2015. Recent progress in RXLR effector research. *Molecular Plant-Microbe Interactions* **28**: 1063-1072.

Armstrong, M.R., Whisson, S.C., Pritchard, L., Bos, J.I., Venter, E., Avrova, A.O., Rehmany, A.P., Böhme, U., Brooks, K., Cherevach, I. and Hamlin, N. 2005. An ancestral oomycete locus contains late blight avirulence gene Avr3a, encoding a protein that is recognised in the host cytoplasm. *Proceedings of the National Academy of Sciences USA* **102**: 7766-7771.

Birch, P.R., Armstrong, M., Bos, J., Boevink, P., Gilroy, E.M., Taylor, R.M., Wawra, S., Pritchard, L., Conti, L., Ewan, R. and Whisson, S.C. 2009. Towards understanding the virulence functions of RXLR effectors of the oomycete plant pathogen *Phytophthora infestans*. *Journal of Experimental Botany* **60**: 1133-1140.

Birch, P.R., Rehmany, A.P., Pritchard, L., Kamoun, S. and Beynon, J.L. 2006. Trafficking arms: oomycete effectors enter host plant cells. *Trends in Microbiology* **14**: 8-11.

Boutemy, L.S., King, S.R., Win, J., Hughes, R.K., Clarke, T.A., Blumenschein, T.M., Kamoun, S. and Banfield, M.J. 2011. Structures of *Phytophthora* RXLR effector proteins: A conserved but adaptable fold underpins functional diversity. *Journal of Biological Chemistry* **286**: 35834-35842.

Chang, K.Y. and Yang, J.R. 2013. Analysis and prediction of highly effective antiviral peptides based on random forests. *PloS One* **8**: e70166. https://doi: 10.1371/journal.pone.0070166.

Chepsergon, J., Motaung, T.E. and Moleleki, L.N. 2021. "Core" RXLR effectors in phytopathogenic oomycetes: A promising way to breeding for durable resistance in plants? *Virulence* **12**: 1921-1935.

Drenth, A. and Sendall, B. 2004. Economic impact of Phytophthora diseases in Southeast Asia. *Diversity and management of Phytophthora in Southeast Asia*. Drenth, A. and Guest, D. I, Southeast Asia, pp. 10-28.

Erwin, D.C. and Ribeiro, O.K. 1996. *Phytophthora Diseases Worldwide*. American Phytopathological Society (APS Press).

Gamage, D.G., Gunaratne, A., Periyannan, G.R. and Russell, T.G. 2019. Applicability of instability index for in vitro protein stability prediction. *Protein and Peptide Letters* **26**: 339-347.

Gangaraj, K.P. and Rajesh, M.K. 2020. Dataset of dual RNA-sequencing of *Phytophthora* palmivora infecting coconut (*Cocos nucifera* L.). *Data in Brief* **30**: doi: 10.1016/j.dib.2020.105455.

Gangaraj, K. P., Muralikrishna, K.S., Antony, G., Binod Bihari, S., Hegde, V. and Rajesh, M.K. 2021. A rapid *in vitro* leaf inoculation assay to investigate *Phytophthora palmivora*–coconut interactions. *Journal of Phytopathology* **169**: 316-328.

Goss, E.M., Press, C.M. and Grünwald, N.J. 2013. Evolution of RXLR-class effectors in the oomycete plant pathogen *Phytophthora ramorum*. *PLoS One* **8**: e79347.

Guo, Y., Dupont, P.Y., Mesarich, C.H., Yang, B., McDougal, R.L., Panda, P., Dijkwel, P., Studholme, D.J., Sambles, C., Win, J. and Wang, Y. 2020. Functional analysis of RXLR effectors from the New Zealand kauri dieback pathogen *Phytophthora agathidicida*. *Molecular Plant Pathology* **21**: 1131-1148.

Guruprasad, K., Reddy, B.B. and Pandit, M.W. 1990. Correlation between stability of a protein and its dipeptide composition: a novel approach for predicting in vivo stability of a protein from its primary sequence. *Protein Engineering, Design and Selection* **4**: 155-161.

Huang, G., Liu, Z., Gu, B., Zhao, H., Jia, J., Fan, G., Meng, Y., Du, Y. and Shan, W. 2019. An RXLR effector secreted by *Phytophthora parasitica* is a virulence factor and triggers cell death in various plants. *Molecular Plant Pathology* **20**: 356-371.

Hunziker, L., Tarallo, M., Gough, K., Guo, M., Hargreaves, C., Loo, T.S., McDougal, R.L., Mesarich, C.H. and Bradshaw, R.E. 2021. Apoplastic effector candidates of a foliar forest pathogen trigger cell death in host and non-host plants. *Scientific Reports* **11**: 19958. https://doi.org/10.1038/s41598-021-99415-5.

Jiang, R.H., Tripathy, S., Govers, F. and Tyler, B.M. 2008. RXLR effector reservoir in two *Phytophthora* species is dominated by a single rapidly evolving superfamily with more than 700 members. *Proceedings of the National Academy of Sciences USA* **105**: 4874-4879.

Judelson, H.S. and Blanco F.A. 2005. The spores of *Phytophthora*: weapons of the plant destroyer. *Nature Reviews Microbiology* **3**: 47-58.

Kamoun, S. 2006. A catalogue of the effector secretome of plant pathogenic oomycetes. *Annual Reviews of Phytopathology* **44**: 41-60.

Liu, Y., Lan, X., Song, S., Yin, L., Dry, IB, Qu, J., Xiang, J. and Lu, J. 2018. *In planta* functional analysis and subcellular localisation of the oomycete pathogen *Plasmopara viticola* candidate RXLR effector repertoire. *Frontiers in Plant Science* **9**: 286. https://doi.org/10.3389/fpls.2018.00286.

Magdeldin, S., Yoshida, Y., Li, H., Maeda, Y., Yokoyama, M., Enany, S., Zhang, Y., Xu, B., Fujinaka, H., Yaoita, E. and Sasaki, S. 2012. Murine colon proteome and characterisation of the protein pathways. *Bio Data Mining* **5**: 1-14.

Maqbool, A., Hughes, R.K., Dagdas, Y.F., Tregidgo, N., Zess, E., Belhaj, K., Round, A., Bozkurt, T.O., Kamoun, S. and Banfield, M.J. 2016. Structural basis of host autophagy-related protein 8 (ATG8) binding by the Irish potato famine pathogen effector protein PexRD54. *Journal of Biological Chemistry* **291**: 20270-20282.

McHau, G.R.A. and Coffey, M. D. 1994. Isozyme diversity in *Phytophthora palmivora*: Evidence for a southeast Asian centre of origin. *Mycological Research* **98**: 1035-1043.

Messaoudi, A., Belguith, H. and Hamida, J.B. 2013. Homology modeling and virtual screening approaches to identify potent inhibitors of VEB-1 β-lactamase. *Theoretical Biology and Medical Modelling* **10**: 1-10.

Petre, B., Contreras, M.P., Bozkurt, T.O., Schattat, M.H., Sklenar, J., Schornack, S., Abd-El-Haliem, A., Castells-Graells, R., Lozano-Duran, R., Dagdas, Y. and Menke, F. 2020. Host-interactor screens of *Phytophthora infestans* RXLR proteins reveal vesicle trafficking as a major effector-targeted process. *The Plant Cell* **33**:1447-1471.

Rehmany, A.P., Gordon, A., Rose, L.E., Allen, R.L., Armstrong, M.R., Whisson, S.C., Kamoun, S., Tyler, B.M., Birch, P.R. and Beynon, J.L. 2005. Differential recognition of highly divergent downy mildew avirulence gene alleles by *RPP1* resistance genes from two *Arabidopsis* lines. *The Plant Cell* **17**(6): 1839-1850.

Rey, T., Chatterjee, A., Buttay, M., Toulotte, J. and Schornack, S. 2015. *Medicago truncatula* symbiosis mutants affected in the interaction with a biotrophic root pathogen. *New Phytologist* **206**: 497-500.

Riolo, M., Aloi, F., La Spada, F., Sciandrello, S., Moricca, S., Santilli, E., Pane, A. and Cacciola, S.O. 2020. Diversity of *Phytophthora* communities across different types of Mediterranean vegetation in a nature reserve area. *Forests* **11**: 853.

Rose, J.K., Ham, K.S., Darvill, A.G. and Albersheim, P. 2002. Molecular cloning and characterisation of glucanase inhibitor proteins: co-evolution of a counter defense mechanism by plant pathogens. *The Plant Cell* **14**: 1329-1345.

Scanu, B., Jung, T., Masigol, H., Linaldeddu, B.T., Jung, M.H., Brandano, A., Mostowfizadeh-Ghalamfarsa, R., Janoušek, J., Riolo, M. and Cacciola, S.O. 2021. *Phytophthora heterospora* sp. nov., a new pseudoconidia-producing sister species of *P. palmivora*. *Journal of Fungi* **7**: 870. https://doi.org/10.3390/jof7100870.

Schornack, S., Huitema, E., Cano, L.M., Bozkurt, T.O., Oliva, R., van Damme, M., Schwizer, S., Raffaele, S., Chaparro Garcia, A., Farrer, R., Segretin, M.E., Bos, J., Haas, B.J., Zody, M.C., Nusbaum, C., Win, J., Thines, M. and Kamoun, S. 2009. Ten things to know about oomycete effectors. *Molecular Plant Pathology* **10**: 795- 803.

Scott, P., Burgess, T. and Hardy, GESJ 2013. Globalisation and *Phytophthora*. *Phytophthora*: *A Global Perspective*. CABI Plant Protection Series, Oxfordshire, UK. pp. 226-232.

Shan, W., Cao, M., Leung, D. and Tyler, B.M. 2004. The *Avr1b* locus of *Phytophthora sojae* encodes an elicitor and a regulator required for avirulence on soybean plants carrying resistance gene Rps 1b. *Molecular Plant-Microbe Interactions* **17**: 394-403.

Singh, Y., Patil, V.U., Dhasmana, A., Chakraborty, S.K., Shukla, P.K. and Rawat, S., 2017. *In silico* study of RXLR effectors of *Phytophthora infestans* HP-10-31, A2 mating type potato late blight pathogen. *International Journal of Advanced Biotechnology and Research* **8**: 398.

Tian, M., Benedetti, B. and Kamoun, S. 2005. A second Kazal-like protease inhibitor from *Phytophthora infestans* inhibits and interacts with the apoplastic pathogenesis-related protease P69B of tomato. *Plant Physiology* **138**: 1785-1793.

Tian, M., Huitema, E., Da Cunha, L., Torto-Alalibo, T. and Kamoun, S. 2004. A Kazal-like extracellular serine protease inhibitor from *Phytophthora infestans* targets the tomato pathogenesis-related protease P69B. *Journal of Biological Chemistry* **279**: 26370-26377.

Tyler, B.M., 2009. Entering and breaking: virulence effector proteins of oomycete plant pathogens. *Cellular Microbiology* **11**: 13-20.

van Poppel, P.M., Guo, J., van de Vondervoort, P.J., Jung, M.W., Birch, P.R., Whisson, S.C. and Govers, F. 2008. The *Phytophthora infestans* avirulence gene *Avr4* encodes an RXLR-dEER effector. *Molecular Plant-Microbe Interactions* **21**: 1460-1470.

Wang, S., McLellan, H., Bukharova, T., He, Q., Murphy, F., Shi, J., Sun, S., van Weymers, P., Ren, Y., Thilliez, G. and Wang, H. 2019. *Phytophthora infestans* RXLR effectors act in concert at diverse subcellular locations to enhance host colonisation. *Journal of Experimental Botany* **70**: 343-356.

Whisson, S.C., Boevink, P.C., Moleleki, L., Avrova, A.O., Morales, J.G., Gilroy, E.M., Armstrong, M.R., Grouffaud, S., Van West, P., Chapman, S. and Hein, I. 2007. A translocation signal for delivery of oomycete effector proteins into host plant cells. *Nature* **450**: 115-118.

Wiederstein, M. and Sippl, M.J. 2007. ProSA-web: interactive web service for the recognition of errors in three-dimensional structures of proteins. *Nucleic Acids Research* **35**: W407-W410.

Win, J., Krasileva, K.V., Kamoun, S., Shirasu, K., Staskawicz, B.J. and Banfield, M.J. 2012. Sequence divergent RXLR effectors share a structural fold conserved across plant pathogenic oomycete species. *PLoS Pathogens* **8**:e1002400. https://doi.org/10.1371/journal.ppat.1002400.

Yaeno, T., Li, H., Chaparro-Garcia, A., Schornack, S., Koshiba, S., Watanabe, S., Kigawa, T., Kamoun, S. and Shirasu, K. 2011. Phosphatidylinositol monophosphate-binding interface in the oomycete RXLR effector AVR3a is required for its stability in host cells to modulate plant immunity. *Proceedings of the National Academy of Sciences USA* **108**: 14682-14687.

Yang, L.N., Liu, H., Duan, G.H., Huang, Y.M., Liu, S., Fang, Z.G., Wu, E.J., Shang, L. and Zhan, J. 2020. The *Phytophthora infestans* AVR2 effector escapes R2 recognition through effector disordering. *Molecular Plant-Microbe Interactions* **33**: 921-931.

Ye, W., Wang, Y. and Wang, Y. 2015. Bioinformatics analysis reveals abundant short alpha-helices as a common structural feature of oomycete RXLR effector proteins. *PLoS One* **10**: e0135240. https://doi: 10.1371/journal.pone.0135240.

Yoshida, K., Schuenemann, V.J., Cano, L.M., Pais, M., Mishra, B., Sharma, R., Lanz, C., Martin, F.N., Kamoun, S., Krause, J. and Thines, M. 2013. The rise and fall of the *Phytophthora infestans* lineage that triggered the Irish potato famine. *Elife* **2**: e00731.

Zhao, L., Zhang, X., Zhang, X., Song, W., Li, X., Feng, R., Yang, C., Huang, Z. and Zhu, C., 2018. Crystal structure of the RXLR effector PcRXLR12 from *Phytophthora capsici*. *Biochemical and Biophysical Research Communications* **503**: 1830-1835.

Zuluaga, A.P., Vega-Arreguín, J.C., Fei, Z., Matas, A.J., Patev, S., Fry, W.E. and Rose, J.K. 2016. Analysis of the tomato leaf transcriptome during successive hemibiotrophic stages of a compatible interaction with the oomycete pathogen *Phytophthora infestans*. *Molecular Plant Pathology* **17**: 42-54.